Berichtsblatt

1. ISBN oder ISSN	2. Berichtsart (Schlussbericht oder Veröffentlichung)

3. Titel

Verbundprojekt VERCHROMT II: Erkennung, Verarbeitung und biologische Konsequenzen von Chromatinschäden nach Teilchenbestrahlung II, Teilprojekt B

4. Autor(en) [Name(n), Vorname(n)]

Prof., Dr. phil. nat. Georg Iliakis

5. Abschlussdatum des Vorhabens
30.06.2025

6. Veröffentlichungsdatum

7. Form der Publikation

8. Durchführende Institution(en) (Name, Adresse)

Institut für Medizinische Strahlenbiologie/Klinik für Radiotherapie
Universitätsklinikum Essen
Hufelandstrasse 55
45147 Essen

9. Ber. Nr. Durchführende Institution

10. Förderkennzeichen
02NUK054B

11. Seitenzahl
33

12. Fördernde Institution (Name, Adresse)

Bundesministerium für
Bildung und Forschung (BMBF)
53170 Bonn

13. Literaturangaben
31

14. Tabellen

15. Abbildungen
2

16. Zusätzliche Angaben

17. Vorgelegt bei (Titel, Ort, Datum)

18. Kurzfassung

Das Projekt baut auf den Erkenntnissen, Ergebnissen und methodischen Entwicklungen des vorangegangenen Verbundprojekts „Verchromt“ auf und verfolgt das Ziel, die Wechselwirkungen zwischen unterschiedlichen Strahlenqualitäten und der dreidimensionalen Kernarchitektur systematisch zu analysieren. Im Zentrum steht das mechanistische Verständnis, wie die durch CTCF, Cohesin und Condensine vermittelte Chromatinorganisation die Induktion, räumliche Verteilung und Reparatur von DNA-Doppelstrangbrüchen sowie die Wahl der beteiligten Reparaturwege beeinflusst. Diese Fragestellungen sind sowohl für die Entwicklung von Konzepten zur selektiven Radiosensibilisierung entarteter Tumorzellen bei gleichzeitiger Schonung von Normalgewebe als auch für das strahlenschutzrelevante Verständnis der erhöhten biologischen Wirksamkeit dicht ionisierender Strahlung von hoher Bedeutung. Aufbauend auf Vorarbeiten, die gezeigt haben, dass Veränderungen der globalen Chromatinorganisation die Nutzung alternativer Endverknüpfungswege (alt-EJ) erheblich beeinflussen, untersucht das Projekt gezielt die funktionellen Konsequenzen von CTCF-, Cohesin- und Condensin-abhängigen Chromatinrestrukturierungen auf das strahleninduzierte Schadensspektrum und die Reparaturwegwahl. Durch die Kombination unterschiedlicher Strahlenqualitäten mit der gezielten Modulation zentraler Chromatinorganisatoren soll ein integriertes Modell entwickelt werden, das die Rolle der Chromatinarchitektur als aktiver Regulator der zellulären Strahlenantwort beschreibt.

19. Schlagwörter
Chromatin, DNA-Doppelstrangbrüche, DNA-Reparatur, dicht ionisierende Strahlung, Teilchenstrahlung

20. Verlag	21. Preis

Document Control Sheet

1. ISBN or ISSN	2. type of document (e.g. report, publication)
3. title Collaborative Project VERCHROMT II: Recognition, Processing and Biological Consequences of Chromatin Damage after Particle Irradiation II, Subproject B	
4. author(s) (family name, first name(s)) Prof., Dr. phil. nat. Georg Iliakis	5. end of project 30.06.2025
	6. publication date
	7. form of publication
8. performing organization(s) (name, address)	9. originator's report no.
	10. reference no. 02NUK054B
	11. no. of pages 33
12. sponsoring agency (name, address) Bundesministerium für Bildung und Forschung (BMBF) 53170 Bonn	13. no. of references 31
	14. no. of tables
	15. no. of figures 2
16. supplementary notes	
17. presented at (title, place, date)	
18. abstract The project builds on the findings, results, and methodological developments of the preceding collaborative project "VERCHROMT" and aims to systematically analyze the interactions between different radiation qualities and the three-dimensional nuclear architecture. Central to the project is a mechanistic understanding of how chromatin organization mediated by CTCF, cohesin, and condensins influences the induction, spatial distribution, and repair of DNA double-strand breaks, as well as the choice of the involved repair pathways. These questions are of high relevance both for the development of concepts for the selective radiosensitization of malignant tumor cells while sparing normal tissue, and for the radiation protection–relevant understanding of the increased biological effectiveness of densely ionizing radiation. Building on prior work demonstrating that alterations in global chromatin organization substantially affect the use of alternative end-joining pathways (alt-EJ), the project specifically investigates the functional consequences of CTCF-, cohesin-, and condensin-dependent chromatin reorganization on the radiation-induced damage spectrum and repair pathway choice. By combining different radiation qualities with the targeted modulation of key chromatin organizers, the project aims to develop an integrated model describing chromatin architecture as an active regulator of the cellular radiation response.	
19. keywords	
20. publisher	21. price

Universitätsklinikum Essen
Institut für Medizinische Strahlenbiologie/Klinik für Radiotherapie
Prof. Dr. phil. nat. G. Iliakis

Schlussbericht für das Projekt 02NUK054B

Erfolgskontrollbericht

„VERCHROMT II: Erkennung, Verarbeitung und biologische Konsequenzen von Chromatinschäden nach Teilchenbestrahlung“

Förderkennzeichen:
02NUK054B

Das diesem Bericht zugrunde liegende Vorhaben wurde mit Mitteln des Bundesministeriums für Forschung, Technologie und Raumfahrt unter dem Förderkennzeichen 02NUK054B gefördert. Die Verantwortung für den Inhalt dieser Veröffentlichung liegt bei den Autoren.

Erfolgskontrollbericht

1. Beitrag der Ergebnisse zu den förderpolitischen Zielen

Die Förderung des Verbundprojekts VERCHROMT II erfolgte im Rahmen des Förderkonzepts „Grundlagenforschung Energie 2020+“ sowie des 7. Energieforschungsprogramms der Bundesregierung, welche grundlegende FuE-Arbeiten in der nuklearen Sicherheits- und Strahlenforschung, den Erhalt wissenschaftlicher Kompetenz sowie die Förderung des wissenschaftlichen Nachwuchses adressieren. Vor diesem Hintergrund leistete das vorliegende Teilprojekt einen substantiellen Beitrag zur Untersuchung grundlegender molekularer Mechanismen der Strahlenwirkung unter Berücksichtigung unterschiedlicher Strahlenqualitäten.

Das Teilprojekt B fokussierte sich auf die Analyse der Rolle der Condensine vermittelten Chromatinorganisation für die DNA-Schadensantwort, die Reparatur von DNA-Doppelstrangbrüchen und die Wahl der beteiligten Reparaturwege. Die erzielten Ergebnisse erweitern das mechanistische Verständnis der zellulären Strahlenantwort und liefern eine wissenschaftliche Grundlage für die Entwicklung verbesserter Konzepte in der Strahlentherapie, insbesondere im Hinblick auf eine selektive Radiosensibilisierung von Tumorzellen bei gleichzeitiger Schonung von Normalgewebe. Darüber hinaus tragen die Ergebnisse zum strahlenschutzrelevanten Verständnis der erhöhten biologischen Wirksamkeit dicht ionisierender Strahlung bei.

Ein weiterer zentraler förderpolitischer Aspekt war die nachhaltige Nachwuchsförderung im Bereich der Strahlenforschung. Im Rahmen des Projekts wurden ein Doktorand und eine Postdoktorandin qualifiziert sowie mehrere Bachelor- und Masterstudierende in die experimentellen Arbeiten eingebunden. Ergänzend wurde die akademische Lehre im Bereich der Strahlenbiophysik gestärkt und der wissenschaftliche Austausch innerhalb des Verbunds gefördert.

Insgesamt trägt das Projekt zur Erreichung der förderpolitischen Ziele des BMBF/BMFTR bei, indem es sowohl den Erkenntnisgewinn in der grundlagenorientierten Strahlenforschung vorantreibt als auch zur langfristigen Sicherung von Fachkompetenz und zur wissenschaftlichen Fundierung zukünftiger Anwendungen in Strahlentherapie und Strahlenschutz beiträgt.

2. Wissenschaftlich-technische Ergebnisse des Vorhabens

Aufbauend auf den im Vorgängerprojekt durchgeführten Tonicity-Experimenten, die erstmals gezeigt hatten, dass globale Veränderungen der Chromatinorganisation die Strahlenantwort und die Nutzung alternativer Reparaturwege maßgeblich beeinflussen, stellt das vorliegende Vorhaben eine konsequente und erfolgreiche Weiterführung dieser Arbeiten dar. Die Untersuchungen vertiefen die zuvor überwiegend phänomenologischen Befunde durch eine mechanistische Analyse zentraler Chromatinorganisatoren und führen diese logisch fort. Im Rahmen des Vorhabens wurde gezeigt, dass die durch Condensine vermittelte Chromatinorganisation ein zentraler Determinant der DNA-Schadensantwort nach ionisierender Strahlung ist. Störungen dieser Chromatinarchitektur führten zu einer signifikanten Radiosensibilisierung, einer beeinträchtigten DSB-Endresektion und einer selektiven Unterdrückung der homologen Rekombination. Für Condensine konnte dabei nachgewiesen werden, dass ihre Funktion ausschließlich in postreplikativen G2-Zellen erforderlich ist und dass ihre Depletion zu einer gleichzeitigen Beeinträchtigung aller resektions-abhängigen Reparaturwege, einschließlich HR, alternativer Endverknüpfung (alt-EJ) und Single-Strand-Annealing (SSA), führt. Die Ergebnisse belegen eine ausgeprägte Zellzyklus- und Strahlenqualitätsabhängigkeit der Reparaturdefekte und unterstreichen die Rolle der dreidimensionalen Chromatinorganisation als aktiver Regulator der Reparaturwegwahl und der zellulären Strahlenantwort.

Darüber hinaus leistete das Vorhaben einen wesentlichen Beitrag zur Nachwuchsförderung und zum langfristigen Kompetenzerhalt in der Strahlenforschung durch die aktive Einbindung von Studierenden und Nachwuchswissenschaftlerinnen und -wissenschaftlern sowie durch die Stärkung des wissenschaftlichen Netzwerks innerhalb des Verbunds.

Durch die kontinuierliche Einbindung von Studierenden in den Forschungsbetrieb wurde zudem ein nachhaltiger Beitrag zur Nachwuchsgewinnung geleistet. Das Projekt förderte das frühzeitige Interesse an strahlenbiologischen Fragestellungen und eröffnete Perspektiven für weiterführende Qualifikationsarbeiten. Insgesamt trug das Vorhaben damit sowohl zur methodischen Weiterentwicklung als auch zur langfristigen Sicherung fachlicher Expertise in der Strahlenforschung bei und schärfte zugleich das Bewusstsein für die Bedeutung strahlenbiologischer Prozesse in medizinischen, umweltrelevanten und raumfahrtbezogenen Anwendungsfeldern.

3. Fortschreibung des Verwertungsplans

Das Projekt lieferte wichtige Erkenntnisse über die zelluläre Reaktion auf unterschiedliche Strahlenqualitäten und deren Wechselwirkung mit der Chromatinorganisation durch Condensine. Diese Ergebnisse tragen zur Optimierung von Strahlentherapien bei, indem sie zeigen, wie Krebszellen selektiv radiosensitiviert werden können, während Normalgewebe geschont bleiben, und liefern zugleich entscheidende Hinweise für Strahlenschutzanwendungen in klinischen, beruflichen oder raumfahrtbezogenen Kontexten. Die etablierten Methoden zur Analyse chromatinabhängiger Reparaturmechanismen sind vollständig dokumentiert und können effizient in Folgeprojekten genutzt werden, wodurch die wissenschaftliche Anschlussfähigkeit des Vorhabens gesichert ist.

Ein weiterer zentraler Erfolg lag in der gezielten Förderung des wissenschaftlichen Nachwuchses. Studierende und Nachwuchswissenschaftlerinnen und -wissenschaftler wurden in experimentelle Arbeiten, methodische Analysen und den wissenschaftlichen Austausch innerhalb des Verbunds eingebunden, erhielten praxisnahe Erfahrungen und konnten ihre Kompetenzen in Planung, Durchführung und Auswertung von Forschungsprojekten erweitern. Lehrveranstaltungen, Forschungspraktika sowie eine MD-Doktorarbeit ermöglichten zudem einen frühzeitigen Zugang zur Strahlenbiologie und stärkten die Vernetzung innerhalb der nationalen und internationalen Forschungscommunity.

4. Ergebnisse, die weiterer mechanistischer Untersuchung bedürfen

Obwohl die Hauptziele des Projekts erreicht wurden, bestehen weiterhin offene mechanistische Fragen, insbesondere im Hinblick auf die zellzyklus-spezifischen Funktionen von CTCF und Cohesin bei der Wahl der DNA-Doppelstrangbruch-Reparaturwege, einschließlich c-NHEJ, HR, alt-EJ und SSA. Es ist bislang unklar, wie genau diese Chromatinorganisatoren in G1-, S- oder G2-Phase die Balance zwischen den verschiedenen Reparaturwegen steuern und welche molekularen Mechanismen diese Wegwahl modulieren. Um die offenen mechanistischen Fragen zu adressieren, ist ein systematisches, zellzyklus-spezifisches Experimentierprogramm geplant. Hierbei werden humane Zelllinien, insbesondere RPE-1 und A549, für die Knockdown-Experimente genutzt, wobei CTCF und Cohesin transient mittels siRNA herabreguliert werden. Die Effizienz des Knockdowns wird durch Western Blot und Immunfluoreszenzfärbung validiert. Um die zellzyklusabhängigen Effekte zu analysieren, werden die Zellen durch EdU-Inkorporation markiert, und G1- bzw. G2-

Phase über spezifische Marker wie Cyclin B1 oder phospho-Histone H3 unterschieden; optional kann eine partielle Synchronisation der Zellen mittels DMSO- oder Thymid-Block durchgeführt werden, um die Auflösung zu verbessern.

DNA-Doppelstrangbrüche werden sowohl durch niedrig-LET Röntgenstrahlung als auch durch hoch-LET Bestrahlung, beispielsweise Kohlenstoffionen am UNILAC-Beschleuniger, induziert, um Unterschiede zwischen Strahlenqualitäten zu untersuchen. Die Analyse der Reparaturwegwahl erfolgt differenziert: c-NHEJ wird über die Dynamik von γH2AX-Foci und durch den Einsatz von DNA-PK-Inhibitoren bestimmt, während HR über Rad51-Foci in S- und G2-Phasen quantifiziert wird. Die Nutzung alternativer, resek-tionsabhängiger Wege wie alt-EJ und SSA wird durch spezifische Reporterassays sowie chemische Inhibitoren von PARP1/2, Polθ und Rad52 analysiert. Zeitreihenmessungen zu mehreren Zeitpunkten nach Bestrahlung (0, 2, 6 und 24 Stunden) erlauben die Darstellung kinetischer Unterschiede in der Reparatur.

Für die quantitative Analyse der Foci werden konfokale Mikroskopie und quantitative bildbasierte Zytometrie (QIBC) eingesetzt. Dabei werden Parameter wie Foci-Größe, Anzahl und Ko-Localization als Indikatoren für die Effizienz der Reparaturwege ausgewertet. Ergänzend werden mechanistische Validierungen durchgeführt, unter anderem durch Co-FISH, ChIP oder superauflösende Mikroskopie, um die Chromatinstruktur an den Schadensstellen und die Rolle von TADs sowie Loop-Extrusion in der Reparaturwegwahl zu untersuchen.

Die Daten statistisch ausgewertet, um die zellzyklusabhängige Beeinflussung der Reparaturwegwahl durch CTCF und Cohesin zu quantifizieren. Auf Grundlage dieser Ergebnisse können mechanistische Hypothesen entwickelt werden, die erklären, wie diese Chromatinorganisatoren die DNA-Doppelstrangbruchreparatur in G1-, S- und G2-Phasen steuern und damit den Balanceakt zwischen fehlerfreien und fehleranfälligen Reparaturwegen determinieren.

Besonders hervorzuheben sind die starken G2-spezifischen Effekte nach Depletion von Condensinen, die bisher nur phänotypisch beschrieben wurden. Die zugrunde liegenden Mechanismen, die zu dieser post-replikativen Sensibilisierung für DNA-Schäden führen, einschließlich möglicher Einflüsse auf Chromatinrestrukturierung, Resektionsprozesse und Rekrutierung von HR-Faktoren, bedürfen noch gezielter experimenteller Aufklärung.

Die Verfügbarkeit spezifischer Condensin- und Cohesin-Inhibitoren in zukünftigen Studien wird es ermöglichen, die bisher gewonnenen Ergebnisse gezielt zu validieren und ihre klinische Anwendbarkeit zu prüfen. Mit solchen pharmakologischen Werkzeugen lassen sich die zellzyklusabhängigen Effekte auf die DNA-Reparatur direkt modulieren, wodurch nicht nur grundlegende Mechanismen weiter entschlüsselt werden können, sondern auch mögliche Strategien für eine selektive Radiosensibilisierung von Tumorzellen unter gleichzeitiger Schonung von Normalgewebe getestet werden können.

5. Verwertung und Sichtbarkeit der Forschungsergebnisse

Die erzielten Ergebnisse des Projekts haben eine hohe Relevanz für die Strahlenbiologische Grundlagenforschung, die DNA-Reparaturforschung sowie die Strahlenonkologie. Die Befunde zur Condensin-vermittelten Chromatinorganisation und deren Einfluss auf die DNA-Schadensantwort wurden in einer Publikation unter dem Titel „Condensins regulate resection-dependent DNA double-strand break repair pathways in replicated chromatin“ zusammengefasst und bei Nucleic Acids Research eingereicht. Der Artikel wurde bereits akzeptiert und wird in Kürze veröffentlicht.

Ein zweiter wissenschaftlicher Artikel ist in Vorbereitung, der die Ergebnisse zu CTCF- und Cohesin-Knockdown sowie deren Auswirkungen auf DNA-Reparaturwege, Chromosomenstabilität und strahleninduzierte Sensitivität zusammenfassen wird. Beide Publikationen werden Open Access erscheinen, um die breite Zugänglichkeit der Ergebnisse für die wissenschaftliche Community sicherzustellen.

Darüber hinaus wurden und werden die Ergebnisse auf nationalen und internationalen Fachtagungen präsentiert, darunter Tagungen der Gesellschaft für Biologische Strahlenforschung (GBS), der Radiation Research Society (RRS), der European Radiation Research Society (ERRS) und der Deutschen Gesellschaft für Radioonkologie (DEGRO). Frühere Konferenzbeiträge umfassten sowohl experimentelle Daten als auch methodische Entwicklungen, was den direkten Austausch mit potenziellen Nutzern und Forschungspartnern erleichtert.

Zukünftig können unveröffentlichte Daten, insbesondere kombinierte Analysen von Condensins, CTCF und Cohesin, zusammen mit neuen experimentellen Resultaten die Grundlage für weitere Publikationen bilden und so die wissenschaftliche Sichtbarkeit und Anwendung der Forschungsergebnisse weiter erhöhen.

6. Einhaltung der Ausgaben- und Zeitplanung

Die im Rahmen des Projektes geplanten Ausgaben wurden insgesamt eingehalten. Die überwiegende Mehrheit der experimentellen Arbeiten, einschließlich der geplanten Bestrahlungsexperimente an den Beschleunigern der GSI, konnte wie vorgesehen durchgeführt werden. Einzig die Wiederholungen der Hoch-LET-Bestrahlungen in den Jahren 2024 und 2025 konnten aufgrund begrenzter Verfügbarkeit von Strahlenzeit nicht realisiert werden, was die Vollständigkeit der experimentellen Wiederholungen einschränkte. Trotz sorgfältiger Planung konnten nicht alle vorgesehenen Experimente mit CTCF- und Cohesin-Knockdown abgeschlossen werden. Die ursprünglich geplanten Analysen, insbesondere detaillierte zellzyklus-spezifische Messungen zur Reparaturwegwahl und zur kinetischen Charakterisierung von c-NHEJ, HR, alt-EJ und SSA, erwiesen sich als deutlich arbeitsintensiver als zunächst angenommen. Pandemiebedingte Einschränkungen während der Corona-Pandemie, einschließlich Zugangsbeschränkungen zu den Laboren, reduzierter Laborkapazitäten und Lieferschwierigkeiten, führten zusätzlich dazu, dass bestimmte zeitkritische Experimente nicht durchgeführt werden konnten. Dennoch konnten wesentliche Kernexperimente erfolgreich umgesetzt werden, sodass zentrale mechanistische Aussagen zur Rolle von CTCF und Cohesin in der DNA-Schadensantwort gewonnen werden konnten.

Darüber hinaus führten die pandemiebedingten Arbeitsbedingungen, zeitweise eingeschränkter Laborbetrieb und Lieferschwierigkeiten zu temporären Verzögerungen im Projektablauf. Diese Herausforderungen konnten jedoch durch die kostenneutrale Verlängerung des Projektes bis Juni 2025 ausgeglichen werden. Die zusätzliche Laufzeit ermöglichte es, die verbleibenden Experimente, Analysen und Auswertungen erfolgreich abzuschließen, sodass die Projektziele trotz der externen Einschränkungen erreicht wurden.

Die Anpassungen im Zeitplan erlaubten zudem eine sorgfältige Durchführung und Optimierung von komplexen experimentellen Ansätzen, insbesondere bei der zellzyklus-spezifischen Analyse von DNA-Reparaturwegen nach hoch- und niedrig-LET-Bestrahlung. Somit wurde die wissenschaftliche Qualität der Ergebnisse gesichert, und die Integrität des Forschungsprojektes blieb vollständig erhalten.

Schlussbericht zum Forschungsvorhaben 02NUK054B

Eingehende Darstellung

Erkennung, Verarbeitung und biologische Konsequenzen von Chromatinschäden nach Teilchenbestrahlung II

(VERCHROMT II)

Laufzeit des Vorhabens

01.01.2020 bis 30.06.2025

Prof. Dr. phil. nat. G. Iliakis

Institut für Medizinische Strahlenbiologie/Klinik für Radiotherapie

Universitätsklinikum Essen

Das diesem Bericht zugrunde liegende Vorhaben wurde mit Mitteln des Bundesministeriums für Forschung, Technologie und Raumfahrt unter dem Förderkennzeichen 02NUK054B gefördert. Die Verantwortung für den Inhalt dieser Veröffentlichung liegt bei den Autoren.

1. Aufgabenstellung

Vorarbeiten in unserem Labor konnten zeigen, dass globale Modulation der Chromatinstruktur, z.B. durch Tonizitätsveränderungen, die Doppelstrangbruch (DSB)-Reparatur durch Homologe Rekombination (HR) erheblich verschlechtern und gleichzeitig die Reparatur durch Single Strand Annealing (SSA) deutlich verbessern (Krieger, Mladenov et al. 2021). Da dieser Eingriff in die Chromatinstruktur jedoch von begrenzter physiologischer Relevanz ist, wird in diesem Projekt die Rolle der Schlüsselkomponenten der Chromatinorganisation untersucht: CTCF, Cohesin und Condensins, die für die globale Organisation des Chromatins essentiell sind (Hirota, Gerlich et al. 2004, Hirano 2012, Schwarzer, Abdennur et al. 2017, Wutz, Várnai et al. 2017) und zudem eine noch nicht aufgeklärte Rolle in der HR spielen (Wood, Liang et al. 2008, Bauerschmidt, Arrichiello et al. 2010, Marin-Gonzalez, Rybczynski et al. 2025). Da die topologische Organisation des Chromatins, u.a. die Reaktion auf DSBs sowie die Wahrscheinlichkeit und Beschaffenheit von Reparaturfehlern (z.B. Translokationen) die zur Karzinogenese führen können, werden planten wir ursprünglich den Einfluss von CTCF, Cohesin, und Condensins auf die Gesamtantwort der Zellen auf DSBs untersuchen. Unsere ersten Versuche haben uns aber darauf hin verleitet auf die Rolle der Kondensine zu konzentrieren. Wir planen die Rolle von CTCF und Cohesins in Folgeprojekten eingehend zu untersuchen.

In diesem Projekt liegt ein besonderer Fokus auf der Analyse der Verarbeitung von ionisierender Strahlung induzierten DSBs. Vorarbeiten zeigten, dass die Herunterregulierung von Condensinen zu einer ausgeprägt erhöhten Strahlenempfindlichkeit von Zellen sowie zu tiefgreifenden Störungen der DNA-Doppelstrangbruchreparatur führte. Insbesondere die starke Beeinträchtigung resek-tions-abhängiger Reparaturwege und die ausgeprägte Zellzyklusabhängigkeit dieser Effekte hoben Condensine als zentrale Regulatoren der zellulären Strahlenantwort hervor. Aufgrund der außergewöhnlichen Stärke und Konsistenz dieser Befunde wurde die systematische Analyse der Condensin-abhängigen Mechanismen der Radiosensibilisierung und der DSB-Reparaturwegwahl zum Hauptfokus des vorliegenden Forschungsvorhabens. Condensine sind essenzielle Regulatoren der Chromatinarchitektur und sind erforderlich für die Chromosomenkondensation, die Organisation des Genoms sowie die Regulation der Genexpression. Säugerzellen exprimieren zwei unterschiedliche Condensin-Komplexe, Condensin I und Condensin II, die jeweils aus den zentralen ATPasen

SMC2 und SMC4 sowie aus spezifischen, nicht-SMC-Regulationsuntereinheiten bestehen (Hirota, Gerlich et al. 2004, Hirano 2012, Walther, Hossain et al. 2018). Condensin I setzt sich aus NCAPD2, NCAPG und NCAPH zusammen, während Condensin II die Untereinheiten NCAPD3, NCAPG2 und NCAPH2 enthält.

Diese beiden Komplexe unterscheiden sich in ihrer subzellulären Lokalisation: Condensin I ist überwiegend zytoplasmatisch und erhält erst nach dem Zerfall der Kernhülle Zugang zur DNA, während Condensin II während des gesamten Zellzyklus im Zellkern lokalisiert ist (Maeshima and Laemmli 2003, Gerlich, Koch et al. 2006). Beide Condensin-Komplexe tragen zur mitotischen Chromosomenkondensation bei, indem sie durch den Mechanismus der Loop-Extrusion DNA-Schleifen bilden und vergrößern (Nasmyth 2001, Abe, Nagasaka et al. 2011, Goloborodko, Imakaev et al. 2016, Gibcus, Samejima et al. 2018, Kong, Cutts et al. 2020). Dabei extrudiert Condensin I DNA-Schleifen schnell, jedoch transient, während Condensin II stabilere Schleifen erzeugt und maßgeblich zur Ausbildung großskaliger chromosomaler Strukturen beiträgt (Kong, Cutts et al. 2020).

2. Voraussetzungen, unter denen das Vorhaben durchgeführt wurde

Eine zentrale Voraussetzung für die Durchführung des Vorhabens war die Verfügbarkeit stabiler und gut charakterisierter und geeigneter humaner Zellkulturmodelle. Die verwendeten Zelllinien (RPE-1 und A549) wurden unter standardisierten Bedingungen kultiviert und ermöglichten reproduzierbare Experimente zur Analyse der DNA-Schadensantwort nach ionisierender Strahlung. Die Etablierung zellzyklusspezifischer Analysen setzte die Möglichkeit zur Identifikation einzelner Zellzyklusphasen auf Einzelzellebene voraus.

Darüber hinaus erforderte das Projekt die Etablierung effizienter und spezifischer siRNA-basierter Knockdown-Strategien zur gezielten Depletion von Condensin-Untereinheiten, CAP-H und CAP-D3, Cohesin und CTCF. Dies schloss die Optimierung von Transfektionsbedingungen, die Validierung der Knockdown-Effizienz auf Protein- und Funktionsebene sowie die Kontrolle möglicher Off-Target-Effekte ein. Nur durch eine konsistente und reproduzierbare Reduktion der Zielproteine war eine belastbare funktionelle Analyse der chromatinabhängigen DNA-Reparaturprozesse möglich.

Eine weitere wesentliche Voraussetzung war der Zugang zu strahlenbiologischer Infrastruktur für definierte Expositionen mit ionisierender Strahlung sowie zu

spezialisierten Methoden zur Erfassung der DNA-Schadensantwort. Hierzu zählten standardisierte Bestrahlungsprotokolle, die Immunfluoreszenzdetektion von DNA-Schadens- und Reparaturmarkern (u. a. γH2AX, 53BP1, RPA70, Rad51) sowie die Anwendung der klassischen Zytogenetik sowie Premature Chromosome Condensation (PCC) zur zytogenetischen Analyse chromosomaler Aberrationen.

Schließlich setzte das Vorhaben die Verfügbarkeit moderner Bildgebungs- und Auswerteplattformen voraus. Die quantitative Analyse der DNA-Schadensantwort erforderte den Einsatz automatisierter Hochdurchsatz-Mikroskopie sowie quantitativer bildbasierter Zytometrie (QIBC), einschließlich EdU-Markierung zur zellzyklusspezifischen Zuordnung einzelner Zellen. Die Etablierung standardisierter Bildanalyse- und Auswertestrategien war entscheidend, um große Datensätze reproduzierbar und statistisch robust auszuwerten und subtile, zellzyklusabhängige Effekte der Chromatinorganisation auf die DNA-Reparatur erfassen zu können.

3. Planung und Ablauf des Vorhabens

Das Vorhaben wurde in inhaltlich und methodisch aufeinander abgestimmte Arbeitsschritte gegliedert, um die Rolle der zentralen Chromatin-organisierenden Faktoren Condensine in der DDR und der Reparatur von DNA-DSBs systematisch zu untersuchen. Die Planung folgte einem integrativen Ansatz, der genetische Modulationen, funktionelle Reparaturassays, zellzyklusspezifische Analysen sowie zytogenetische Endpunkte kombinierte.

Zu Beginn wurden siRNA-basierte Knockdown-Strategien für Condensin-Untereinheiten etabliert und in normalen humanen Fibroblasten (82-8 hTert), epithelialen Zellen (RPE-1) sowie in humanen Tumorzelllinien (A549, U2OS) validiert. Diese genetischen Interventionen bildeten die methodische Grundlage für alle weiteren Analysen und ermöglichten eine gezielte Untersuchung der Auswirkungen veränderter Chromatinorganisation auf die DNA-Schadensantwort.

Im nächsten Schritt wurde der Einfluss von Condensinen auf die Reparaturwegwahl von DSBs analysiert. Hierzu kamen etablierte U2OS-Reporterzelllinien zum Einsatz (Gunn, Bennardo et al. 2011), die eine differenzierte funktionelle Bewertung der HR, des klassischen nicht-homologen End-Joinings (cNHEJ) sowie alternativer Endverknüpfungswege (alt-EJ) und Single Strand Annealing (SSA) erlauben. Ergänzend wurde die HR detailliert durch die quantitative Analyse von Rad51-Foci in

S- und G2-Phasen-Zellen mittels konfokaler Mikroskopie charakterisiert, um resektions-abhängige Reparaturprozesse zellzyklusspezifisch zu erfassen.

Die funktionelle Analyse des cNHEJ erfolgte dosisabhängig. Nach hohen Strahlendosen wurde die Reparatur mittels Pulsfeld-Gelelektrophorese (PFGE) untersucht, während im Niedrigdosisbereich die γH2AX-Foci mithilfe konfokaler Mikroskopie quantitativ ausgewertet wurden. Besonderes Augenmerk lag dabei auf der Größe und Dynamik der γH2AX-Foci als Indikator für die chromatinabhängige Ausbreitung von DDR-Signalen. Zusätzlich wurden DNA-PK-Inhibitoren eingesetzt, um den Beitrag alt-EJ unter Bedingungen gestörter Chromatinorganisation zu analysieren.

Parallel dazu wurde der Einfluss von Condensinen auf die ATM- und ATR-abhängige Signaltransduktion sowie auf die Aktivierung zellzyklusspezifischer Kontrollpunkte untersucht. Die Analysen unterschieden gezielt zwischen in der S- oder G2-Phase bestrahlten Zellen, um phasenspezifische Effekte auf den G2- und S-Phasen-Kontrollpunkt zu erfassen.

Abschließend wurden die chromosomalen Konsequenzen einer gestörten Chromatinorganisation untersucht. Mithilfe klassischer zytogenetischer Analysen (Soni, Siemann et al. 2014, Soni, Siemann et al. 2015, Soni, Murmann-Konda et al. 2020) wurde die Bildung von Chromosomen- und Chromatidenaberrationen in normalen humanen Fibroblasten sowie in RPE-1-hTERT-Zellen nach Knockdown von CTCF, Cohesin oder Condensinen erfasst. Der Fokus lag hierbei auf der G2-Phase, um die langfristigen Auswirkungen fehlerhafter DSB-Reparatur auf die genomische Stabilität zu bewerten.

Der Ablauf des Vorhabens war durch eine kontinuierliche Auswertung der experimentellen Ergebnisse gekennzeichnet, wodurch die einzelnen Arbeitsschritte flexibel aufeinander abgestimmt und bei Bedarf gezielt vertieft werden konnten. Dieses iterative Vorgehen gewährleistete eine konsistente Bearbeitung aller Fragestellungen und eine integrierte Bewertung der Rolle höhergeordneter Chromatin Organisation in der DNA-Schadensantwort.

4. Wissenschaftliche Ergebnisse des Vorhabens

Zu Beginn des Projekts wurde der Einfluss der Chromatinarchitektur-regulierenden Faktoren Cohesin und CTCF auf die DDR nach ionisierender Strahlung untersucht.

Das siRNA-vermittelte Knockdown von Cohesin und CTCF führte in der normalen humanen Epithelzelllinie RPE-1 zu einer signifikanten Radiosensibilisierung (Abb. 1).

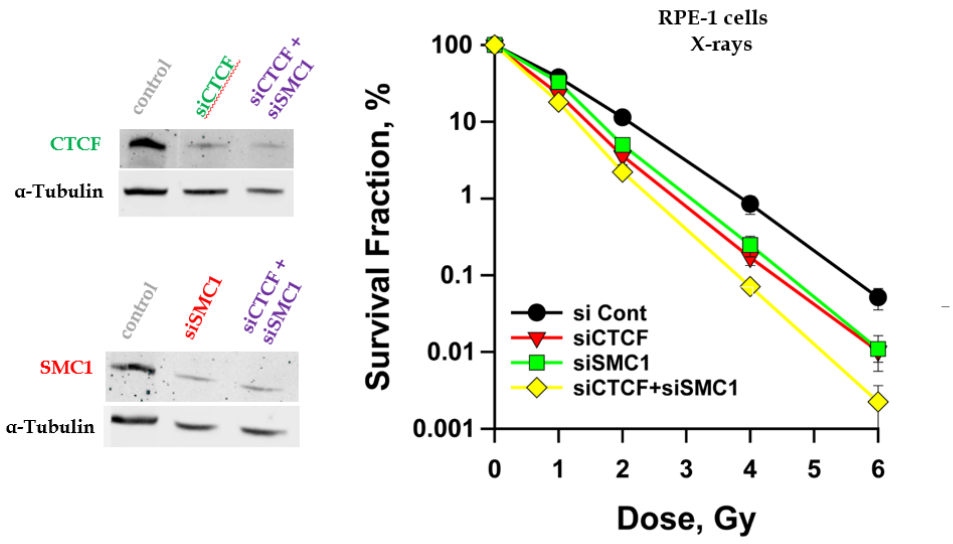

Abbildung 1: Einfluss des Knockdowns von SMC1 und CTCF auf die Radiosensitivierung von RPE-1-Zellen

Auf molekularer Ebene zeigte sich eine deutliche Beeinträchtigung der DDR-Signalkaskade, die mit einer Reduktion der HR einherging. Diese Defekte äußerten sich in einer verminderten DSB-Endresektion (Abb. 2, links) sowie einer reduzierten Rekrutierung zentraler HR-Faktoren,Rad51 (Abb. 2, rechts), was auf eine essentielle Rolle von Cohesin und CTCF bei der effizienten HR-vermittelten Reparatur strahleninduzierter DNA-DSBs hinweist. Diese Ergebnisse etablierten Chromatinorganisation als einen entscheidenden Regulator der HR und der zellulären Strahlenresistenz.

Die zytogenetische Analyse nach Teilchenbestrahlung mit Kohlenstoffionen an der GSI zeigte insbesondere nach Knockdown von CTCF oder Cohesin das Auftreten einzelner massiv geschädigter Chromosomen bei gleichzeitig überwiegend unbeschädigten Chromosomen. Dieses Befundmuster spricht für eine stark lokalisierte, hoch-LET-typische Schadensentstehung und weist darauf hin, dass eine gestörte Chromatinorganisation die Verarbeitung komplexer DNA-Schäden zusätzlich beeinträchtigt. Derzeit werden geeignete Kriterien zur systematischen Interpretation und quantitativen Bewertung dieser Befunde erarbeitet.

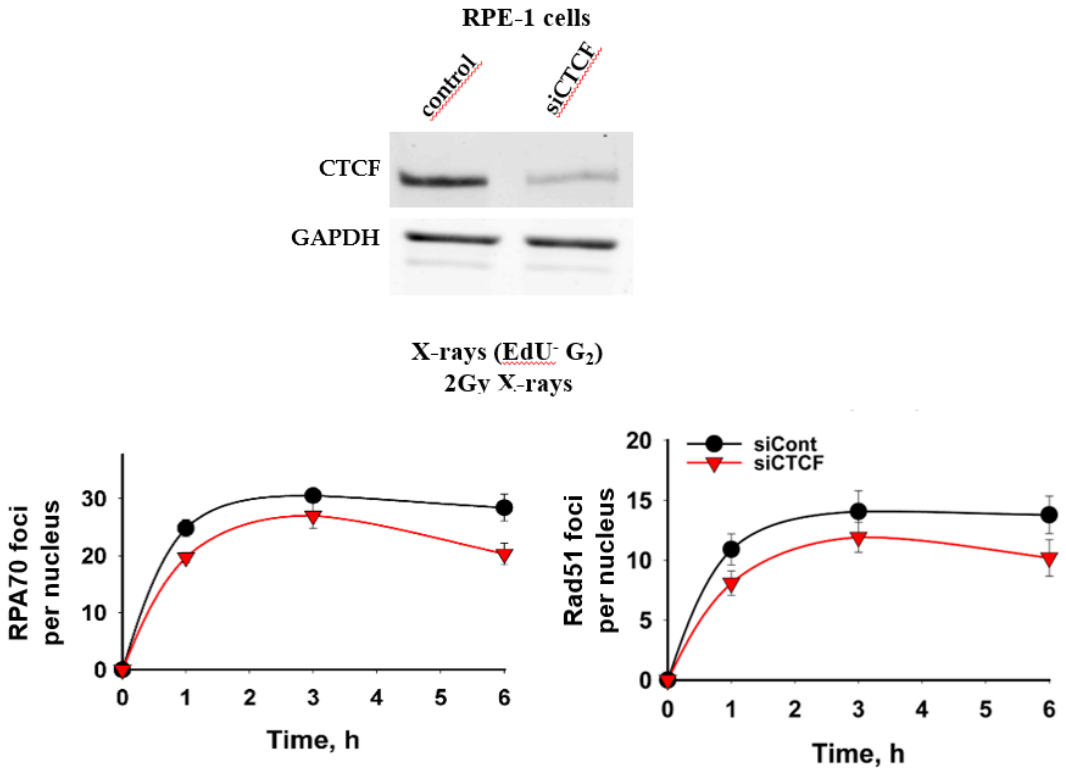

Abbildung 2: Einfluss des Knockdowns von SMC1 und CTCF auf durch ionisierende Strahlung induzierte RPA70- und Rad51-Foci

Aufbauend auf diesen Befunden wurde der Einfluss der durch CAP-H (Condensin I) und CAP-D3 (Condensin II) vermittelten Chromatinorganisation auf die Reparatur von durch ionisierende Strahlung induzierten DSBs untersucht. Ein besonderer Fokus lag auf der Modulation der DSB-Reparaturwege in der Lungenkarzinom-Zelllinie A549 im Vergleich zur normalen humanen Epithelzelllinie RPE-1, um Unterschiede zwischen normalen und malignen Zellen sowie die zellzyklusabhängige Rolle der Condensine in der DNA-Schadensantwort zu charakterisieren.

In Übereinstimmung mit den Ergebnissen zeigte das Knockdown einzelner Condensine (Condensin I oder II) nur geringe Effekte auf die Strahlenempfindlichkeit, während das kombinierte Knockdown von Condensin I und II essenziell für die Radiosensitivität der Zellen war (Siehe Appendix 1, Figure 19 und Figure 20).

Eine detaillierte zellzyklusspezifische Analyse der DNA-Schadensantwort erfolgte mithilfe quantitativer bildbasierter Zytometrie (QIBC) nach EdU-Markierung und Immunfluoreszenzfärbung von γH2AX- und 53BP1-Foci. Dabei zeigte sich, dass die DSB-Reparatur in der G1- und S-Phase durch das Knockdown von Condensin I und II nicht beeinträchtigt ist, wohingegen in G2-Zellen eine ausgeprägte Suppression der

γH2AX- und 53BP1-Foci-Auflösung beobachtet wurde, was auf einen deutlichen Reparaturdefekt in dieser Zellzyklusphase hinweist (Siehe Appendix 1, Figure 22, Figure 23).

In beiden Zellen führte das kombinierte Condensin-Knockdown zu einer deutlichen Beeinträchtigung der Resektion von IR-induzierten DSBs, gemessen anhand von RPA70-Foci in G2-Zellen, wenn auch weniger stark ausgeprägt als in RPE-1-Zellen (Siehe Appendix 1, Figure 30). Parallel dazu war die Rekrutierung von Rad51 stark reduziert, was auf eine ausgeprägte Unterdrückung der HR hindeutet (Siehe Appendix 1, Figure 31).

Die Analyse des G2-Checkpoints zeigte nach Knockdown von Condensin I und II einen vergleichsweisen schwächeren Effekt, wie er auch in RPE-1-Zellen beobachtet wurde. Die kombinierte Hemmung der Kinasen ATM und ATR führte hingegen zu einer nahezu vollständigen Aufhebung des G2-Checkpoints (Siehe Appendix 1, Figure 32).

Zusätzlich wurde der Einfluss von Cohesin und CTCF auf die chromosomale Stabilität untersucht. Nach Knockdown dieser Faktoren wurde in RPE-1-Zellen mittels Premature Chromosome Condensation (PCC) nach Röntgenbestrahlung ein signifikanter Anstieg von Chromatidenbrüchen beobachtet, der auf eine beeinträchtigte Reparatur dieser Chromatidenbrüche im Vergleich zu Kontrollzellen hinweist (Siehe Appendix 1, Figure 34).

Zur weiteren Validierung wurde SMC2, eine gemeinsame Untereinheit von Condensin I und II, untersucht. Die Suppression von SMC2 führte zu deutlichen Veränderungen der Zellzyklusverteilung und zu einer drastisch reduzierten Ausplattierungseffizienz in beiden Zelllinien, was auf eine essenzielle Rolle der Condensine für die Zelllebensfähigkeit hinweist. Aufgrund dieses starken Effekts war eine detaillierte Analyse der Radiosensitivität nach SMC2-Knockdown nicht möglich (Siehe Appendix 1 Figure 21).

Ergänzend wurde geprüft, ob die Hemmung alternativer resektions-abhängiger Reparaturwege (alt-EJ und SSA) zusätzliche Effekte auf die DNA-Schadensantwort zeigt. Die chemische Inhibition von PARP1/2, Polθ und Rad52 führte jedoch zu keiner weiteren Verstärkung der beobachteten Reparaturdefekte, was darauf hindeutet, dass die durch Condensin-Knockdown verursachten Effekte primär die HR betreffen.

Diese Ergebnisse verdeutlichen, dass eine intakte dreidimensionale Chromatinorganisation eine zentrale Voraussetzung für eine effiziente DNA-

Schadensantwort ist. Cohesin und Condensin sind evolutionär konservierte SMC-Komplexe, die mittels ATP-abhängiger Loop-Extrusion die räumliche Architektur des Genoms in höheren Eukaryoten aktiv formen. Cohesin organisiert interphasische Chromatin-Loops und Topologically Associating Domains (TADs) und schafft damit strukturelle Rahmenbedingungen für die koordinierte Rekrutierung und Stabilisierung von DNA-Reparaturfaktoren an Schadensstellen. Die beobachteten Defekte in der DDR-Signalweiterleitung und der HR nach Condensin-Knockdown sprechen dafür, dass gestörte Loop-Extrusion und Domänengrenzen die effiziente Endresektion und den Aufbau von HR-Reparaturplattformen beeinträchtigen.

Insbesondere Condensin I und II treiben die großskalige Chromatinkompaktierung und -reorganisation in der G2-Phase voran, einer Zellzyklusphase, in der homologe Rekombination als dominanter Reparaturweg zur Verfügung steht. Vor diesem Hintergrund ist es naheliegend in der Zukunft zu untersuchen, ob Condensin-vermittelte Chromatinrestrukturierung durch vergleichbare Loop-Extrusionsmechanismen die Zugänglichkeit, Prozessivität und Koordination der resek-tions-abhängigen Reparaturwege, insbesondere der HR, an strahleninduzierten DSBs steuert.

Insgesamt zeigen die Ergebnisse, dass eine intakte dreidimensionale Chromatinorganisation eine zentrale Voraussetzung für die effiziente und fehlerfreie homologe Rekombination bei der Reparatur von DNA-Doppelstrangbrüchen darstellt. Die räumliche Struktur des Genoms beeinflusst dabei nicht nur die initiale Erkennung von DNA-Schäden, sondern auch die nachfolgenden Schritte der Signalweiterleitung, Endverarbeitung und Rekrutierung spezialisierter Reparaturfaktoren. Störungen dieser Architektur führen zu einer funktionellen Entkopplung der DDR-Komponenten und begünstigen ineffiziente oder fehleranfällige Reparaturprozesse.

Cohesin und CTCF übernehmen in diesem Kontext eine Schlüsselrolle, indem sie durch die Organisation von Chromatin-Loops und Domänengrenzen stabile strukturelle Rahmenbedingungen schaffen, die eine koordinierte Assemblierung von Reparaturkomplexen an DSBs ermöglichen. Die beobachteten Defekte in der DSB-Endresektion und der HR nach Depletion dieser Faktoren sprechen dafür, dass eine gestörte Loop-Extrusion und veränderte TAD-Architektur die lokale Chromatinumgebung an Schadensstellen nachhaltig beeinträchtigen und damit die

Etablierung resektions-abhängiger Reparaturplattformen verhindern (Lang, Li et al. 2017, Chiolo, Altmeyer et al. 2025, Marin-Gonzalez, Rybczynski et al. 2025).

Condensine wirken nach ähnlichen mechanistischen Prinzipien, übernehmen jedoch eine funktionell und zeitlich spezialisierte Rolle. Insbesondere in der G2-Phase des Zellzyklus, in der homologe Rekombination als bevorzugter Reparaturweg zur Verfügung steht, ist der durch Condensin I und II vermittelte Chromatinumbau entscheidend für die Prozessivität und Koordination der HR. Die strikt auf die G2-Phase begrenzten Reparaturdefekte nach Condensin-Depletion verdeutlichen, dass die großskalige Reorganisation des Chromatins in dieser Zellzyklusphase eine notwendige Voraussetzung für den effizienten Zugang der HR-Maschinerie zu resektierten DNA-Enden darstellt.

Über ihre gut etablierte mitotische Funktion hinaus sind Condensine auch in Interphasekernen aktiv und tragen zur Genomkompartimentierung sowie zur transkriptionellen Regulation bei (Zhang, Paulson et al. 2016, Wu, Fatkhutdinov et al. 2019, Hoencamp, Dudchenko et al. 2021, Lancaster, Patel et al. 2021). Die im Rahmen dieses Projekts gewonnenen Ergebnisse liefern darüber hinaus starke funktionelle Hinweise darauf, dass Condensine bereits in der Interphase, insbesondere in postreplikativen G2-Zellen, eine zentrale Rolle spielen und aktiv die DNA-Schadensantwort sowie resek-tions-abhängige Reparaturprozesse koordinieren. Damit tragen diese Befunde wesentlich dazu bei, dass bislang vorherrschende Paradigma zu erweitern, wonach Condensine primär auf die Chromosomenkondensation während der Metaphase beschränkt sind. Eine Depletion von Condensinen führt zu einer ausgeprägten Dekondensation des Chromatins (Martin, Murray et al. 2016, Baergen, Jeusset et al. 2019) und unterstreicht ihre zentrale Rolle für die Aufrechterhaltung höherordentlicher Chromatinstrukturen. Neben Condensinen sind Cohesin und das Architekturprotein CTCF entscheidende Regulatoren der Chromatinorganisation. Cohesin vermittelt die Bildung von Chromatin-Loops und TADs, während CTCF als positionsspezifischer Bindungspartner Domänengrenzen definiert. Frühere Arbeiten weisen zudem darauf hin, dass Cohesin und CTCF über ihre strukturelle Funktion hinaus an der Rekrutierung und Stabilisierung von DNA-Reparaturfaktoren beteiligt sind. Condensine übernehmen dabei insbesondere Aufgaben in der großskaligen Chromatinrestrukturierung, wobei ihre funktionelle Relevanz in der Interphase und im Kontext der DNA-Reparatur zunehmend deutlich wird (Zhang, Paulson et al. 2016, Wu,

Fatkhutdinov et al. 2019, Hoencamp, Dudchenko et al. 2021, Lancaster, Patel et al. 2021).

Zusammenfassend liefern die Ergebnisse neue mechanistische Einblicke in die zellzyklusabhängige Regulation der DNA-Doppelstrangbruchreparatur durch Chromatinarchitektur. Sie zeigen, dass Chromatinorganisation nicht lediglich einen passiven strukturellen Rahmen darstellt, sondern aktiv und dynamisch die Wahl und Effizienz von Reparaturwegen steuert. Damit tragen die Daten wesentlich zum Verständnis der molekularen Grundlagen genomischer Stabilität bei und unterstreichen die Bedeutung chromatinorganisierender Faktoren als potenzielle Modulatoren der zellulären Strahlenantwort und der Tumorentstehung.

5. Angaben zum wissenschaftlichen und technischen Stand

Das Vorhaben knüpfte unmittelbar an den etablierten wissenschaftlichen Kenntnisstand zur Rolle der dreidimensionalen Chromatinorganisation in der Regulation der DNA-Schadensantwort an. In den vergangenen Jahren haben zahlreiche Studien gezeigt, dass die räumliche Anordnung des Genoms einen entscheidenden Einfluss auf die Erkennung, Signalweiterleitung und Reparatur von DSBs ausübt. Insbesondere wurde deutlich, dass DNA-Doppelstrangbrüche nicht isoliert, sondern stets im Kontext höhergeordneter, zellzyklusabhängig organisierter Chromatinstrukturen verarbeitet werden. Veränderungen dieser Strukturen beeinflussen nicht nur die räumliche Zugänglichkeit von Schadensstellen, sondern steuern maßgeblich die Reparaturwegwahl sowie die Häufigkeit fehlerhafter Reparaturereignisse. Dabei kommt der postreplikativen Chromatinumgebung eine besondere Bedeutung zu, da die Architektur des Chromatins in G2-Zellen entscheidend bestimmt, ob resek-tions-abhängige Reparaturmechanismen effizient etabliert oder zugunsten potenziell fehleranfälliger Alternativwege eingeschränkt werden.

Vor diesem Hintergrund zielte das Projekt darauf ab, die bislang nur unzureichend verstandene Rolle dieser Chromatin-organisierenden Faktoren in der DDR systematisch zu untersuchen und ihre Bedeutung für die Verarbeitung von DSBs unterschiedlicher Komplexität zu analysieren. Besonderes Augenmerk lag dabei auf der Frage, inwieweit Veränderungen der Chromatinarchitektur die Wahl zwischen verschiedenen DSB-Reparaturwegen, insbesondere HR, cNHEJ und alternativen Endverknüpfungsmechanismen, beeinflussen.

Methodisch basierte das Vorhaben auf einem breiten Spektrum etablierter molekular- und zellbiologischer Verfahren. Die gezielte Modulation der Chromatinorganisation erfolgte mittels siRNA-vermittelter Genunterdrückung einzelner Untereinheiten von Cohesin, Condensin I und II sowie von CTCF. Die Effizienz und Spezifität dieser Knockdowns wurden sowohl auf Protein- als auch auf Funktionsebene validiert. Zur Analyse der DNA-Schadensantwort kamen Immunfluoreszenz-basierte Foci-Analysen zentraler DDR-Marker (u. a. γH2AX, 53BP1, RPA70, Rad51) zum Einsatz, die eine zeitlich und zellzyklusspezifisch aufgelöste Untersuchung der DSB-Erkennung und -Reparatur ermöglichten. Ergänzend wurden Reporter-Assays verwendet, die eine funktionelle Quantifizierung einzelner DSB-Reparaturwege erlauben.

Zur Erfassung chromosomaler Endpunkte und langfristiger Konsequenzen fehlerhafter DSB-Reparatur wurden zytogenetische Methoden wie die PCC eingesetzt. Diese Technik erlaubte eine detaillierte Analyse von Chromosomen- und Chromatidenaberrationen nach Bestrahlung und stellte damit ein wichtiges Bindeglied zwischen molekularen Reparaturdefekten und genomischer Instabilität dar. Ergänzend kamen etablierte Inhibitoren zentraler DDR-Kinasen (ATM, ATR, DNA-PK) zum Einsatz, um Signaltransduktionswege gezielt zu modulieren und funktionell einzuordnen.

Die Planung und Durchführung des Vorhabens stützten sich auf eine umfassende Auswertung der einschlägigen internationalen Fachliteratur sowie auf den kontinuierlichen Zugriff auf wissenschaftliche Publikationsdatenbanken und elektronische Informations- und Dokumentationsdienste. Der enge Bezug zum aktuellen Stand der Forschung gewährleistete eine fundierte experimentelle Ausrichtung des Projekts und ermöglichte eine präzise Einordnung der erzielten Ergebnisse in den bestehenden wissenschaftlichen Kontext.

6. Die wichtigsten Positionen des zahlenmäßigen Nachweises

Für das Forschungsvorhaben wurden vom BMBF Finanzmittel in Höhe von 913.833,00 Euro bereitgestellt, die sowohl Personalkosten als auch Sach- und Reisemittel abdecken.

Personal

Der überwiegende Teil der Fördermittel wurde für die Finanzierung von Personal eingesetzt. Im Rahmen der Förderung konnten zwei Postdoktorandenstellen bereitgestellt werden. Einsparungen durch den Zeitpunkt der vorzeitigen Stellenwechsel von Frau Dr. Lisa-Marie Krieger ermöglichten eine flexible Mittelverwendung zugunsten der Postdoktorandenstelle von Herrn Dr. Aashish Soni. Dadurch konnte eine kostenneutrale Verlängerung des Projekts bis Juni 2025 realisiert werden, wodurch pandemiebedingte Verzögerungen erfolgreich kompensiert werden konnten.

Sach- und Reisemittel

Die bereitgestellten Sachmittel wurden vorrangig für laborbezogene Verbrauchsmaterialien eingesetzt, die für die Durchführung der Experimente erforderlich waren. Dazu zählen insbesondere Zellkulturmaterialien (Medien, Zusätze, Petrischalen, Flaschen), Kits und Einwegmaterialien für EdU-Assays, Inhibitoren, Antikörper, DNA-Farbstoffe und weitere Chemikalien.

Die Reisemittel dienten der Teilnahme der Projektmitarbeiter an nationalen und internationalen Konferenzen, um die Forschungsergebnisse zu präsentieren. Zusätzliche Tagungsteilnahmen wurden aus der Grundfinanzierung der Arbeitsgruppe getragen.

7. Notwendigkeit und Angemessenheit der geleisteten Arbeit

Die im Rahmen des Vorhabens durchgeführten Arbeiten waren zur Erreichung der bewilligten Projektziele notwendig und sachlich begründet. Ziel des Projekts war es, die funktionelle Bedeutung der dreidimensionalen Chromatinorganisation für die DNA-Schadensantwort nach ionisierender Strahlung mechanistisch zu analysieren. Diese Fragestellung erfordert experimentelle Ansätze, die über Standarduntersuchungen hinausgehen, insbesondere zellzyklus-spezifische Analysen sowie den Vergleich unterschiedlicher Strahlenqualitäten.

Der gewählte experimentelle Umfang war erforderlich, um belastbare Aussagen zur Rolle von Condensinen in der Regulation von DNA-Doppelstrangbruch-Reparaturwegen treffen zu können. Die detaillierte Auflösung von Reparaturprozessen in Abhängigkeit vom Zellzyklus sowie die Analyse resektions-abhängiger Signal- und Reparaturwege machten einen erhöhten personellen und methodischen Aufwand

notwendig, der jedoch in einem angemessenen Verhältnis zum wissenschaftlichen Erkenntnisgewinn stand.

Im Projektverlauf zeigte sich zudem, dass einzelne Untersuchungen arbeits- und zeitintensiver waren als ursprünglich angenommen. Entsprechende inhaltliche Schwerpunktsetzungen und Anpassungen dienten einer effizienten Nutzung der bewilligten Mittel und stellten sicher, dass die zentralen wissenschaftlichen Fragestellungen mit der erforderlichen Tiefe bearbeitet werden konnten. Die geleisteten Arbeiten waren daher insgesamt zweckmäßig, wirtschaftlich und angemessen und bilden eine belastbare Grundlage für die erzielten Ergebnisse sowie für weiterführende Forschungsaktivitäten.

8. Voraussichtlicher Nutzen, insbesondere Verwertbarkeit des Ergebnisses im Sinne des fortgeschriebenen Verwertungsplans

Die Arbeiten zeigen, dass Condensine zentrale Regulatoren der DNA-Doppelstrangbruch-Reparatur in repliziertem Chromatin sind. Insbesondere in der G2-Phase führt die Depletion von Condensinen zu ausgeprägten Reparaturdefekten und signifikanter Radiosensitivierung, während die G1- und S-Phase weitgehend unbeeinträchtigt bleibt. Diese Ergebnisse verdeutlichen die entscheidende Rolle von Condensinen für die Organisation der Chromatinumgebung und die effiziente Etablierung resektions-abhängiger Reparaturplattformen nach Strahlung.

Die gewonnenen Erkenntnisse sind direkt verwertbar, da spezifische Inhibitoren gegen Condensin-Komponenten zukünftig eine gezielte Strahlensensitivierung von Tumorzellen ermöglichen könnten, ohne Normalgewebe zu schädigen. Dies bietet sowohl Chancen für die Optimierung strahlentherapeutischer Konzepte als auch für die präklinische Entwicklung neuer Therapiestrategien.

Darüber hinaus liefert das Projekt wichtige Grundlagenkenntnisse zur Chromatinorganisation und zur DNA-Reparatur, die sowohl für die Strahlenbiologie als auch für strahlenschutzrelevante Fragestellungen relevant sind. Gleichzeitig stärkt das Vorhaben den Kompetenzaufbau im Bereich der Strahlenbiologie und bildet eine solide Basis für zukünftige Forschungsprojekte. Im Sinne des fortgeschriebenen Verwertungsplans sind für die nähere Zukunft weiterführende, mechanistisch ausgerichtete Experimente mit gezieltem Knockdown von CTCF und Cohesin vorgesehen. Der Schwerpunkt liegt dabei auf der systematischen Analyse zellzyklusabhängiger Effekte auf die Reparaturwegwahl von DNA-

Doppelstrangbrüchen, insbesondere im Hinblick auf c-NHEJ, HR, alt-EJ und SSA nach Bestrahlung mit unterschiedlichen Strahlenqualitäten. Die so gewonnenen Daten sollen die Grundlage für weiterführende Publikationen sowie für die Konzeption von Anschlussprojekten bilden, die die klinische Relevanz der identifizierten Chromatin-abhängigen Reparaturmechanismen weiter prüfen und perspektivisch für strahlentherapeutische Anwendungen nutzbar machen.

9. Während der Durchführung des Vorhabens dem ZE bekannt gewordener Fortschritt auf dem Gebiet des Vorhabens bei anderen Stellen

Während der Projektlaufzeit wurden bedeutende mechanistische Fortschritte zu Chromatin-Architekturfaktoren in der DNA-Schadensantwort veröffentlicht, die die Aktualität und Anschlussfähigkeit der eigenen Ergebnisse bestätigen. So zeigt eine Studie, dass CTCF die Richtung und Dynamik der Cohesin-vermittelten Schleifenextrusion steuert, was die Bildung topologisch assoziierter Domänen (TADs) beeinflusst und direkte Konsequenzen für die DNA-Schadensantwort hat (Davidson, Barth et al. 2023). Parallel wurde gezeigt, dass Cohesin zwei getrennte Rollen in der Reparatur von DNA-Doppelstrangbrüche übernimmt: einerseits als architektonisches Strukturprotein, das die Chromatinstruktur stabilisiert, und andererseits als ein durch ATM-vermittelte Phosphorylierung aktivierter Faktor, der die Effizienz der Reparaturprozesse steigert (Fedkenheuer, Shang et al. 2025). Im Bereich der Condensine wurde gezeigt, dass Condensin II mit der BLM-Helicase interagiert und so die Replikationsdynamik sowie Reparaturprozesse unterstützt (Rodemoyer, Kariyawasam et al. 2025). Darüber hinaus gibt es derzeit keine weitere Publikation, die in die gleiche Richtung wie die vorliegende Arbeit geht, sodass diese Ergebnisse bislang einzigartig sind.

Insgesamt zeigen diese Originalstudien, dass die funktionelle Verbindung zwischen Chromatinarchitektur und DNA-Reparatur ein aktives Feld ist, und bestätigen die wissenschaftliche Relevanz und Anschlussfähigkeit der eigenen Projektergebnisse.

10. Zusammenarbeit mit anderen Stellen

Während der Laufzeit des Projekts wurden in Zusammenarbeit mit externen Partnern Experimente zur Analyse der DNA-Schadensantwort und der chromosomalen Stabilität nach Exposition gegenüber hoch-LET-Kohlenstoff-Ionen an der UNILAC der GSI Helmholtzzentrum für Schwerionenforschung (Darmstadt) durchgeführt. Die zu untersuchenden Zelllinien wurden am Universitätsklinikum präpariert und funktionell

modifiziert (siRNA-vermitteltes Knockdown von CTCF, Cohesin und Condensinen), während die Bestrahlungen mit Kohlenstoffionen sowie die anschließende zytogenetische Analyse in enger Zusammenarbeit mit den Partnern an der GSI realisiert wurden. Diese Experimente ermöglichten den Vergleich der DNA-Schadensantwort und der Chromosomenaberrationsbildung nach niedrig-LET-Röntgenstrahlung und hoch-LET-Teilchenstrahlung unter definierten Bedingungen der Chromatinorganisation.

Der wissenschaftliche Austausch und die Diskussion der Projektergebnisse erfolgten kontinuierlich auf nationalen und internationalen Fachtreffen, darunter die Jahrestagungen der Deutschen Gesellschaft für Biologische Strahlenforschung (DeGBS), der Radiation Research Society (RRS), der European Radiation Research Society (ERRS) sowie der Deutschen Gesellschaft für Radioonkologie (DEGRO). Diese Veranstaltungen dienten der kritischen Einordnung der eigenen Ergebnisse in den aktuellen Stand der Forschung, dem Austausch methodischer Erfahrungen und der Initiierung neuer wissenschaftlicher Kooperationen.

Darüber hinaus bestand während der gesamten Projektlaufzeit eine enge und regelmäßige Zusammenarbeit zwischen den beteiligten Forschergruppen. Diese erfolgte in Form von projektbezogenen Treffen, bei denen die jeweils neuesten experimentellen Ergebnisse in Vorträgen vorgestellt, methodische Aspekte diskutiert und das weitere Vorgehen koordiniert wurden. Der kontinuierliche wissenschaftliche Austausch trug wesentlich zur Qualitätssicherung der Experimente, zur Interpretation der Ergebnisse sowie zur erfolgreichen Umsetzung des interdisziplinären Projektansatzes bei.

11. Erfolgte und geplante Veröffentlichungen des Ergebnisses nach Nr. 5

11.1 Publikationen (peer-review)

1. **Liu M.,** Wei Y., **Weber L.M.**, Mladenov E., Lin X., Mladenova V., Shafaat R.O., Pantelias G.E., Gkika E., Stuschke M., **Soni, A.**§, and **Iliakis G**§. (2026). "Condensins regulate resection-dependent DNA double-strand break repair pathways in replicated chromatin." Nucleic Acids Research. §Corresponding Authors
2. Mladenov, E.*, Pressler, M.*, Mladenova, V., **Soni, A.**, Li, F., Heinzelmann, F., Esser, J.N., Hessenow, R., Gkika, E., Jendrossek, V., Timmermann, B., Stuschke, M., and **Iliakis, G.** (2026). Evidence for Quasi-High-LET Biological

Effects in Clinical Proton Beams That Suppress c-NHEJ and Enhance HR and Alt-EJ. Cells, 15. *Contributed equally

3. Lin, X.§, Qiu,Y, **Soni A.**, Stuschke,M. and **Iliakis G.**§ 2025. 'Reversing regulatory safeguards: Targeting the ATR pathway to overcome PARP inhibitor resistance', Mol Ther Oncol, 33: 200934. §Corresponding Authors
4. **Soni, A.***, Beisser D.*, Mladenov E. *, Höller M., Wohlers I., Nikolov V., Magin S., Mussfeldt T., Klein-Hitpass L., Cornforth M. N., Loucas B. D., Rahmann S., and **Iliakis G.** (2025). "NGS Detects Extensive Genomic Alterations in Survivors of Irradiated Normal Human Fibroblast Cells." Radiat Res. 203:37-52 *Contributed equally
5. Lin, X., **Soni, A.** §, R. Hessenow, Y. Sun, E. Mladenov, M. Guberina, M. Stuschke and **G. Iliakis**§ (2024). "Talazoparib enhances resection at DSBs and renders HR-proficient cancer cells susceptible to Poltheta inhibition." Radiother Oncol 200: 110475. §Corresponding Authors
6. Luo, D., Mladenov, E., **Soni, A.**, Stuschke, M., and **Iliakis, G.** (2023). The p38/MK2 Pathway Functions as Chk1-Backup Downstream of ATM/ATR in G2-Checkpoint Activation in Cells Exposed to Ionizing Radiation. Cells (Basel), May 14;12 (10):1387.
7. Li, F., Mladenov, E., Sun, Y., **Soni, A.**, Stuschke, M., Timmermann, B., and **Iliakis, G.** (2023) Low CDK Activity and Enhanced Degradation by APC/CCDH1 Abolishes CtIP Activity and Alt-EJ in Quiescent Cells. Cells (Basel), Jun 1;12 (11):1530.
8. **Soni, A.,** Lin, X., Mladenov, E., Mladenova, V., Stuschke, M., and **Iliakis, G.** (2022) BMN673 Is a PARP Inhibitor with Unique Radiosensitizing Properties: Mechanisms and Potential in Radiation Therapy. Cancers (Basel), Nov 16;14(22):5619.
9. Pei, X., Mladenov, E., **Soni, A.,** Li, F., Stuschke, M., and **Iliakis, G.** (2022) PTEN Loss Enhances Error-Prone DSB Processing and Tumor Cell Radiosensitivity by Suppressing RAD51 Expression and Homologous Recombination. Int J Mol Sci, Oct 25;23(21).
10. **Soni, A.,** Duan, X., Stuschke, M., and **Iliakis, G.** (2022) ATR Contributes More Than ATM in Intra-S-Phase Checkpoint Activation after IR, and DNA-PKcs Facilitates Recovery: Evidence for Modular Integration of ATM/ATR/DNA-PKcs Functions. Int J Mol Sci, Jul 6;23(14):7506.

11. Xiao, H., Li, F., Mladenov, E., **Soni, A.**, Mladenova, V., Pan, B., Dueva, R., Stuschke, M., Timmermann, B., and **Iliakis, G.** (2022). Increased Resection at DSBs in G(2)-Phase Is a Unique Phenotype Associated with DNA-PKcs Defects That Is Not Shared by Other Factors of c-NHEJ. Cells, Jul2;11(13):2099.
12. Hassiepen C.*, **Soni A.***, Rudolf I., Boron V., Oeck S., **Iliakis G.**, Schramm A. (2021), "NTRK1/TrkA activation overrides the G2/M-checkpoint upon irradiation". Cancers (Basel), 2021 Nov 30;13 (23):6023. *Contributed equally.
13. **Krieger, L.M.**, Mladenov E., **Soni A.,** Demond M., Stuschke M., and **Iliakis G.** (2021). "Disruption of chromatin dynamics by hypotonic stress suppresses HR and shifts DSB processing to error-prone SSA." International Journal of Molecular Sciences, 2021 Oct 11;22(20):10957.
14. Murmann-Konda T., **Soni, A.**§, Stuschke M., and **Iliakis G**§. (2021). "Analysis of chromatid break repair detects a homologous recombination to no-homologous end-joining switch with increasing load of DNA double-strand breaks." Mutation Research/Genetic Toxicology and Environmental Mutagenesis, 793, 2-8. 2021 Jul; 867: 503372 §Corresponding Authors

11.2 Doktorarbeit

Ein Teil der hier berichteten Ergebnisse wurde im Rahmen einer M.D.-Doktorarbeit umfassend dargestellt. In dieser Arbeit werden insbesondere die Ergebnisse zur Rolle der Condensine in der DNA-Schadensantwort sowie deren Einfluss auf die Wahl der DNA-Doppelstrangbruch-Reparaturwege hervorgehoben. Zusätzlich befindet sich eine Publikation mit den Ergebnissen dieses Projekts derzeit in der Publikationsphase (siehe 6.2). Die M.D.-Doktorarbeit von Liu M. ist diesem Bericht als Appendix 1 beigefügt.

Appendix 1:

Liu, M. Promotion zum Dr. med.: ``Effects of condensins suppression on DSB-induced signaling and the choice of the DSB repair pathway. ``

12. Zitierte Literatur

Abe, S., K. Nagasaka, Y. Hirayama, H. Kozuka-Hata, M. Oyama, Y. Aoyagi, C. Obuse and T. Hirota (2011). "The initial phase of chromosome condensation requires Cdk1-mediated phosphorylation of the CAP-D3 subunit of condensin II." Genes & Development **25**(8): 863-874.

Baergen, A. K., L. M. Jeusset, Z. Lichtensztejn and K. J. McManus (2019). "Diminished Condensin Gene Expression Drives Chromosome Instability That May Contribute to Colorectal Cancer Pathogenesis." Cancers (Basel) **11**(8).

Bauerschmidt, C., C. Arrichiello, S. Burdak-Rothkamm, M. Woodcock, M. A. Hill, D. L. Stevens and K. Rothkamm (2010). "Cohesin promotes the repair of ionizing radiation-induced DNA double-strand breaks in replicated chromatin." Nucleic Acids Research **38**(2): 477-487.

Chiolo, I., M. Altmeyer, G. Legube and K. Mekhail (2025). "Nuclear and genome dynamics underlying DNA double-strand break repair." Nature Reviews Molecular Cell Biology **26**(7): 538-557.

Davidson, I. F., R. Barth, M. Zaczek, J. van der Torre, W. Tang, K. Nagasaka, R. Janissen, J. Kerssemakers, G. Wutz, C. Dekker and J. M. Peters (2023). "CTCF is a DNA-tension-dependent barrier to cohesin-mediated loop extrusion." Nature **616**(7958): 822-827.

Fedkenheuer, M., Y. Shang, S. Jung, K. Fedkenheuer, S. Park, D. Mazza, R. Sebastian, H. Nagashima, D. Zong, H. Tan, S. K. Jaiswal, H. Fu, A. Cruz, S. V. Vartak, J. Wisniewski, V. Sartorelli, J. J. O'Shea, L. Elnitski, A. Nussenzweig, M. I. Aladjem, F.-L. Meng and R. Casellas (2025). "A dual role of Cohesin in DNA DSB repair." Nature Communications **16**(1): 843.

Gerlich, D., B. Koch, F. Dupeux, J. M. Peters and J. Ellenberg (2006). "Live-cell imaging reveals a stable cohesin-chromatin interaction after but not before DNA replication." Curr Biol **16**(15): 1571-1578.

Gibcus, J. H., K. Samejima, A. Goloborodko, I. Samejima, N. Naumova, J. Nuebler, M. T. Kanemaki, L. Xie, J. R. Paulson, W. C. Earnshaw, L. A. Mirny and J. Dekker (2018). "A pathway for mitotic chromosome formation." Science **359**(6376).

Goloborodko, A., M. V. Imakaev, J. F. Marko and L. Mirny (2016). "Compaction and segregation of sister chromatids via active loop extrusion." Elife **5**.

Gunn, A., N. Bennardo, A. Cheng and J. M. Stark (2011). "Correct End Use during End Joining of Multiple Chromosomal Double Strand Breaks Is Influenced by Repair Protein RAD50, DNA-dependent Protein Kinase DNA-PKcs, and Transcription Context." Journal of Biological Chemistry **286**(49): 42470-42482.

Hirano, T. (2012). "Condensins: universal organizers of chromosomes with diverse functions." Genes & Development **26**(15): 1659-1678.

Hirota, T., D. Gerlich, B. Koch, J. Ellenberg and J. M. Peters (2004). "Distinct functions of condensin I and II in mitotic chromosome assembly." J Cell Sci **117**(Pt 26): 6435-6445.

Hoencamp, C., O. Dudchenko, A. M. O. Elbatsh, S. Brahmachari, J. A. Raaijmakers, T. van Schaik, Á. Sedeño Cacciatore, V. G. Contessoto, R. G. H. P. van Heesbeen, B. van den Broek, A. N. Mhaskar, H. Teunissen, B. G. St Hilaire, D. Weisz, A. D. Omer, M. Pham, Z. Colaric, Z. Yang, S. S. P. Rao, N. Mitra, C. Lui, W. Yao, R. Khan, L. L. Moroz, A. Kohn, J. St. Leger, A. Mena, K. Holcroft, M. C. Gambetta, F. Lim, E. Farley, N. Stein, A. Haddad, D. Chauss, A. S. Mutlu, M. C. Wang, N. D. Young, E. Hildebrandt, H. H. Cheng, C. J. Knight, T. L. U. Burnham, K. A. Hovel, A. J. Beel, P.-J. Mattei, R. D. Kornberg, W. C. Warren, G. Cary, J. L. Gómez-Skarmeta, V. Hinman, K. Lindblad-Toh, F. Di Palma, K. Maeshima, A. S. Multani, S. Pathak, L. Nel-Themaat, R. R. Behringer, P. Kaur, R. H. Medema, B. van Steensel, E. de Wit, J. N. Onuchic, M. Di Pierro, E.

Lieberman Aiden and B. D. Rowland (2021). "3D genomics across the tree of life reveals condensin II as a determinant of architecture type." Science **372**(6545): 984-989.
Kong, M., E. E. Cutts, D. Pan, F. Beuron, T. Kaliyappan, C. Xue, E. P. Morris, A. Musacchio, A. Vannini and E. C. Greene (2020). "Human Condensin I and II Drive Extensive ATP-Dependent Compaction of Nucleosome-Bound DNA." Molecular Cell **79**(1): 99-114.e119.
Krieger, L. M., E. Mladenov, A. Soni, M. Demond, M. Stuschke and G. Iliakis (2021). "Disruption of Chromatin Dynamics by Hypotonic Stress Suppresses HR and Shifts DSB Processing to Error-Prone SSA." Int J Mol Sci **22**(20).
Lancaster, L., H. Patel, G. Kelly and F. Uhlmann (2021). "A role for condensin in mediating transcriptional adaptation to environmental stimuli." Life Sci Alliance **4**(7).
Lang, F., X. Li, W. Zheng, Z. Li, D. Lu, G. Chen, D. Gong, L. Yang, J. Fu, P. Shi and J. Zhou (2017). "CTCF prevents genomic instability by promoting homologous recombination-directed DNA double-strand break repair." Proc Natl Acad Sci U S A **114**(41): 10912-10917.
Maeshima, K. and U. K. Laemmli (2003). "A two-step scaffolding model for mitotic chromosome assembly." Dev Cell **4**(4): 467-480.
Marin-Gonzalez, A., A. T. Rybczynski, N. M. Nilavar, D. Nguyen, A. G. Li, V. Karwacki-Neisius, R. S. Zou, F. J. Avilés-Vázquez, M. T. Kanemaki, R. Scully and T. Ha (2025). "Cohesin drives chromatin scanning during the RAD51-mediated homology search." Science **390**(6777): eadw1928.
Martin, C. A., J. E. Murray, P. Carroll, A. Leitch, K. J. Mackenzie, M. Halachev, A. E. Fetit, C. Keith, L. S. Bicknell, A. Fluteau, P. Gautier, E. A. Hall, S. Joss, G. Soares, J. Silva, M. B. Bober, A. Duker, C. A. Wise, A. J. Quigley, S. R. Phadke, A. J. Wood, P. Vagnarelli and A. P. Jackson (2016). "Mutations in genes encoding condensin complex proteins cause microcephaly through decatenation failure at mitosis." Genes Dev **30**(19): 2158-2172.
Nasmyth, K. (2001). "Disseminating the genome: joining, resolving, and separating sister chromatids during mitosis and meiosis." Annu Rev Genet **35**: 673-745.
Rodemoyer, B., G. Kariyawasam, V. Subramanian and K. Schmidt (2025). "Condensin II interacts with BLM helicase in S phase to maintain genome stability." Commun Biol **8**(1): 492.
Schwarzer, W., N. Abdennur, A. Goloborodko, A. Pekowska, G. Fudenberg, Y. Loe-Mie, N. A. Fonseca, W. Huber, C. H. Haering, L. Mirny and F. Spitz (2017). "Two independent modes of chromatin organization revealed by cohesin removal." Nature **551**: 51.
Soni, A., T. Murmann-Konda, M. Siemann-Loekes, G. E. Pantelias and G. Iliakis (2020). "Chromosome breaks generated by low doses of ionizing radiation in G2-phase are processed exclusively by gene conversion." DNA Repair (Amst) **89**: 102828.
Soni, A., M. Siemann, M. Grabos, T. Murmann, G. E. Pantelias and G. Iliakis (2014). "Requirement for Parp-1 and DNA ligases 1 or 3 but not of Xrcc1 in chromosomal translocation formation by backup end joining." Nucleic Acids Research **42**(10): 6380-6392.
Soni, A., M. Siemann, G. E. Pantelias and G. Iliakis (2015). "Marked cell cycle-dependent contribution of alternative end joining to formation of chromosome translocations by stochastically induced DNA double strand breaks in human cells." Mutation Research **793**: 2-8.
Walther, N., M. J. Hossain, A. Z. Politi, B. Koch, M. Kueblbeck, Ø. Ødegård-Fougner, M. Lampe and J. Ellenberg (2018). "A quantitative map of human Condensins provides

new insights into mitotic chromosome architecture." The Journal of Cell Biology **217**(7): 2309-2328.
Wood, J. L., Y. Liang, K. Li and J. Chen (2008). "Microcephalin/MCPH1 Associates with the Condensin II Complex to Function in Homologous Recombination Repair." Journal of Biological Chemistry **283**(43): 29586-29592.
Wu, S., N. Fatkhutdinov, L. Rosin, J. M. Luppino, O. Iwasaki, H. Tanizawa, H. Y. Tang, A. V. Kossenkov, A. Gardini, K. I. Noma, D. W. Speicher, E. F. Joyce and R. Zhang (2019). "ARID1A spatially partitions interphase chromosomes." Sci Adv **5**(5): eaaw5294.
Wutz, G., C. Várnai, K. Nagasaka, D. A. Cisneros, R. R. Stocsits, W. Tang, S. Schoenfelder, G. Jessberger, M. Muhar, M. J. Hossain, N. Walther, B. Koch, M. Kueblbeck, J. Ellenberg, J. Zuber, P. Fraser and J. M. Peters (2017). "Topologically associating domains and chromatin loops depend on cohesin and are regulated by CTCF, WAPL, and PDS5 proteins." The EMBO Journal **36**(24): 3573.
Zhang, T., J. R. Paulson, M. Bakhrebah, J. H. Kim, C. Nowell, P. Kalitsis and D. F. Hudson (2016). "Condensin I and II behaviour in interphase nuclei and cells undergoing premature chromosome condensation." Chromosome Res **24**(2): 243-269.

Medizinische Fakultät

der

Universität Duisburg-Essen

Klinik und Poliklinik für Strahlentherapie

Bereich für Experimentelle Strahlenbiologie

Effects of condensins suppression on DSB-induced signaling and the choice of the DSB repair pathway

Inaugural-Dissertation

zur

Erlangung des Doktorgrades der Medizin

durch die Medizinische Fakultät

der Universität Duisburg-Essen

Vorgelegt von

Mei Liu

aus Sichuan, P.R. China

October 2024

Dekan:

1. Gutachter:

2. Gutachter:

Tag der mündlichen Prüfung:

1. Introduction

1.1 Radiation and DNA damages

Radiation constitutes energy in the form of electromagnetic waves or moving subatomic particles. It can be divided into natural radiation and human-made radiation. Natural radiation sources include natural radionuclides from the soil, water, air, and cosmic rays. Humans are exposed to various forms of radiation daily, which can come from the air, food, water, and even naturally occurring radioactive substances in the body. The primary source of human ionizing radiation (IR) exposure is naturally occurring IR.

Human-made radiation refers to exposures caused by human activities, primarily medical exposures, which accounts for 98 percent of such exposure. Depending on how radiation affects matter, it can be classified as either ionizing or non-ionizing. Non-ionizing radiation includes visible light, heat, radar, microwaves, and radio waves. This type of radiation does not carry enough energy to ionize atoms or molecules, but deposits energy in materials as it passes through them.

On the other hand, ionizing radiation, such as X-rays, gamma rays, and protons, has higher energy than non-ionizing radiation. It is capable of breaking molecular bonds and displacing or removing electrons from atoms as it passes through the material. This electron displacement results in the formation of ions and can cause changes in the living cells of plants, animals, and humans. Ionizing radiation can pose serious health hazards, including burns, radiation sickness, various types of cancer, and genetic damage. Therefore, the use of ionizing radiation requires elaborate radiological protection measures.

In medical settings, ionizing radiation is commonly generated by X-ray machines, radiopharmaceuticals, and other medical devices for diagnosis and radiation therapy. As DNA is the principal target for the biological effects of radiation, including cell killing, carcinogenesis, and mutation, the effects of radiation are often studied by inducing DNA damage. X-rays and gamma rays are frequently used by researchers to induce random DNA damages. In this thesis, we utilized X-rays to investigate DNA double-strand break (DSB) repair and DSB-induced signaling. The associated processes of X-ray-induced DSBs can be accurately controlled in terms of exposure time and dose administration, ensuring a linear increase in generated lesions per unit of radiation dose.

The effects of ionizing radiation are caused by the absorption of its kinetic or electromagnetic energy. For low-energy photons such as X-rays and gamma rays, the primary mechanism of energy deposition in matter is the photoelectric process. High-energy photons, on the other hand, primarily interact with electrons in the valence shell of atoms through the Compton process, transferring their energy to the electron and ejecting it from its atomic shell (Hall and Giaccia 2006).

Different types of particle radiation have different ionization patterns along their particle tracks, which are characterized by the linear energy transfer (LET) parameter, measured in energy (keV) deposited in irradiated matter per unit length (µm). X-rays are electromagnetic waves and are considered low LET radiation, as they cause sparsely ionizing events (Allen et al. 2011). DSBs induced by X-rays and gamma rays often exhibit a 3'-phosphoglycolate and a 5'-OH at the DNA ends. In contrast, high-LET radiation, such as neutrons and alpha particles, produce ionization events in close proximity to each other along their tracks, resulting in direct DSBs through the generation of clustered lesions. These direct DSBs are often accompanied by other types of lesions, such as base damage or loss, near the DSB site(Figure 1) (Schipler and Iliakis 2013).

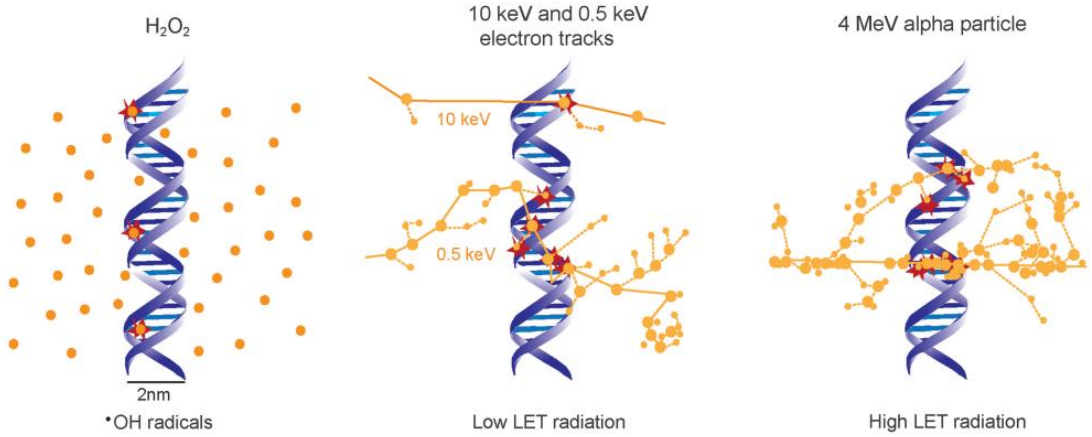

Figure 1: The distribution of events that induce DNA damage varies between exposure to H_2O_2 and low or high LET radiation. The distribution of DNA damage induced by OH radicals from H_2O_2 is rather evenly distributed in space, as the producing radicals are evenly distributed in space. Ionization events in the case of IR localize along the particle tracks (Large dots represent ionization events, while small dots indicate excitations along the tracks) (Schipler and Iliakis 2013).

There is a type of double-stranded breaks (DSBs) that are generated by restriction endonucleases (RE)(Bryant and Johnston 1993). By binding as a homodimer to specific

DNA sequences and disrupting the phosphodiester bonds on both strands, this family of proteins can generate either blunt or staggered DNA ends. REs are often utilized as model reagents to create DSBs at particular sites of a DNA molecule and to study the cellular responses associated with this damage. The use of the rare cutting homing endonuclease, I-SceI, has become increasingly popular due to its unique properties (Jasin 1996; Mladenova, Mladenov, and Iliakis 2016). One of the benefits of this method is that DSBs can be generated at precise locations within the genome, enabling researchers to analyze specific repair pathways through the use of appropriately designed reporters (Rouet, Smih, and Jasin 1994).

1.2 DNA damage response （DDR）

Our body's cells are constantly exposed to sources that can damage their DNA, both from within the cell (endogenous) and outside the cell (exogenous). If this DNA damage is left unrepaired, it can perpetuate errors through subsequent cell divisions and lead to genome instability (Tiwari and Wilson 2019). Studies suggest that approximately 10^5 DNA lesions occur spontaneously each day in the mammalian genome (Patel et al. 2020). To ensure the faithful replication and transmission of genetic information to future generations, mammalian cells have evolved a highly conserved and sophisticated DDR system to identify and repair damaged DNA (Hoeijmakers 2009).

1.2.1 DNA damage signaling

DDR is a complex system of signaling pathways required for preserving and accurately transmitting genetic information through cell generations. It coordinates DNA damage repair with checkpoint activation and facilitates in this way the removal of DNA lesions. DDR responses alert the cell to the presence of DSBs and set the stage for DNA lesion processing, adaptation, or programmed cell death. Incorrectly repaired DNA lesions can result in mutations, while unrepaired damage can lead to cellular apoptosis or senescence (Ciccia and Elledge 2010). Dysregulation of DDR and the encompassing repair systems can cause human disorders associated with developmental, immunological, and neurological disorders, accelerated aging, and developmental abnormalities, and is a major driver of cancer (Ribezzo, Shiloh, and Schumacher 2016; Nastasi, Mannarino, and D'Incalci 2020).

In response to unrepaired DNA damage, signaling cascades initiate, which require the coordinated actions of various proteins categorized as DNA damage sensors, transducers, mediators, and effectors (Polo and Jackson 2011)(Figure 2). DNA damage sensors detect structural changes or DSBs in the DNA and initiate the signaling response. DNA sensor proteins recruit apical kinases, such as ataxia-telangiectasia mutated (ATM) (via the MRN complex) and ataxia-telangiectasia and Rad3-related (ATR) (via RPA and the 9-1-1 complex) bound by ATR-interacting protein (ATRIP). DNA sensor proteins include the Mre11-Rad50-Nbs1 (MRN) complex (Yu et al. 2012), Poly (ADP-ribose) polymerase 1 (PARP-1), and the Ku heterodimer.

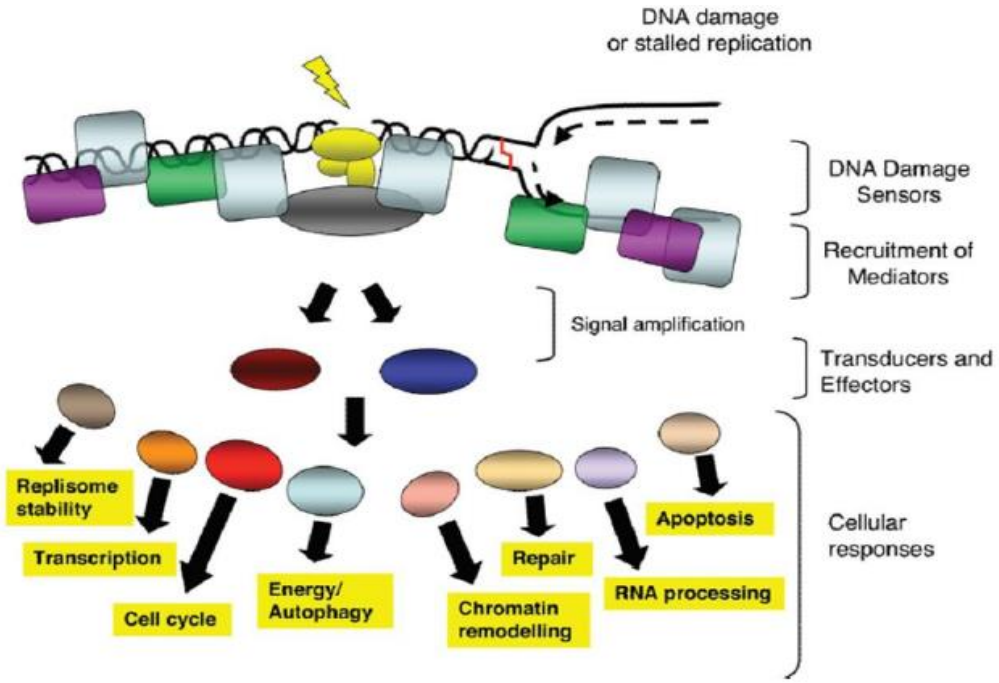

Figure 2: Schematic outline of the DNA damage response (DDR). The presence of a lesion in the DNA can lead to stalled replication forks, which are recognized by a variety of DNA damage sensors. The same holds for directly induced DNA DSBs. These sensors can recruit mediators to initiate signaling pathways that impact a wide variety of cellular processes as indicated (Jackson and Bartek 2009).

The MRN complex is another DNA sensor protein consisting of Mre11, Rad50, and the Nijmegen breakage syndrome 1 (NBS1) subunits. Mre11, the core enzyme of the MRN complex, uses two DNA binding motifs to bind to DNA and is associated with Rad50. Mre11 and Rad50 play a role in bridging and stabilizing broken DNA ends and are involved in replication fork stability(Williams et al. 2008). The Nijmegen breakage syndrome 1 (NBS1) protein, which is independent of Rad50, interacts with and recruits

ATM, the apical DDR kinase, as a component of the MRN complex to activate ATM (Falck, Coates, and Jackson 2005).

PARP-1 is another DNA sensor protein that binds to single-strand breaks (SSBs) and DSBs with its two zinc finger motifs. It initiates the poly (ADP-ribosylation) of a great variety of proteins including itself (Wang et al. 2006). PARP-1 also binds to other forms of DNA damage (Kedar et al. 2012) and plays a role in the repair of SSBs (Dantzer et al. 2000).

Ku70/80, as a key component of the nonhomologous end-joining (NHEJ) pathway, acts as the third DNA sensor protein. It binds to DNA ends and recruits other proteins to facilitate the processing and ligation of the broken ends.

Rpa is a protein that cooperates with its partner, Atr-interacting protein (Atrip), and Rad9-Rad1-Hus1 to detect single-stranded DNA (ssDNA). SsDNA is produced during the resection of DSBs and at stalled or collapsed replication forks during the DNA synthesis (S) phase. Rpa recruits the apical kinase Atr to the damaged site through its partner protein, ATRIP (Cortez et al. 2001).

The mediators and transducers of DDR amplify and pass the signal received from upstream proteins to effector proteins, resulting in several cellular responses, including cell cycle checkpoint activation, DNA repair, and transcriptional inhibition (Polo and Jackson 2011; Williams et al. 2008). Transducer kinases activate effector kinases, such as Chk1 (mainly phosphorylated by ATR) and Chk2 (mainly phosphorylated by ATM), with the help of mediator proteins such as MDC1 (mediator of DNA damage checkpoint), 53BP1 (p53-binding protein 1), BRCA1 for ATM and ATR, and TopBP1 (topoisomerase-binding protein 1) and Claspin for ATR. The signal is then propagated throughout the nucleus by activated Chk1 and Chk2, converging on downstream effectors such as p53 and the cell division cycle 25 (CDC25) phosphatases. The ultimate targets of these signaling cascades include transcription factors, cell cycle regulators, apoptotic machinery, and DNA repair factors (Harrison and Haber 2006). If the damage remains unresolved, the DDR activates apoptotic pathways or directs cells to senescence (Sulli, Di Micco, and d'Adda di Fagagna 2012) (Figure 3).

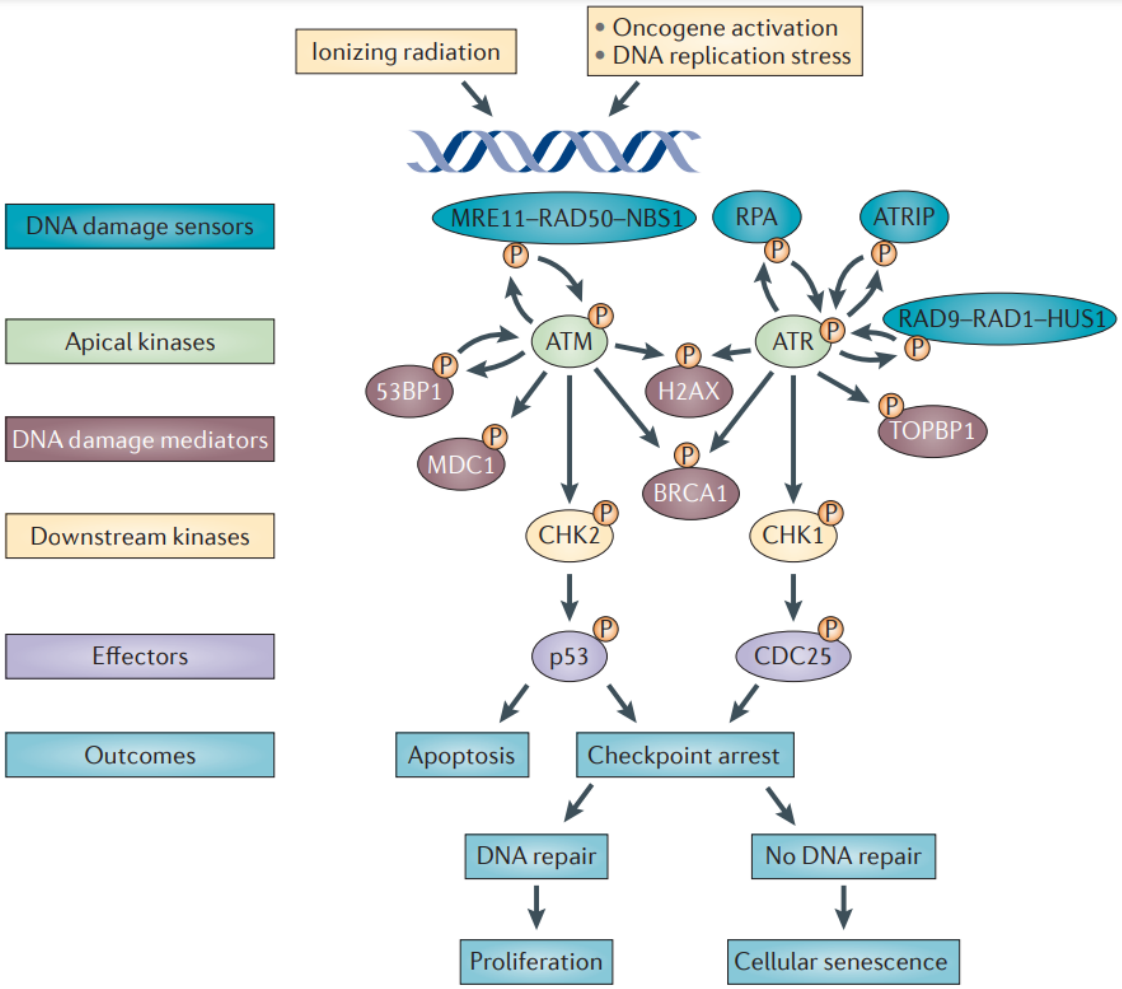

Figure 3: Outline of DNA damage signaling. Key DDR pathways induce cell cycle arrest, DSB repair, apoptosis, or senescence (Sulli, Di Micco, and d'Adda di Fagagna 2012).

1.2.2 Cell cycle and DNA damage checkpoints

1.2.2.1 Cell cycle

The cell cycle consists of four phases: G1, S, G2, and M phase (Figure 4). Its purpose is to maintain the genetic information of DNA from one cell generation to the next. The cell starts in the G1 phase immediately after completing the M phase, during which it grows by increasing in size. Once it reaches a certain size and receives the appropriate signals, it enters the S phase. In the S phase, DNA synthesis takes place as the cell duplicates its hereditary material through DNA replication, forming a copy of each chromosome. In the subsequent G2 phase, the cell verifies the completion of DNA replication and makes necessary preparations for cell division. Following this, the chromosomes undergo separation through mitosis (M), resulting in the division of the cell into two daughter cells.

Through this mechanism, the cell's genetic information is transmitted intact to a new generation of cells. After division, the cells return to G1, and the cell cycle begins again.

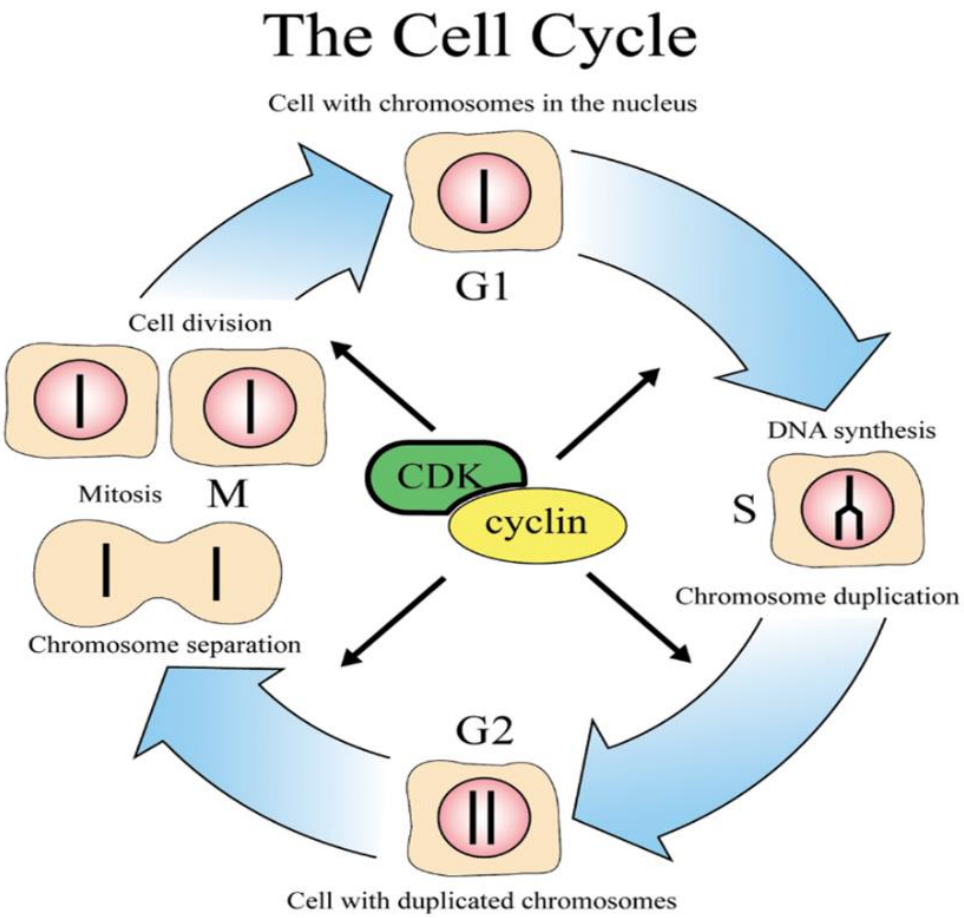

Figure 4: The cell cycle. The cell cycle is divided into G1, S, G2, and M phases. CDK-molecules function as engines and the cyclins as a gearbox controlling whether the engine will run, will enter an idling state, or drive the cell from one phase to the next (Source : https://www.nobelprize.org/prizes/medicine/2001/press-release/).

The progression of the cell cycle is tightly regulated by a complex machinery of cyclins and cyclin-dependent kinases (Cdks). Cyclins are proteins that are synthesized and degraded during each cell cycle and do not possess enzymatic activity themselves. They bind to their respective Cdks and activate the Cdk enzymatic activity. The cyclin-Cdk complex, responsible for regulating the cell cycle, is the active complex. Throughout each stage of the cell cycle, different cyclins are synthesized and degraded periodically, while the protein expression of Cdks remains constant. Activation of cyclin-Cdk complexes promotes the initiation and progression of cell cycle phases, while the degradation of cyclins leads to the termination of these phases.

It is important to note that the next cell cycle begins only when a cell cycle-inducing stimulus is present (Massagué 2004). If this stimulus fails to occur during G1, or if the cellular environment is unfavorable, cyclin synthesis does not initiate, and the cell exits the active cycle. In this condition, cells exit the cell cycle and enter a post-mitotic state called the G0 phase (Zetterberg and Larsson 1985).

1.2.2.2 DNA damage checkpoints

The primary purpose of the DNA damage response (DDR) is to maintain genome stability by coordinating DNA repair and cell cycle progression. However, the repair process requires a certain amount of time to complete. If there is not enough time available, the repair may not be fully accomplished. In such cases, the resulting damage can have severe effects if the cell has already entered the next cell cycle before the DNA breaks have been completely repaired. Therefore, cells have a mechanism for pausing the cell cycle to ensure that damaged DNA is repaired before cell division proceeds. This mechanism is known as the DNA damage checkpoint, which plays a crucial role in the process.

Cyclin-dependent kinases (CDKs) along with their regulatory subunits called cyclins regulate the progression through the cell cycle and are substrates of signaling cascades activated in response to DNA damage (Löbrich and Jeggo 2017). These signaling cascades activate cell cycle checkpoints that temporarily halt cell cycle progression, allowing time for DNA repair to occur. The activation of checkpoint kinases, such as ATM (ataxia telangiectasia mutated) and ATR (ataxia telangiectasia and Rad3-related), leads to the inhibition of CDK activity through phosphorylation of key regulatory proteins. This inhibition prevents the cell from entering the next phase of the cell cycle until the DNA damage is adequately repaired.

By halting the cell cycle at specific checkpoints, the DNA damage response ensures that damaged DNA is repaired before cell division proceeds, minimizing the risk of transmitting genetic abnormalities to daughter cells.

1.3 DNA repair mechanisms

To maintain genomic stability and repair DNA damage, cells have evolved intricate repair mechanisms to handle various types of DNA lesions that can occur (Figure 5).

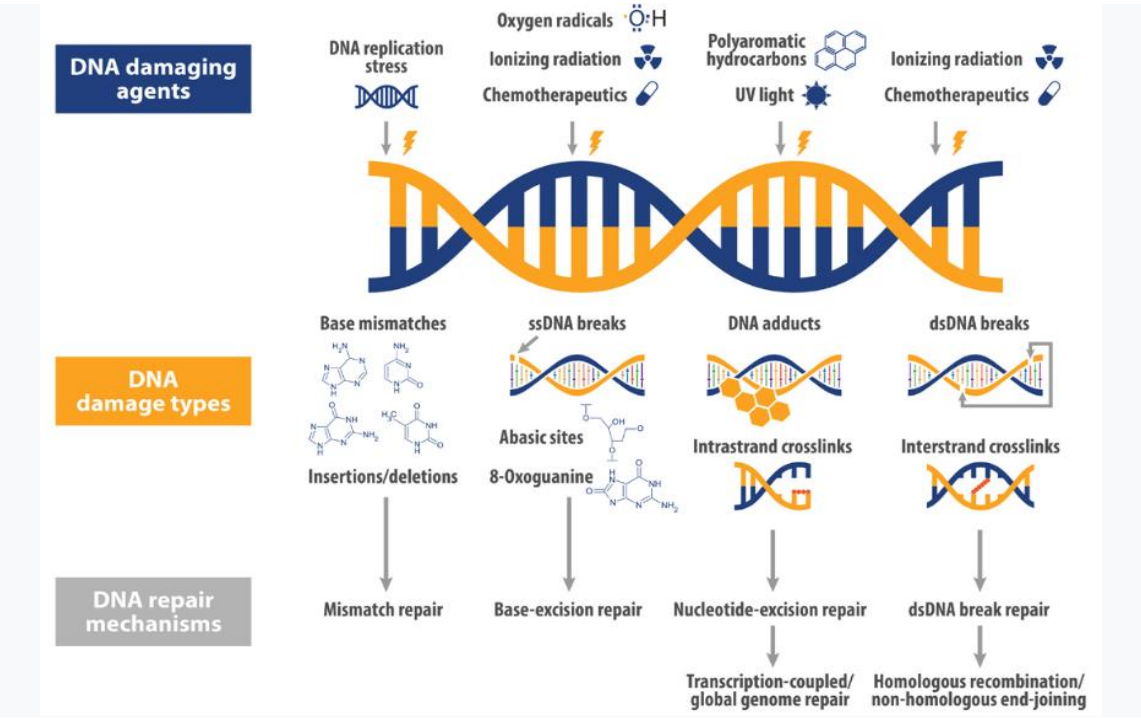

Figure 5: DNA repair pathways. Mammalian cells have developed specialized pathways to sense, respond to, and repair base mismatches, SSBs, DNA adducts, and DSBs (Source: https://blog.crownbio.com/dna-damage-response-and-dna-repair-in-cancer).

1.3.1. Mismatch repair pathway

The mismatch repair (MMR) pathway plays a vital role in maintaining genome stability by correcting base-base mismatches and small insertion errors that occur during DNA replication, such as nucleotide misincorporation by DNA polymerase and template slippage (Figure 5). Additionally, MMR corrects mispairs arising from the spontaneous deamination of 5-methylcytosine and resolves heteroduplexes formed during genetic recombination.

The MMR process involves four main components:

1. Sensors (Msh2-Msh6 or Msh2-Msh3 complexes) that recognize and identify the mismatched base pairs.

2. MMR factors (MLH1-PMS2, MLH1-PMS1, and MLH1-MLH3) that recruit the exonuclease EX01 for further processing.

3. Recognition of the newly synthesized DNA strand containing the mismatch and subsequent removal of incorrect or altered nucleotides.

4. Resynthesis and ligation of the excised DNA segment.

Dysfunction of the MMR pathway leads to a "mutator" cellular phenotype characterized by an increased frequency of spontaneous mutations and greater microsatellite instability (MSI). In humans, mutations in several MMR genes can predispose individuals to hereditary nonpolyposis colorectal carcinoma (HNPCC) and other sporadic tumors that exhibit MSI.

1.3.2 Base Excision Repair (BER)

The base excision repair (BER) pathway is responsible for repairing single-base mutations and multiple-base errors caused by ionizing radiation and endogenous mutagens, which pose significant threat to genomic fidelity and stability. The BER pathway is initiated by one of eleven DNA glycosylases, which recognizes and removes the damaged base in the case of single-base mutations. After the base is removed, the sugar residue is subsequently excised by an apurinic endonuclease 1 (APE1).

Following the base excision step, a distinct group of proteins is involved in either the short-patch pathway or the long-patch pathway. In the short-patch pathway, a single missing base in the exposed gap is filled in by a DNA polymerase enzyme, and then the nick is sealed by a DNA ligase enzyme. On the other hand, in the long-patch pathway, multiple bases are added to the gap before it is ultimately sealed by a DNA ligase enzyme.

Through these steps, the BER pathway efficiently repairs single-base mutations and multiple-base errors, safeguarding the integrity of the genome.

1.3.3 Nucleotide Excision Repair (NER)

Nucleotide excision repair (NER) is the primary pathway used by mammals to remove bulky adducts in DNA, such as pyrimidine dimers. There are two subpathways within NER: global genome repair (GGR or GG-NER) and transcription-coupled repair (TCR or TC-NER). The GG-NER process is responsible for genome-wide repair, meaning that lesions in both coding and non-coding regions of DNA can be removed. On the other hand, TC-NER specifically targets lesions in the DNA strands of actively transcribed genes.

NER is a complex multi-step process that involves a large network of more than 30 proteins. The mechanism of GG-NER and TC-NER differs primarily in the initial recognition of the damaged base, while the subsequent steps used to repair the damage are the same for both subpathways.

Deficiencies in NER are associated with xeroderma pigmentosum, an inherited disorder characterized by extreme susceptibility to skin cancer.

1.3.4 DNA DSBs repair

DNA DSBs are the most severe types of DNA damage that can compromise genomic stability and cell viability. DSBs can arise from exogenous sources like UV radiation, ionizing radiation, and certain chemicals, as well as endogenous factors such as cellular metabolites, reactive oxygen species, and errors during DNA replication. Failure to repair DSBs properly can lead to severe diseases, including cancer, growth and mental retardation, immune deficiency, and developmental defects.

It is estimated that approximately 10-100 DNA DSBs are occurring per nucleus of each human cell per day. To repair DSBs, vertebrate cells utilize several pathways, each with varying levels of fidelity and speed, employing different mechanisms to restore the original genomic sequence.

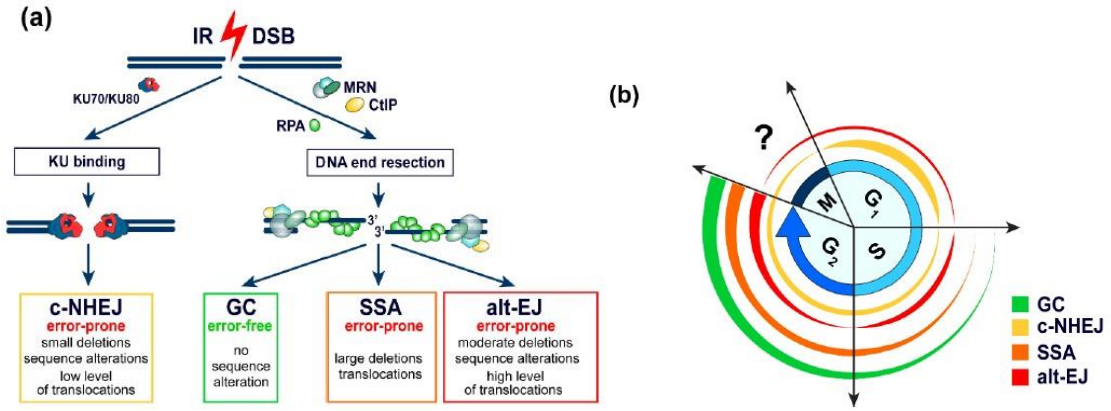

Figure 6: DSB repair pathways and their cell cycle dependence. (a) DSB repair pathways: The classical non-homologous end joining (c-NHEJ) pathway, which does not require extensive DNA end resection, is initiated by the strong binding of the KU heterodimer and subsequent recruitment of DNA-PKcs protein kinase. This pathway is believed to inhibit and limit DNA end resection-dependent processing of DSBs. On the other hand, precisely controlled DNA end resection is the initial step for other DSB processing pathways such as homologous recombination (HR) (known also as gene conversion (GC)), single-strand annealing (SSA), and alternative end joining (alt-EJ). (b) Cell cycle dependence of DSB processing pathways: The above-mentioned DSB processing pathways exhibit distinct dependencies on the cell cycle (Iliakis, Mladenov, and Mladenova 2019).

One key control point in the DSB repair pathway is the processing of the 5' DNA end through a process known as DNA end resection or simply resection. DSBs can be repaired

through both DNA end resection-independent and DNA end resection-dependent pathways (Figure 6).

1.3.4.1 C-NHEJ

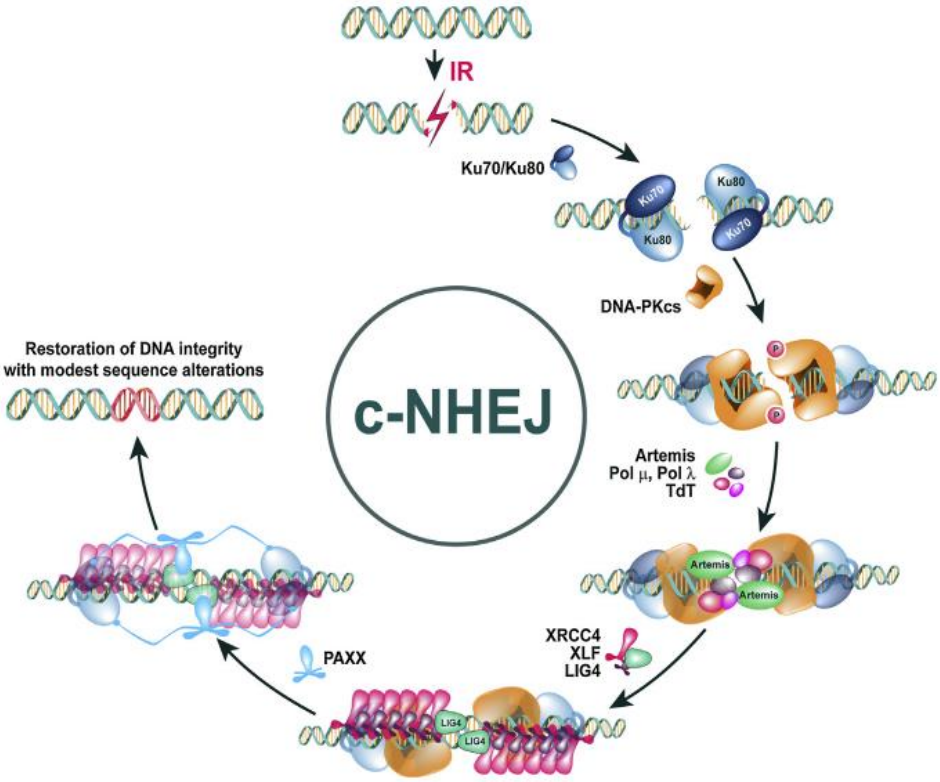

Figure 7: Schematic drawing of c-NHEJ mechanism. C-NHEJ pathway operates throughout the entire cell cycle. It is initiated by the robust binding of the Ku heterodimer and the subsequent recruitment of DNA-PKcs protein kinase. This mechanism is thought to inhibit and limit the DNA end resection-dependent processing of DSBs. Since c-NHEJ does not utilize a template for repair, it is considered to be error-prone (Mladenov et al. 2016). See text for more details.

A group of sensors is rapidly activated in response to DSBs. These sensors include the ATM and ATR protein kinases, which not only promote DNA repair but also halt the cell cycle progression until the break is accurately repaired. One crucial step in this process is DNA end resection, which determines the choice of the DSB repair pathway.

The competition between HR and NHEJ pathways is regulated by various factors, including the protein 53BP1. While ATM protein's primary role is to facilitate the processing of broken DNA ends, it is suppressed by 53BP1. This suppression reduces the production of recombinogenic single-stranded DNA and favors c-NHEJ over HR. The MRN complex plays a vital role in regulating this process (Figure 7).

The c-NHEJ pathway can be described as a five-step process. First, the broken DNA ends are recognized through Ku binding. Second, the DNA-PKcs is recruited. Third, the DNA ends undergo processing. Fourth, either fill-in synthesis or end bridging takes place. Finally, the DNA ends are ligated to complete the repair process.

The initiation of the c-NHEJ pathway occurs through the rapid and strong binding of the Ku70/Ku80 (Ku) heterodimer to the broken DNA ends. This binding event recruits the DNA-dependent protein kinase catalytic subunit (DNA-PKcs), leading to the formation of the active DNA-PK holoenzyme. The DNA-PK holoenzyme, due to its substantial size, serves as a recruitment scaffold for other components of the c-NHEJ pathway. Additionally, the kinase activity of DNA-PKcs plays a regulatory role by phosphorylating several proteins, including itself. Another protein called Artemis, which possesses endonuclease activity, forms a physical complex with DNA-PKcs and Ku. This complex is capable of phosphorylating Artemis and activating its endonuclease activity, allowing it to process various DNA structures.

To fill gaps in the DNA and add new nucleotides in a non-complementary manner, members of the X family DNA polymerases (Pol μ, Pol λ) and TdT (terminal deoxynucleotidyl transferase) are involved. Their DNA synthesis activity prepares the DNA ends for the final ligation step in the repair process. For DNA end rejoining, a ligation complex composed of DNA ligase 4 (Lig4), XRCC4, XLF (XRCC4-like factor), and PAXX (paralog of XRCC4 and XLF) comes into play. This complex, recruited by the Ku/DNA-PK complex, plays a critical role in the final step of the c-NHEJ repair process.

In terms of efficiency, the c-NHEJ pathway operates with remarkable speed and removes DNA ends from the genome in a cell cycle-independent manner. It is faster than many repair pathways that deal with base lesions confined to a single DNA strand. However, c-NHEJ is considered an error-prone mechanism as it simply ligates broken DNA ends without restoring the original DNA sequence. Moreover, c-NHEJ lacks inherent mechanisms to ensure the joining of the correct DNA ends, which can lead to the erroneous ligation of non-compatible DNA molecules. This can potentially result in chromosomal translocations, a type of genetic abnormality that can cause severe health problems.

1.3.4.2 DNA-End-Resection-Dependent Rejoining of DSBs by HR, SSA, and alt-EJ

1.3.4.2.1 HR

HR is the sole DSB repair pathway known to faithfully restore the original DNA sequence during the repair of DSBs. HR not only joins the broken DNA ends but also preserves the genetic integrity of the DNA (Figure 8).

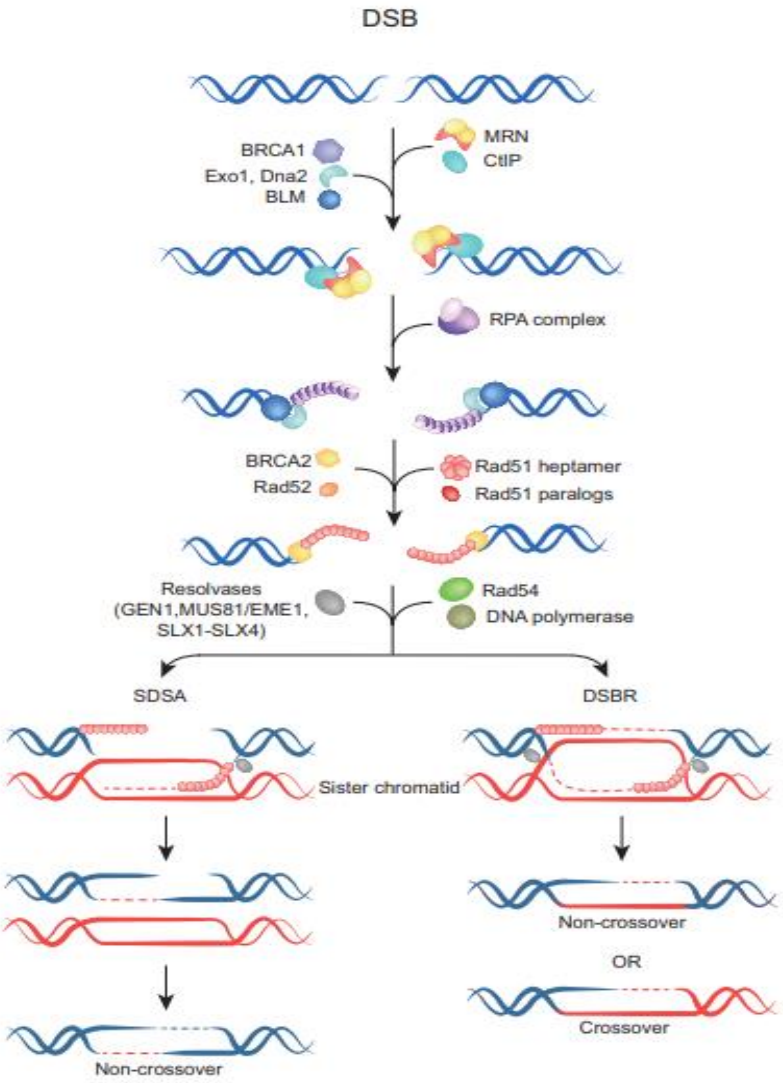

Figure 8: Schematic representation of the mechanism of HR. HR starts with precisely controlled DNA end resection and uses the homologous sister chromatid as a template for error-free repair. The repair is limited to late S- and G2-phase of the cell cycle. Two possible outcomes can occur after HRR: non-crossover and crossover products (Dueva and Iliakis 2013). For more details see text.

In contrast to c-NHEJ, which can rejoin broken DNA ends without sequence homology, HR is a highly accurate repair mechanism that requires the physical contact of an

undamaged chromatid or chromosome to serve as a template for repair. Resection of DNA ends is a crucial step in HR, which generates 3'-ssDNA overhangs that facilitate the process of strand invasion during the search for homology on the sister chromatid. Due to this requirement for template search and homology, HR is highly regulated during the cell cycle and primarily active in the late S and G2 phases. However, the homology search process is time-consuming, making HR slower compared to other repair pathways.

The initial step of HR involves the recognition of DNA damage, followed by the processing of double-stranded DNA ends into 3' DNA single-stranded tails. Several proteins are involved in this process. The MRN complex, consisting of Rad50, Nbs1 and Mre11, forms the core and provides both DNA binding and enzymatic activities. Mre11 activates single-strand endonuclease and 3'-5' exonuclease activities, while Rad50 regulates ATPase and adenylate kinase activities. Nbs1, the third component of the MRN complex, is recruited to DSBs and plays a crucial role in the activation of ATM. CtIP, which interacts with Nbs1, is essential for the activation of the MRN complex and the initiation of end resection. Exo1, DNA2, WRN, and BLM helicases facilitate the extension of the DNA end resection process.

Following resection, the resulting 3'-ssDNA is coated by replication protein A (RPA), which plays a role in eliminating the formation of secondary structures. RPA is then replaced by Rad51 recombinase with the assistance of BRCA2, Rad52, and Rad51 paralogs (Rad51B, Rad51C, Rad51D, XRCC2, and XRCC3). This leads to the formation of the Rad51 nucleoprotein filament, which invades the intact sister chromatid to search for homologous sequences and forms a structure called the displacement loop (D-loop). The DNA annealing process is facilitated by the HRR mediator Rad52. Once homology is found, the 3'-end of the invading strand undergoes extension and Rad51 is removed by Rad54 and its paralog Rad54B to initiate strand extension.

Homology-based repair of DSBs can occur through two different pathways: synthesis-dependent strand annealing (SDSA) and double-strand break repair (DSBR) pathways (see Figure 9). In SDSA, the 3'-end of the invading strand is extended for a limited distance, detaches from the template, and then reconnects with the original DNA end through ligation. This is the most common outcome in HR and results in the creation of a single Holliday Junction (HJ), leading to the formation of non-crossover products. In

contrast, DSBR generates two X-shaped HJs, which can produce either crossover or non-crossover products depending on how the intermediate DNA strands are cleaved by specialized enzymes. The resolution of these HJs involves several proteins, including GEN1, MUS81/EME1, and SLX1-SLX4.

1.3.4.2.2 Alt-EJ

It has been discovered that when HR and c-NHEJ mechanisms fail to repair DNA DSBs, an alternative end-joining (alt-EJ) pathway comes into play. Alt-EJ is a third mechanism based on the principle of end-joining (Figure 9). While our understanding of alt-EJ is still evolving, many details have already been uncovered and confirmed. Alt-EJ operates similarly to c-NHEJ by joining two DNA ends together. However, unlike c-NHEJ, alt-EJ requires DNA-end resection, which exposes microhomologies.

When DNA DSBs are induced, Parp-1, one of the earliest proteins involved in alt-EJ, detects the breaks and binds to the damaged DNA ends. The Parp family consists of polymerases that catalyze poly (ADP-ribosyl) ation (PARylation) events in proteins. Although Parp-1 may have lower efficiency in binding DNA ends compared to Ku, once it is bound, it can promote the redirection of DNA DSBs towards the alt-EJ pathway instead of c-NHEJ processing. The broken ends are further stabilized by histone 1 (H1), which also contributes to the activation of Parp-1. Subsequent end resection is carried out by the MRN complex and CtIP. Alt-EJ involves the alignment of DNA ends based on microhomologies. Polθ may play a role in this process by elongating ssDNA with overhangs at the ends of DSBs. Additionally, Polθ may repress Rad51 and influence the selection of the DNA DSB repair pathway when redirected to the resection-dependent repair pathway by the MRN complex and CtIP. The repair process continues from this point. With the ligation step and the involvement of Lig1 and Lig3/XRCC1, while the linker histone H1 may serve as an alignment factor (Schipler and Iliakis 2013). Alt-EJ is active throughout the cell cycle but exhibits significant fluctuations in activity, with its maximum activity occurring in the G2 phase. During G2 phase, alt-EJ also functions as a backup pathway to HR. However, alt-EJ activity decreases in the G1 phase due to its reliance on DNA end resection. In fact, alt-EJ is often inactive in resting G0 cells. While alt-EJ serves as a mechanism to remove DSBs and acts as a backup when the primary

repair pathways fail, it is a highly mutagenic pathway that can lead to significant sequence alterations in the junctions and the formation of chromosomal translocations (Figure 9).

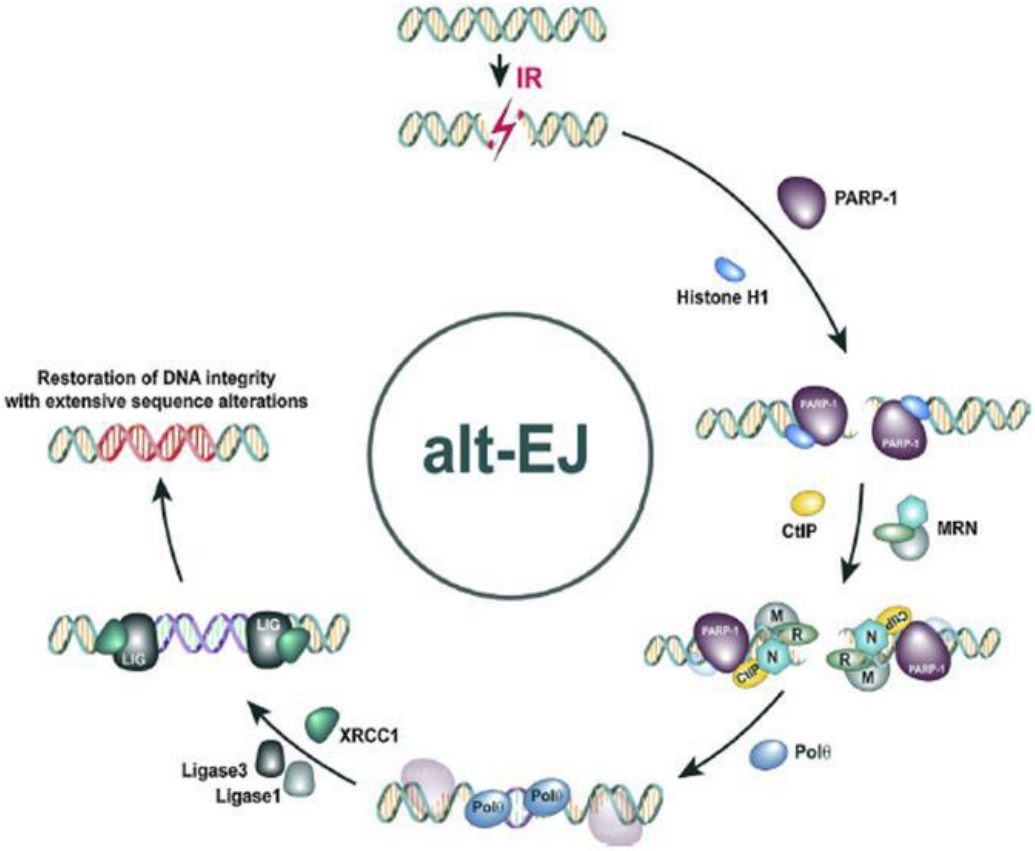

Figure 9: Schematic mechanism of alt-EJ. Alt-EJ serves as a backup repair mechanism to both cNHEJ and HRR pathways. It remains active throughout the cell cycle but displays significant fluctuations in activity depending on the cell cycle phase. The initial sensing of DNA DSBs is mediated by Parp-1, which is followed by DNA end resection facilitated by the MRN complex and CtIP. The processed DNA ends are then further modified by Polθ before the final ligation step, which involves Lig1 and Lig3. These sequential steps in alt-EJ ensure the repair of DNA double-strand breaks (Mladenov et al. 2016). For more details see text.

1.3.4.2.3 SSA

Alongside HR and end-joining processes, SSA is another DSB repair pathway that relies on homology. Unlike HR, SSA utilizes regions of homology within the same DNA molecule for repair. Upon DNA damage, extensive resection of the DSB ends is initiated, likely facilitated by the MRN complex and CtIP. Unlike HR, SSA does not involve RAD51 but instead utilizes the strand-annealing protein RAD52 to anneal the exposed homologous DNA sequences flanking the DSB. Following annealing, the XPF–ERCC1 and MSH2–MSH3 complexes are responsible for removing protruding DNA ends. The

resulting nicks are then ligated by DNA Lig1 to restore the integrity of the DNA molecule. It is important to note that although SSA relies on homology, it is an error-prone repair pathway that leads to sequence deletions and the formation of translocations. Similar to HR, SSA exhibits cell cycle dependence, with maximum activity observed during S and G2 phases. Furthermore, loss of Rad51, Rad54, or BRCA2 can enhance SSA activity, suggesting a backup role for SSA in the absence of HRR. For further details, please refer to the provided references (Mladenov et al. 2016; Ivanov et al. 1996; Ochs et al. 2016; Rothenberg et al. 2008; Bhargava, Onyango, and Stark 2016) (Figure 10).

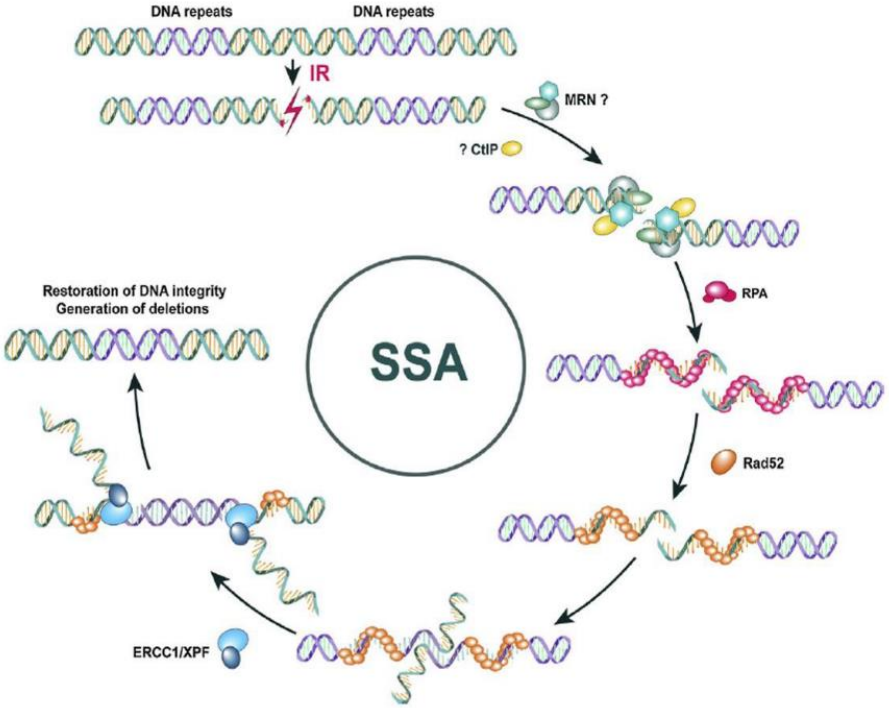

Figure 10: Schematic mechanism of SSA. SSA is a mutagenic repair pathway leading to the deletion of the sequence and formation of translocations. It has DNA end resection-dependent and cell cycle dependent manner (Mladenov et al. 2016). For more details see text.

1.4 Condensins

The expression of condensins protein genes is necessary for the proliferation and migration of human cancer cells, and loss of condensins expression has been associated with the development of cancers and developmental disorders.

Yeast and other lower eukaryotes typically possess a single condensin complex. Mammalian cells have two distinct condensin complexes: condensin I and condensin II ((Hirota et al. 2004; Hirano 2012) (Figure 11). These complexes differ in their protein

composition and cellular localization during the cell cycle. Both complexes contain two Structural Maintenance of Chromosomes (SMC) subunits, SMC2 and SMC4, which form the enzymatic (ATPase) and structural core. Each complex also includes three unique non-SMC subunits or Chromatin Associated Proteins (CAPs).

A HEAT repeat is a protein tandem repeat structural motif composed of two alpha helices linked by a short loop. HEAT repeats can form alpha solenoids, a type of solenoid protein domain found in several cytoplasmic proteins. Condensin I consists of HEAT subunits NCAPD2 (non-SMC condensin I complex subunit D2) and NCAPG (non-SMC condensin I complex subunit G), and the kleisin family protein NCAPH (non-SMC condensin I complex subunit H). Condensin II includes HEAT subunits NCAPD3 (non-SMC condensin II complex subunit D3） and NCAPG2 (non-SMC condensin II complex subunit G2), and the kleisin family protein NCAPH2 (non-SMC condensin II complex subunit H2). The CAP proteins are crucial for stabilizing the condensin holocomplex, enhancing ATPase activity, and interacting with histones (Bazett-Jones, Kimura, and Hirano 2002; Abe et al. 2011; Piazza et al. 2014; Kong et al. 2020).

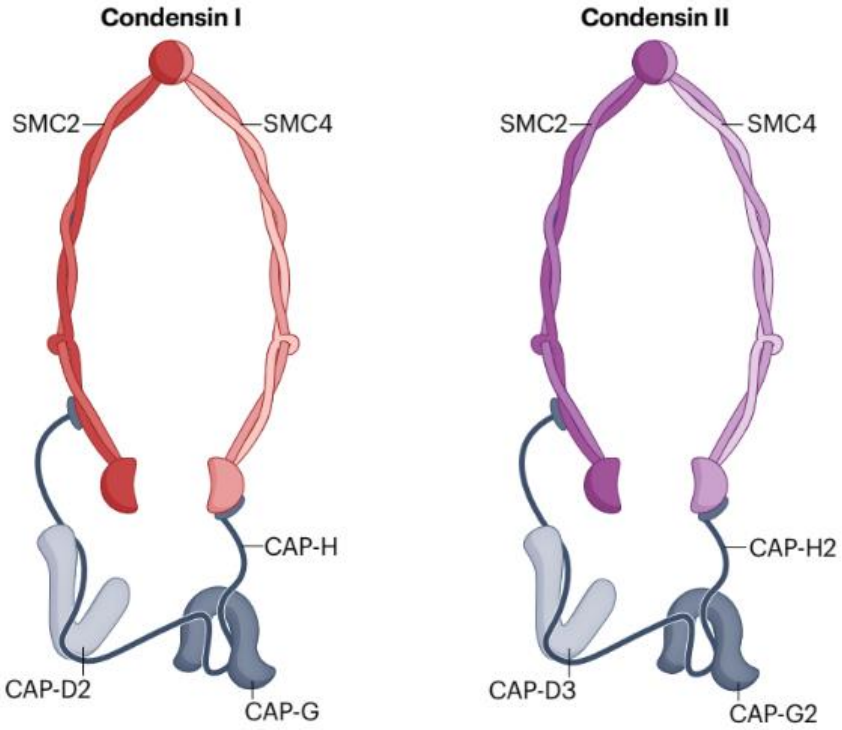

Figure 11: Schematic depiction of the overall organization and constituent components of condensin complexes (Hoencamp and Rowland 2023).

Under normal conditions, condensin II is present in the nucleus and cytoplasm throughout the cell cycle, whereas condensin I is mainly cytoplasmic and interacts with DNA after the nuclear envelope breaks down during mitosis (Maeshima and Laemmli 2003; Gerlich et al. 2006). Both human condensins compact chromosomes in mitosis but differ in their regulation and contribution (Hirano 2012). The two condensins also differ in their ability to extrude DNA (Kong et al. 2020). In single molecule experiments, condensins I bound to DNA for much shorter periods of time than condensins II, but extruded loops 2–53 times faster. Chromosomes become compacted into a series of ~100-kb loops in less than ten minutes (Gibcus et al. 2018).

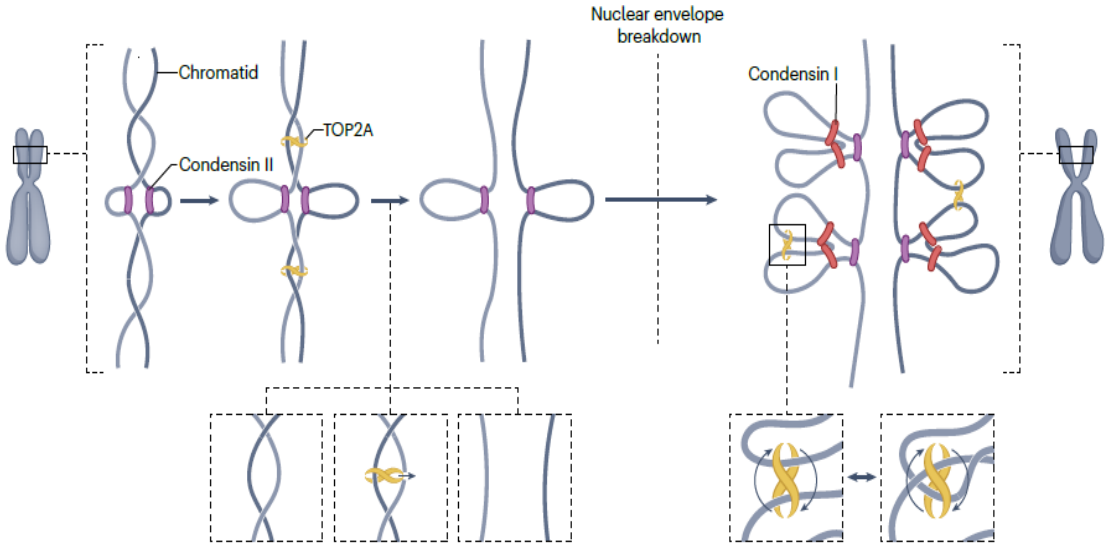

Figure 12: Chromosome formation by condensin loop extrusion. As mitosis begins, condensin II initiates the formation of chromatin loops, facilitating topoisomerase 2A (TOP2A)-mediated resolution of sister chromatids and the development of rod-like chromosomes during mitotic prophase. After the nuclear envelope disintegrates, condensin I further segments the chromatin loops created by condensin II into smaller, nested loops. Regions of DNA in close proximity are knotted and unknotted by TOP2A, leading to additional chromatin compaction (Hoencamp and Rowland 2023).

More than twenty years ago, it was proposed that SMC complexes shape chromatin by forming and progressively enlarging DNA loops (Nasmyth 2001). Recently, a growing body of in vivo and in vitro evidence has supported the notion that condensin complexes carry out this function. These loop structures can naturally form through a process known as loop extrusion. Loop extrusion has been suggested as a mechanism for chromosome compaction (Nasmyth 2001; Riggs 1990; Ryu et al. 2022) and has been investigated

through simulations (Goloborodko et al. 2016) (Terakawa et al. 2017). Condensin II is responsible for generating outer loops, whereas condensin I forms inner loops (Figure 12). Furthermore, recent studies have shown that condensin proteins play a role in regulating chromosome organization and gene expression within the interphase nuclei of vertebrate cells (Zhang et al. 2016; Hoencamp et al. 2021; Wu et al. 2019; Lancaster et al. 2021)

Condensins function by forming chromosomal loops through their conserved SMC ring structure, which consists of a V-shaped dimer of SMC ATPase subunits. Cohesin is another SMC complex. Cohesin is recruited to chromatin in a manner dependent on the DNA damage response factors Mre11, γH2AX, ATR, and Scc2 (Kim et al. 2002; Ström et al. 2004; Unal et al. 2004; Ström et al. 2007; Unal, Heidinger-Pauli, and Koshland 2007). Sister chromatid cohesion can promote repair using the sister chromatid as a template, rather than using the homologous chromosome or other genomic regions in trans (Covo et al. 2010; Piazza et al. 2021). For HR to be successful, chromatids should be kept in proximity by cohesin and condensins. Depletion of condensin proteins results in chromosome decondensation, highlighting their importance in maintaining chromatin compaction. For instance, hypotonic stress has been shown to induce global chromatin decompaction, which compromises regulated chromatin dynamics and genomic stability by suppressing DSB processing by HR, and allowing error-prone processing by alt-EJ and SSA (Krieger et al. 2021).

Other lines of evidence suggest that condensins promote DNA repair. Condensin II might play a role in promoting HR (Wood et al. 2007; Wood et al. 2008), whereas condensin I has been reported to cooperate with poly (ADP-ribose) polymerase 1 in interphase to facilitate the repair of single-stranded DNA breaks (Kong et al. 2011; Heale et al. 2006). Additionally, condensin I is depleted from DNA at under-replicated sites in mitosis, possibly to allow for mitotic DNA synthesis and the completion of replication at these sites (Boteva et al. 2020).

It has become apparent that condensins have crucial functions in each phase of the cell cycle. These complexes shape the genome, bring together distant genomic regions, contribute to DNA repair, prepare chromatin for mitosis, and ultimately ensure proper chromosome segregation and the formation of daughter cells with identical karyotypes.

Although recent years have yielded new insights into how SMC complexes control DNA repair, we are only beginning to grasp the full extent of their contribution and how these different activities are regulated. The precise mechanisms by which changes in condensin levels affect and disrupt DSB repair, as well as the activation of DDR and cell cycle checkpoints, are not yet fully understood. The objective of our study was to investigate the specific role of condensin in X-ray-induced DSB repair. Understanding this role could potentially lead to the development of new strategies to protect individuals from the harmful effects of ionizing radiation and increase the sensitivity of tumor cells to radiation therapy.

2. Aims of this thesis

This thesis aims to investigate the role of the condensins protein complex in DNA damage repair, with a particular focus on its contribution to maintaining cell viability following ionizing radiation (IR). Specifically, the study seeks to determine how the suppression of condensin I and II impacts radiosensitivity in RPE-1 hTert and A549 cells, and whether this could represent a novel therapeutic target for enhancing radiotherapy. Additionally, the thesis explores the molecular mechanisms by which condensins knockdown affects DSBs repair pathways, including HR, SSA, alt-EJ, and c-NHEJ. Another key objective is to assess how condensins influence the G2/M checkpoint response, which is crucial for DNA repair prior to cell division, and their role in ensuring genomic stability. Finally, the study aims to elucidate the importance of condensins in chromatid break repair, chromosome condensation, and their potential as a target to improve the efficacy of cancer therapies. Through these objectives, the thesis seeks to expand our understanding of condensin complexes in the context of DNA repair and genomic stability.

3. Materials and Methods

3.1 Materials

Table 1 Cell culture and growth

Growth medium	Supplier
Dulbecco's Modified Eagle Medium (DMEM)	Sigma-Aldrich
McCoy's 5A medium	Sigma-Aldrich

Table 2 Cell lines and corresponding growth media

Cell line	Cell type	Origin	Growth medium
RPE-1 hTert	Retina pigmented epithelium	Human	DMEM+10 % serum
A549	Adenocarcinoma	Human	McCoy's 5A+10 % serum
U2OS 279A EJ2-GFP	Osteosarcoma	Human	McCoy's 5A+10 % serum
U2OS 280A EJ5-GFP	Osteosarcoma	Human	McCoy's 5A+10 % serum
U2OS 282C DR-GFP	Osteosarcoma	Human	McCoy's 5A+10 % serum
U2OS 283C SA-GFP	Osteosarcoma	Human	McCoy's 5A+10 % serum

Table 3 Antibodies

Antibody	Host/type	Dilution	Incubation time	Supplier
anti-mouse Alexa Fluor 488	Goat/polyclonal	1:400 (IF/FC)	1 h	Invitrogen
anti-mouse Alexa Fluor 647	Goat/polyclonal	1:400 (IF)	1 h	Invitrogen
anti-mouse IRDye 680LT	Goat/polyclonal	1:10000 (WB)	1 h	Li-COR Biosciences
anti-rabbit IRDye 680LT	Goat/polyclonal	1:10000 (WB)	1 h	Li-COR Biosciences
anti-rabbit IRDye 800LT	Goat/polyclonal	1:1000 (WB)	1 h	Li-COR Biosciences
Beta Actin	Rabbit/polyclonal	1:30000 (WB)	overnight	Gene Tex

GAPDH	Mouse/monoclonal	1:20000 (WB)	overnight	UBP Bio
CAP-H	Rabbit/monoclonal	1:1000 (WB)	overnight	Bethyl Laboratie
CAP-D3	Rabbit/monoclonal	1:2500 (WB)	overnight	Bethyl Laborаties
RPA70B	Mouse/monoclonal	1:500 (IF/FC)	1.5 h	IFMSB, UK Essen
Rad51(14B4)	Mouse/monoclonal	1:400 (IF/FC)	1.5 h	Gene Tex
53BP1	Mouse/monoclonal	1:500 (IF/FC)	1.5 h	Abcam plc
ɣH2AX	Mouse/monoclonal	1:200 (IF/FC)	1.5 h	Abcam plc

Table 4 Plasmids used for transfection

Plasmid	Description
pCMV-3xNLS-ISceI	I-SceI expressing plasmid
pEGFP-N1	EGFP expressing plasmid

Table 5 siRNA sequences used for transfection

Target mRNA	siRNA sequence (5' → 3')	Provider
CAPH-1	GGC-ACC-AGG-UUA-CUU-AAG-A55	Eurogentec
CAPH-2	ACA-CGC-AGA-UUA-CGG-AAC-A55	Eurogentec
CAPH-3	CGA-AGC-AGA-UCG-GAA-GUG-U55	Eurogentec
CAPH-4	CUU-UAG-GCC-UCG-ACG-CAA-A55	Eurogentec
SMC2-1	CAG-GUG-GUU-AUU-GGU-GGU-AGA-55	Eurogentec
SMC2-2	CUG-AAA-CGU-CGA-UAC-ACU-AUA-55	Eurogentec
SMC2-3	CAG-GUU-CGG-GCU-UCU-AAU-UUA-55	Eurogentec
SMC2-4	UUG-GAU-CUU-UCU-CAU-ACC-CAA-55	Eurogentec
NCAPD3	CAU-GGA-UCU-AUG-GAG-AGU-AUU-55	Eurogentec
negative control siRNA	UUC UCC GAA CGU GUC ACG UdTdT	Eurogentec

Table 6 RNA Interference programs

Cell line	Program
RPE-1 hTert	GenePulser Xcell™ electroporation systems
A549	Nucleofector® X-20
U2OS 279A EJ2-GFP	Nucleofector® X-01
U2OS 280A EJ5-GFP	Nucleofector® X-01

U2OS 282C DR-GFP	Nucleofector® X-01
U2OS 283C SA-GFP	Nucleofector® X-01

Table 7 EdU Click-iT reaction cocktail

Stock solution	Working concentration
1 M Tris pH 7.4	100 mM
1 × PBS	
10 mM CuSO4	1.25 mM
1 mM Azide dye (Alexa Fluor 647)	1.25 μM
500 mM Ascorbic Acid	12.5 mM

Table 8 Chemicals

Chemicals	Supplier
4’,6-diamidino-2-phenylindole (DAPI)	SERVA
5-Ethynyl-2’-deoxyuridine (EdU)	SERVA
Acetic acid	Roth
Acetone	J.T. Baker
Aluminium sulfate, Al2(SO4)3	Roth
Ammonium persulfate (APS)	Sigma-Aldrich
Acrylamide/Bis-acrylamide, 30% solution	Sigma-Aldrich
Ascorbic acid	Roth
Beta (β)-mercaptoethanol	Merck
Bovine serum albumin (BSA) fraction V	Roth
Bromophenol blue (BrPBlue)	Sigma-Aldrich
6-Carboxyfluorescein Azide	Roth
Coomassie brilliant blue G-250	Serva
Copper (II) sulfate pentahydrate (CuSO4)	Sigma-Aldrich
Crystal violet	Merck
Calyculin A	Sigma-Aldrich
Dimethyl sulfoxide (DMSO)	Sigma-Aldrich
Ethanol (EtOH)	Sigma-Aldrich
Ethylenediaminetetraacetic acid (EDTA)	Roth
Fetal bovine serum	Sigma-Aldrich

Glycerol	Sigma-Aldrich
Glycine	Roth
Glucose	Roth
Hydrochloric acid (HCl)	Roth
HEPES (4-(2-hydroxyethyl)-1-piperazineethansulfonic acid)	Roth
KU 55933 (ATMi)	Haoyuan ChemExpress
Magnesium chloride (MgCl2)	Sigma-Aldrich
Methanol (MeOH)	J.T. Baker
N-Laurylsarcosine (NLS)	Merck
Non-fat dry milk	Roth
Paraformaldehyde (PFA)	Roth
Potassium chloride (KCl)	Roth
PromoFluor antifade reagent	PromoKine
Propidium iodide (PI)	Sigma-Aldrich
Protease inhibitor	Roche
RIPA buffer	Thermo Scientific
RNase A	Applichem
Sodium chloride (NaCl)	Roth
Sodium dodecyl sulfate (SDS)	Roth
Sodium hydroxide (NaOH)	Roth
Tetramethylethylenediamine (TEMED)	Roth
TRIS Pufferan®	Roth
Triton X-100	Roth
Trypsin	Biochrom
Tween 20	Roth
VE-821 (ATRi)	Haoyuan ChemExpress

Table 9 Drugs

Drug	**Drug description**	**Designation**	**Working concentration**
KU 55933	Specific inhibitor of ATM	ATMi	10 μM
VE-821	Specific inhibitor of ATR	ATRi	5 μM

Table 10 Solutions for flow cytometry

Solutions	Abbreviation	Compounds
Blocking buffer	PBG	0.2 % gelatin 0.5 % BSA (fraction V) 1 × PBS pH 7.4
Permeabilization solution		0.25 % Triton X-100 1 × PBS pH 7.4
Fixation solution	PFA	3 % paraformaldehyde 2 % Sucrose 50 ul 4N NaOH/500 ml 1 × PBS
Propidium iodide staining	PI	40 µg/ml propidium iodide 62 µg/ml RNaseA Buffer for RNaseA, pH 7.6 10 mM Tris 100 mM EDTA 50 mM NaCl Buffer for PI staining 0.1 M Tris 0.1 M NaCl 5 mM $MgCl_2$ 0.05 % Triton X-100

Table 11 Solutions for SDS-PAGE and immunoblotting

Solutions	Compounds
10 × running buffer	0.025 M Tris-HCl 0.192 M glycine 0.1 % SDS
4 × stacking gel buffer	0.5 M Tris-HCl, pH 6.8 0.4 % SDS
4 × resolving gel buffer	1.5 M Tris-HCl, pH 8.8 0.4 % SDS
2 × sample loading buffer	0.065 M Tris-HCl, pH 6.8 0.01 M EDTA 20 % glycerol 3 % SDS 0.02 % BrPBlue 5 % DTT
5 % stacking gel	16.8 % Rotiphorese® Gel 30 bidest. H_2O 0.125 M 4 × stacking gel buffer 0.1 % SDS 0.1 % APS 0.2 % TEMED
10 % resolving gel	34 % Rotiphorese® Gel 30 bidest. H_2O 0.37 M 4 × resolving gel buffer

	0.1 % SDS 0.1 % APS 0.1 % TEMED
4 × electrode buffer4	0.1 M Tris-HCl, pH 8.3 0.7 M glycine
western blot transfer buffer	25 % 4 × electrode buffer 20 % MeOH
5xBradford reagent	500 mg Coomassie Briliant Blue G-250 250 ml 95% ethanol 500 ml 85% phosphoric acid 250 ml pure sterile H_2O

Table 12 Gels for SDS-PAGE and immunoblotting

Gels	Supplier
4–20% Mini-PROTEAN ® TGX™ Precast Protein Gels, 12-well, 20 µl	BIO-RAD

Table 13 Software

Software	Supplier
EndNote 21	Thomson Reuters, USA
ZEN 2.6	Carl Zeiss AG
ImageJ	Image Processing and Analysis in Java,USA
ImarisXT 8.0.2	Bitplane AG, Switzerland
Kaluza 1.2	Beckman Coulter, USA
LasAF	Leica Microsystems，Germany
Microsoft Office 2013	Microsoft, USA
MultiCycle AV DNA Analysis	Phoenix Flow Systems, USA
Odyssey® Infrared Imaging System	LiCor Biosciences USA
Adobe Photoshop CS 5	Adobe Systems Inc. USA
SigmaPlot 14.0	Systat Software Inc. USA

Table 14 Major laboratory apparatuses

Laboratory apparatus	Model	Supplier
Bright field microscopy	VANOX-T	Olympus, Japan
Cell and Particle Counter	Z2 Coulter Counter®	Beckman Coulter Inc., USA
Cell culture CO2 incubators	MCO-18 AC(UV)	Sanyo, Japan
Centrifuge	MultifugeTM 3 S-R	Heraeus, Germany
Centrifuge (tabletop)	Biofuge FrescoTM	Heraeus, Germany

Electroporation device	NucleofectorTM I	Lonza Cologne GmbH, Germany
Flow cytometer	GalliosTM	Beckman Coulter Inc., USA
Laminar flow cabinet	HERAsafeTM	Heraeus, Germany
Infrared imaging system	Odyssey®	LI-COR Biosciences, Germany
Inverted phase contrast microscope	Motic AE 31	Motic, China
Nucleofector Bright-field microscopy		Nucleofector® Technology, Lonza Olympus VANOX-T, Japan
pH meter	InoLab®	WTW GmbH, Germany
SDS-PAGE equipment		Bio-Rad, USA
UV/VIS Spectrophotometer	UV-2401 PC	Shimadzu, Japan
X-ray machine, Isovolt 320		General Electric
GenePulser Xcell™ electroporation		Bio-Rad
Axio Scan Z1		ZEISS

3.2 Methods

3.2.1 Cell culture

Cells are cultured at 37 °C in a humidified incubator with 5% CO2. All growth media are supplemented with 100 µg/ml penicillin and 100 µg/ml streptomycin. The cells are maintained in 100 mm cell culture dishes containing 15 ml of growth medium with 10% fetal bovine serum (FBS). The cell lines and media used are detailed in Table 1 and Table 2. Cell lines are routinely passaged to prevent overgrowth and to ensure a stable, reproducible source of cells for experiments. To passage or collect cells, they are washed with 1x phosphate-buffered saline (PBS) and incubated in 1 ml of a 0.05% trypsin/EDTA solution for 2-5 minutes on a warm plate (42 °C) to detach them from the dish surface. After detachment, the cells are collected and resuspended in 5-7 ml of growth medium containing 10% FBS. Cell numbers are then measured using a Beckman Coulter Counter (Multisizer Z2). For the experiments, after transfection, the cells are plated in either 35 mm or 60 mm dishes with 2 ml or 5 ml of medium, respectively, or in 25 cm² flasks with 5 ml of medium. To avoid genetic drift, cells are discarded after approximately 30

passages. After thawing frozen cells, the initial two passages are not used for experiments. The cells used in experiments are in the exponential growth phase.

3.2.2 Transfection of cells with siRNA

In this thesis, siRNA duplexes are transfected into cultured eukaryotic cells using either Nucleofector® Technology (Lonza) or the GenePulser Xcell™ electroporation system, depending on the cell line (Table 6). These methods involve applying short electric pulses to temporarily destabilize the cell membrane, making it permeable, which allows siRNA oligonucleotides in the surrounding medium to enter the cytoplasm.

Cells are seeded on 100 mm dishes two days before transfection. To prevent cell death and resistance to macromolecule uptake post-transfection, cells are kept in the log phase of growth. They are harvested by trypsinization and centrifuged at 980 rpm for 3 minutes at room temperature. Up to 3 - 5 × 10^6 cells are resuspended in 100 µl of a custom transfection buffer (80 mM NaCl, 5 mM KCl, 12 mM glucose, 25 mM HEPES, 40 mM Na2HPO4/NaH2PO4, 20 mM MgCl2, 0.4 mM Ca (NO3)2), and 100 - 200 µmol siRNA is added (Table 5). The cells are then quickly transferred into an Ingenio® cuvette and subjected to either nucleofection® or the GenePulser Xcell™ electroporation system according to the specified program (Table 6). After electroporation, the sample is immediately transferred from the cuvette to freshly prepared, pre-warmed (37 °C) growth medium. The transfected cells are utilized for experiments 48 hours after transfection. For Western blot analysis, cells are plated in 100 mm dishes, and protein detection is performed 48 hours post-transfection. The efficiency of siRNA delivery is confirmed using a Green Fluorescent Protein (GFP) expression vector, with green fluorescence measured by flow cytometry 24 hours after transfection. Transfection efficiency is determined as the percentage of cells expressing GFP protein in the population.

3.2.3 X-ray irradiation

Cells are irradiated using an X-ray machine equipped with an MXR320 (Comet) X-ray tube, an ISOVOLT Titan (General Electrics) generator, and an Xrad320 (PXi) control unit, operating at 320 kV and 12.5 mA with a 1.65 mm aluminum filter. The irradiation occurs at room temperature in standard cell culture dishes, with distances adjusted according to dish sizes and rotation of the irradiation table to ensure uniform exposure. Cells in 30-60 mm diameter culture dishes are irradiated at a distance of 50 cm with a

dose rate of 3.6 Gy/min. For G2-checkpoint assays， cells in 25 cm^2 flasks are irradiated on a thin-walled aluminum box filled with pre-warmed water to maintain temperature stability, at a distance of 66 cm and a dose rate of 3.2 Gy/min. For G2 PCC assays, Cells in 25 cm2 flasks are irradiated at a distance of 50 cm with a dose rate of 3.6 Gy/min. Control samples undergo the same procedure without irradiation.

3.2.4 Clonogenic Survival Assay

Clonogenic survival assays are conducted to evaluate cell radiosensitivity to killing. Following siRNA transfection, 0.3 - 0.6 $x10^6$ cells are seeded in 60 mm dishes and incubated at 37°C with 5% CO_2. After two days of growth, the cells are either irradiated or directly harvested and reseeded in low numbers, targeting 30 - 150 colonies per 60 mm dish. After 11 - 14 days of incubation at 37°C with 5% CO_2, the colonies are stained with 1% crystal violet in 70% EtOH and counted.

3.2.5 Drug treatments

To treat cells with kinase inhibitors, a fresh, pre-warmed growth medium containing each drug is added to the cells one hour before irradiation, and the treatment is maintained until the cells are collected at various time points. The final concentrations of the drugs are provided in Table 9. Control cells receive an equal volume of DMSO. Post-irradiation, the cells are returned to the incubator or warm room for the designated time intervals. All experiments measuring the mitotic index are conducted in a warm room located near the irradiation source, specifically designed to minimize temperature fluctuations and ensure the accuracy of sensitive assays.

3.2.6 Flow cytometry

Flow cytometry (FC) using a Beckman Coulter Gallios flow cytometer is employed for analyzing cell cycle distribution and determining the mitotic index (MI) through H3pS10 labeling.

3.2.6.1 Cell cycle distribution

To determine cell cycle distribution, the fluorescence signal of the intercalating agent PI is analyzed, which emits red fluorescence excited by an Argon laser (488 nm). PI binds to double-stranded nucleic acids, and to eliminate signals from dsRNA, RNase is added. The intensity of the measured fluorescent signal is directly proportional to the amount of DNA and is utilized to ascertain the percentages of cells in the G1, S, and G2/M phases.

Since PI cannot penetrate cell membranes, cells must be permeabilized before staining with PI.

For cell cycle analysis, cells are collected, fixed in cold 70% EtOH, and stored at 4°C. Before flow cytometry (FC), cells are centrifuged at 4°C for 5 minutes at 1,500 rpm. Ethanol is removed, and the cell pellet is resuspended and incubated for 30 minutes at 37°C in PI staining solution (refer to Table 10). Gating based on forward and side scattering is applied to select cells of interest (single cells).

3.2.6.2 Determination of mitotic index

To determine the proportion of cells in mitosis, a two-parameter flow cytometry (FC) approach is used. Since cells in the M-phase have the same DNA content as G2-phase cells, phospho-Serine10 of histone H3 (H3pS10) staining is employed as a marker for mitotic cells, in addition to the standard PI staining.

For the determination of the mitotic index (MI), approximately 10^5 cells are plated in 25 cm^2 cell culture flasks. After one day of growth at 37°C and 5% CO_2, the flask caps are closed to maintain a steady CO_2 atmosphere, and the flasks are moved to a warm room set at a constant temperature of 37°C. To avoid the impact of temperature fluctuations on the MI, all subsequent steps are performed in the warm room at 37°C. The only exception is irradiation, which is carried out on a warm plate to minimize temperature changes.

Mitotic cells round up and can easily detach from the flask surface, so the growth medium is collected into 15 ml tubes instead of being aspirated. The cells are then washed with prewarmed 1X PBS, which is also collected into the same tubes. Cells are detached by trypsinization and collected in the prewarmed medium in the same tubes. After centrifugation at 1,200 rpm for 5 minutes at 4°C, the supernatant is removed, and the cells are fixed in cold 70% EtOH and stored overnight at -20°C.

To prepare for antibody labeling, cells are centrifuged at 2,000 rpm for 5 min at 4 °C and the supernatant is removed. 150 µl of primary antibodies diluted in PBG (see Table 3) are added and cells are incubated for 1.5 h at RT while shaking. For washing, 1 ml of 1X PBS is added to the samples before centrifugation and removal of the supernatant. This step is repeated once. Afterward, cells are incubated in 100 µl of secondary antibodies diluted 1:400 in PBG for 1 h at RT (see Table 3) while shaking in the dark. Cells are washed again with 1X PBS before centrifugation and then incubated in PI staining solution for

30 min at RT. Measurement is performed by Beckman Coulter Gallios flow cytometer. If treated with ATMi, ATRi (concentrations in Table 9), or DMSO (as a control), these are added 1 hour before irradiation.

3.2.7 G2 premature chromosome condensation (PCCs)

Approximately 0.2 - 0.6 x 10^6 cells are plated in 25 cm² cell culture flasks for cytogenetic experiments after transfection with siRNA. After two days of growth, the cells are irradiated with 0.5Gy X-ray. 50 nM Calyculin-A is added for 45 minutes before harvesting at the respective time point to induce PCC. The time of Calyculin-A treatment is included in the indicated repair time. After 45 minutes of incubation with the drug, the cultures are harvested. The cells are then centrifuged at 1200 rpm for 5 min at 4 °C to obtain a firm pellet with a clear supernatant. After discarding the supernatant, a hypotonic solution (75 mM KCl) is added dropwise to the cells to a final volume of 7 ml. The cells are resuspended in this solution and incubated for 14 minutes at room temperature. Then, an equal volume of methanol-acetic acid (3:1) is added before centrifuging for 7 minutes at 1,200 rpm at 4°C. The supernatant is removed, and the cells are resuspended in 7 ml of methanol-acetic acid for fixation and stored overnight at 4°C. The fixation procedure is repeated three times in Cornoy's fixative the next day. 15 µl fixed cells suspension is dropped on clean, wetted glass microscope slides, which are then allowed to air dry overnight. After drying, slides are stained with 6% Giemsa stain prepared in Sorenson's buffer for 10 minutes. After staining, slides are rinsed with tap water and allowed to air dry for several hours. Finally, slides are mounted using Entellan and covered with a coverslip. About 100 G2- PCCs are scored for excess PCC fragments at each experimental time point and results are summarized from three independent experiments. During scoring, chromatid breaks and gaps are considered – the latter only when they appear longer than the chromatid width. The analysis is done using bright field microscopy (Olympus VANOX-T, Japan).

3.2.8 Reporter system

U2OS GFP reporter cell lines (Gunn and Stark 2012) are employed to measure the repair of I-SceI induced DSBs by a specific DSB repair pathway. DR-GFP construct is used for analyzing HRR. EJ5-GFP construct is used for analyzing NHEJ (total end-joining or distal end-joining).SA-GFP construct is used for analyzing single-strand annealing (SSA) and the EJ2-GFP construct is used for analyzing alt-EJ (Mladenov et al. 2020). These

reporters are stably integrated into the genomes of the corresponding cell lines. Transfection of cells with I-SceI expression plasmid (1 µg pDNA/10^6 cells) was carried out 48 h after transfection with siRNA. The I-SceI mediated DSB was, thus, induced at the corresponding site and its repair by the indicated DSB repair pathway generated a GFP signal that was measured with a Gallios® flow cytometer (Beckman Coulter) 48 h later.

3.2.9 Immunofluorescence staining

For immunofluorescence experiments, approximately 2 - 6 × 10^6 cells are seeded into 35 mm dishes containing Ø 20 mm glass coverslips following transfection. After a growth period of two days, the cells are subjected to irradiation (0 - 2 Gy) and maintained at 37 °C with 5 % CO2 until the specified time points for examining IRIF formation (1 - 6 hours). To identify cells in the S-phase during irradiation, they are additionally incubated with 10 µM of the thymidine analog EdU for 30 min at 37 °C with 5 % CO2 before irradiation. Following irradiation, the cells are washed with 1X PBS and a fresh standard growth medium is added. For fixation, the medium is removed, and the cells are washed with 1X PBS before being incubated in 2 ml of 2 % PFA (with an optional 2 % sucrose) in 1X PBS for 15 min at room temperature (RT). The PFA solution is then removed, and the cells are washed with 1X PBS. For permeabilization, 2 ml of P-solution (100 mM Tris pH 7.4, 50 mM EDTA in bidest. H_2O) containing 0.5 % Triton X-100 is added for 7 min at RT. After removing the P-solution and performing another wash with 1X PBS, the cells are incubated in 2 ml of PBG (0.2 % gelatin, 0.5 % BSA fraction V in 1X PBS) overnight at 4 °C. Post-blocking, the cells are incubated with primary antibodies (diluted in PBG, Table 3) for 1.5 h at RT. The coverslips are then washed three times with 1X PBS for 5 min. Secondary antibodies conjugated with Alexa Fluor dyes (Table 3) are diluted 1:400 in PBG and incubated with the cells for 60 min at RT in the dark. The coverslips are washed one time with 1X PBS. If EdU incorporation was performed earlier, EdU is labeled using the Click-iT reaction cocktail (see Table 7) by incubating the cells in 90 µl of EdU labeling solution for 30 min at RT. Following this, the coverslips are washed two times with 1X PBS before incubating the cells with DAPI (50 ng/ml) for 10 minutes at RT in the dark to stain the DNA. Finally, the cells are washed two times with 1X PBS and mounted on microscopic slides using PromoFluor Antifade Reagent. After the

mounting medium solidifies in the dark at RT, 3D images are scanned using an Axion Scan Z1 Slide Scanner.

3.2.10 PAGE and immunoblotting

Immunoblotting is utilized to detect specific proteins by separating them based on their molecular weight. In this thesis, the focus is on the analysis of the proteins CAP-H and CAP-D3. Following protein extraction, the concentration is measured using the Bradford reagent assay. Subsequently, 60 µg of protein extract is mixed in a 1:1 ratio with 2 × sample loading buffer (see Table 11) and denatured by heating at 96 °C for 5 minutes. Before loading onto the gel, the samples are briefly centrifuged at 13,000 rpm. During SDS polyacrylamide gel electrophoresis (SDS-PAGE), CAP-H and CAP-D3 proteins are separated on a 10% SDS polyacrylamide gel under a constant voltage of 120 V for 105 to 120 minutes. Alternatively, when using Mini-PROTEAN TGX precast gels, the proteins are separated on a 4-15% polyacrylamide gel under the same constant voltage and duration.

For Western blotting, the proteins separated on the polyacrylamide gel are transferred onto an Odyssey® 0.22 µm nitrocellulose membrane using a wet transfer apparatus at 280 mA 2 hours, with the temperature maintained at 4 °C. Following the transfer, the membrane is blocked for 1 hour at room temperature with 5% non-fat dry milk in 1X TBS (25 mM Tris-HCl, pH 7.6, 150 mM NaCl) while gently shaking. The membrane is then incubated overnight at 4 °C with primary antibodies diluted in 5% non-fat dry milk in TBS-T (1X TBS with 0.05% Tween-20), as specified in Table 3. After primary antibody incubation, the membrane is washed three times for 10 minutes each with TBS-T before being incubated with secondary antibodies (diluted in TBS-T as per Table 3) for 1 hour at room temperature. This is followed by another three washing steps with TBS-T for 10 minutes each. Finally, the membrane is allowed to dry, and the detection of CAP-H and CAP-D3 is carried out using the Odyssey® Infrared Imaging System (LI-COR Biosciences).

4. Statistical analysis

The majority of the data comes from at least three independent experiments, with the results expressed as the mean ± standard deviation. SigmaPlot 14 was used to generate the graphs. For the dependent observations, the logarithms of the normalized surviving fractions from each experiment were analyzed, covering a minimum of three cell culture plates. Nonlinear regression curve fitting (SigmaPlot 14) was employed for the statistical analysis of the colony assays.

Statistical significance was determined using the Student's t-test routine available in SigmaPlot 14. Statistical significance was indicated as * $p < 0.05$, ** $p < 0.01$, *** $p < 0.001$, ****$p<0.0001$.

5. Results

5.1 Origin of the Retinal pigment epithelial cell line (RPE-1) and lung carcinoma epithelial cells (A549)

Radiation therapy is a widely used treatment modality for cancer, particularly for carcinomas derived from epithelial cells, which account for over 80% of malignant tumors. To study the repair mechanisms involved in DSB repair after IR, it is appropriate to use a normal epithelial cell line as a model for normal tissue and follow up with human tumor cell lines to model tumors. RPE-1 cells, derived from normal human retinal pigment epithelium (RPE) cells and immortalized with the human telomerase reverse transcriptase (hTert) gene, can serve as a model for this purpose.

Introducing hTert into RPE-1 cells restores telomerase activity, thereby extending their replicative lifespan without affecting the DNA damage response (DDR) or causing abnormal cell growth and oncogenic transformation (Jiang et al. 1999). The RPE-1 hTert cell line was generated by transfecting the RPE-340 cell line with the pGRN145 plasmid that expresses hTert (ATCC® CRL-4000™) (Matsunaga et al. 1999; Bodnar et al. 1998)

The immortalization of RPE-1 hTert cells allows long-term cultivation, which is crucial for investigating DNA repair processes occurring over multiple cell cycles and in different phases of the cell cycle. RPE-1 hTert cells can be readily cultured in vitro and exhibit a robust and efficient DDR upon exposure to IR. This response involves the activation of DNA damage checkpoint pathways, DNA repair mechanisms, and cell cycle arrest to suppress the propagation of damaged DNA into progeny.

The combination of RPE-1 hTert cell line's widespread use for studying DDR with its ease for in vitro culturing and its immortalized nature, makes it well-suited for experiments on the role of condensins on DSB repair after IR.

Tumor cell lines are physiologically different from normal cells and show often different responses to DNA damage that generate opportunities for the treatment of the corresponding tumors. It was therefore relevant to examine the role of condensins in representative tumor cell lines. Since tumor cells originate from actual tumors, they retain several of the genetic alterations found in these cancers, and may even predict their response to radiation. A549 cells, derived from human lung adenocarcinoma, possess a

wild-type p53 gene. These cells exhibit a robust and well-characterized DNA damage response, making them an excellent model for studying DSB-induced signaling. Their ability to activate the ATM and ATR pathways, which are essential for initiating DSB repair, allows for an accurate assessment of the effects of condensin suppression on these pathways.

Known for their high transfection efficiency, A549 cells and RPE-1 hTert cells are advantageous for experiments involving gene knockdown (Xiao et al. 2022; Pei et al. 2022) or overexpression. Efficient transfection allows for effective suppression of condensins proteins using siRNA, ensuring reliable and reproducible results in subsequent analyses of their consequences on DSB repair pathways.

The A549 cell line has been extensively used in previous studies to investigate various aspects of DNA repair mechanisms (Luo et al. 2023; Xiao et al. 2022; Mladenov et al. 2020; Wang et al. 2019). This extensive background knowledge facilitates the design and interpretation of experiments, as well as the comparison of new findings with the existing literature.

5.1.1 Cell growth characteristics of RPE-1 hTert cells and A549 cells

To establish optimal growth conditions for the experiments described in this study, an initial number of 1×10^5 cells is plated in 60 mm dishes with 5 ml of growth medium. The cell population is then monitored and recorded over several days to track proliferation (Figure 13A, C). Additionally, the distribution of cells across different stages of the cell cycle is analyzed using propidium iodide (PI) staining and one parameter flow cytometry (FC) (Figure 13B, D). This analysis provides insights into the cell cycle dynamics and allows characterization of the cell population at various stages of growth.

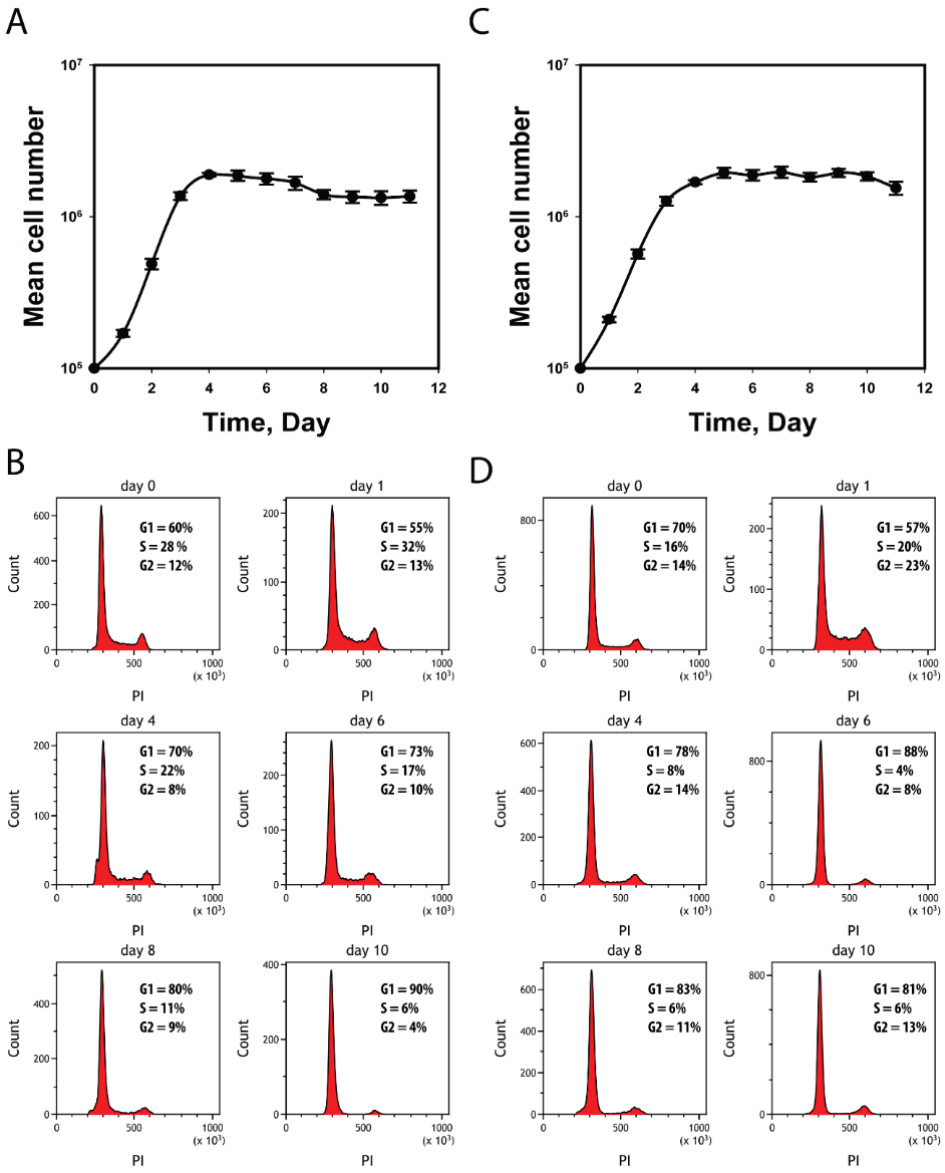

Figure 13: Growth curve of RPE-1 hTert cells and A549 cells. (A): After plating 10^5 cells per dish and allowing for growth over several days, the number of RPE-1 hTert cells was determined using a Beckman Coulter Counter. The data presented here represent the means ± SD from three independent experiments. (B): The cell cycle distribution of representative cultures was assessed at the indicated time points by FC analysis (PI staining). (C): Same as panel (A), but for A549 cells. (D): Same as panel (B), but for A549 cells.

5.1.2 Clonogenic survival assay

The clonogenic survival assay is a well-established technique used to assess the ability of cells to undergo multiple divisions and form colonies after exposure to different treatments, such as radiation, chemotherapy, or drug therapy. In this study, RPE-1 hTert cells and A549 cells in the exponential growth phase were exposed to varying doses of X-rays, ranging from 0 to 8 Gy. As the X-ray dose increased, there was a gradual decrease

in the colony-forming ability of the cells. At the highest dose of 8 Gy, very few or no colonies were observed in RPE-1 hTert cells (Figure 14A), indicating that higher doses of X-rays significantly impair their clonogenic potential. However, in the case of A549 cells, a much larger number of colonies were observed at the 8 Gy dose (Figure 14B). These findings demonstrate that the two cell lines exhibit markedly different radiosensitivities to X-ray irradiation (Figure 14C).

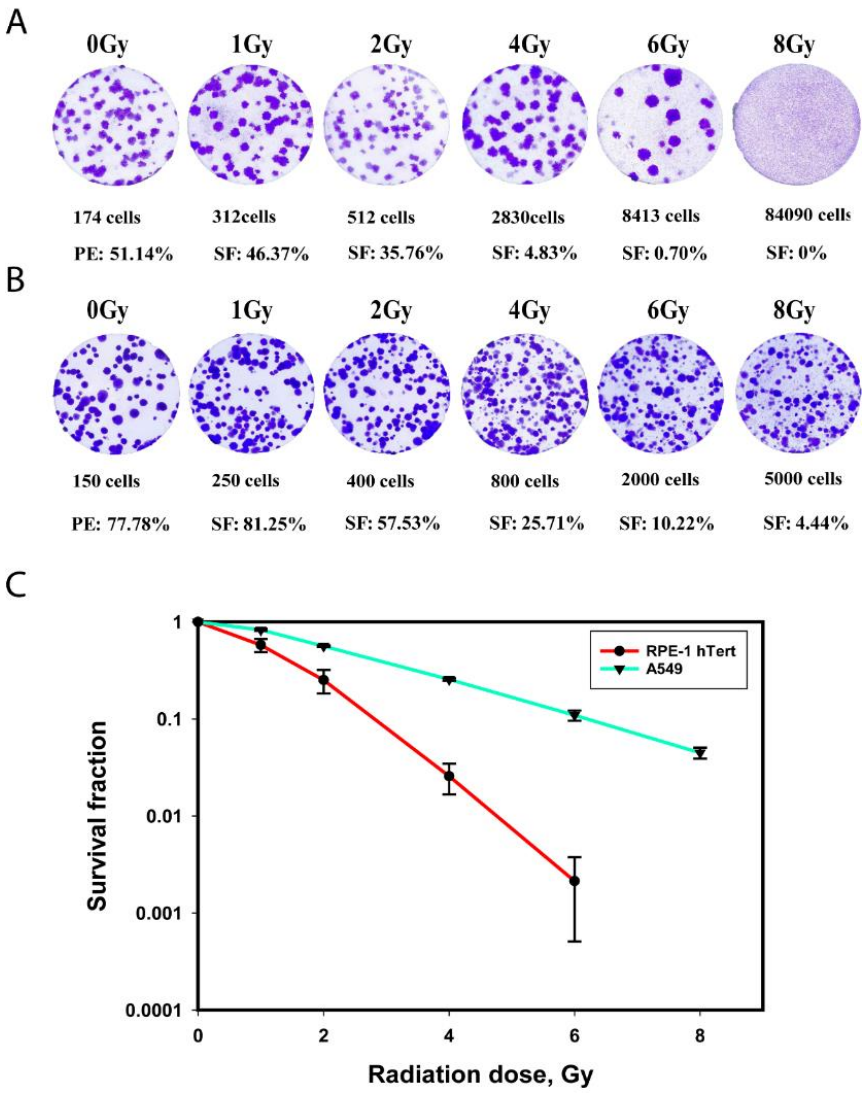

Figure 14: Clonogenic survival assay of RPE-1 hTert cells and A549 cells. (A) Representative images of colony formation of RPE-1 hTert cells. Exponentially growing cells were irradiated with different dose of X-rays and seeded for colony formation at the indicated numbers per dish, 11 days post IR cells were stained with crystal violet and colonies were counted. (B) Same as panel (A), but for A549 cells, 14 days post IR cells were stained with crystal violet and colonies were counted. (PE: plating efficiency, SF: surviving fraction. PE =Number of colonies counted/Number of unirradiated cells seeded x 100, SF= Colonies counted/ [Cells seeded × (PE/ l00)]. (C) Survival curve for cells exposed to IR. Data shown here represent means ± SD from three determinations in three experiments.

5.2 Analysis of expression of the condensin I and II subunits in RPE-1 hTert cells

To examine the expression of condensin I subunit CAP-H, condensin II subunit CAP-D3, and shared subunit SMC2 proteins in untreated RPE-1 hTert cells, western blotting was performed under various conditions. Positive bands indicating protein presence were observed for CAP-H and SMC2 when using both a 10% gel and a 4%-15% gradient gel (Figure 15C, D, E, F). However, the use of a 4%-15% gradient gel proved to be more effective compared to a 10% gel under the same experimental conditions employed. Conversely, CAP-D3 protein was not detected when using a 10% gel; only the 4%-15% gradient gel yielded a positive result (Figure 15A, B). These findings highlight the importance of gel composition in achieving optimal detection of specific protein targets.

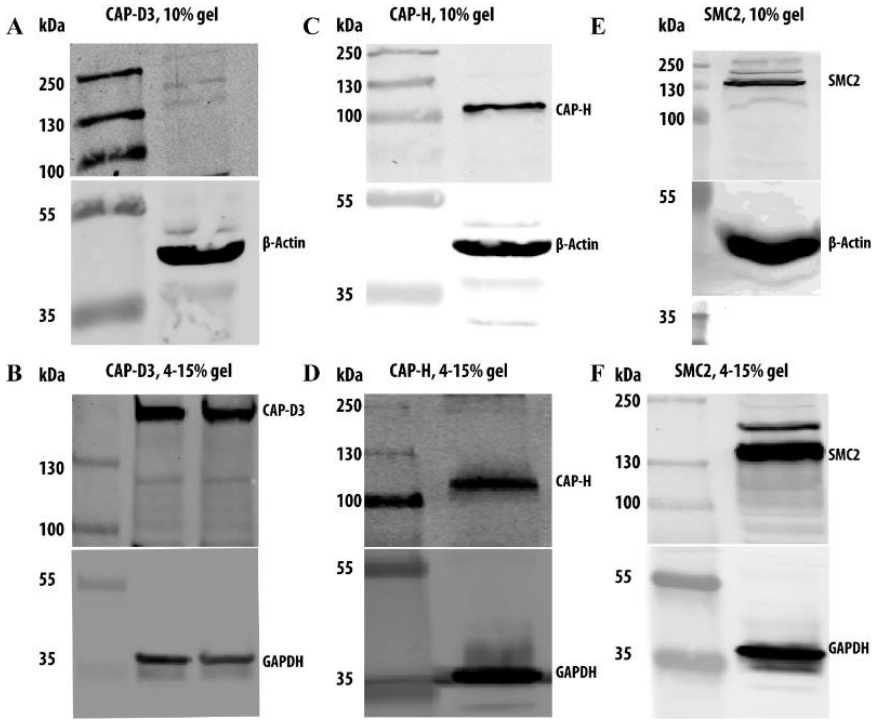

Figure 15: Detection CAP-H and CAP-D3 by western blotting using different gel constitutions. (A, B) Detection of human CAP-D3 using a 10% gel and a 4-15% gradient gel, respectively. Only the 4-15% gel detected the CAP-D3 protein. (C, D) Detection of human CAP-H using a 10% gel and a 4-15% gradient gel, respectively. Positive bands were observed in both cases. (E, F) Detection of human SMC2 using a 10% gel and a 4-15% gradient gel respectively. Positive bands were observed in both cases. However, the 4-15% gradient gel bands appear clearer and stronger.

Based on the results, in subsequent experiments, the expression of CAP-H, CAP-D3, and SMC2 was examined using 4%-15% gels.

5.3 Knockdown efficiency-test for CAP-H and SMC2 in RPE-1 hTert cells.

As the RPE-1 hTert cells naturally express condensin, it was essential to reduce the expression of condensin through siRNA knockdown in order to study its contributions to DSB repair and checkpoint control in irradiated cells. As a guide for the efficiency of siRNA transfection, a Green Fluorescent Protein (GFP) expression vector was co-transfected. The fluorescence emitted by GFP was measured by flow cytometry at 24 h and 48 h post-transfection (Figure 16). This assessment allowed for the evaluation of transfection efficiency and served as a predictor of successful knockdown of condensin expression in the RPE-1 hTert cells.

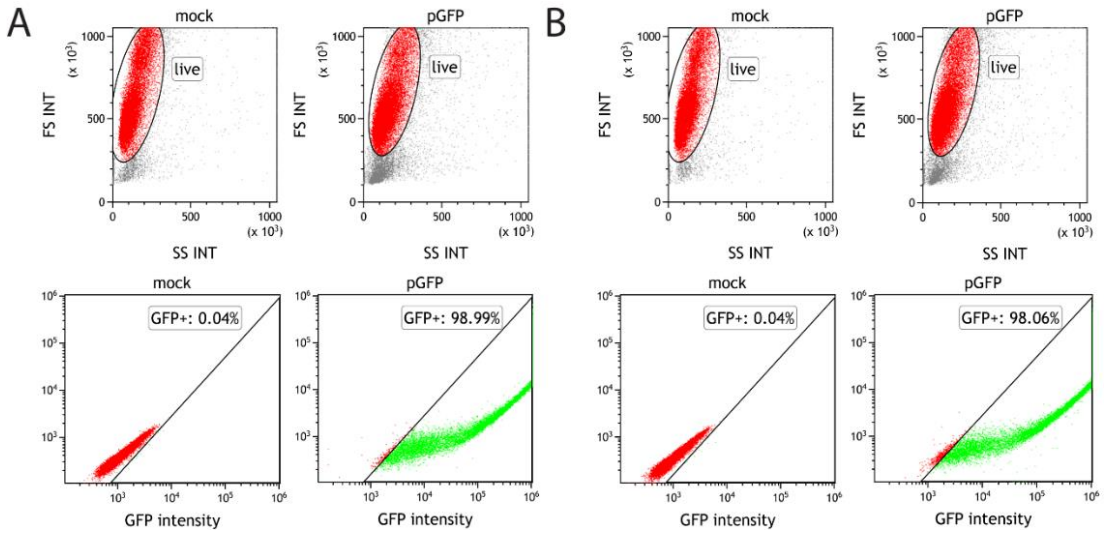

Figure 16: Transfection efficiency measured by GFP intensity in RPE-1 hTert cells. (A) Histograms of cell viability and GFP intensity in RPE-1 hTert cells 24 h after transfection with mock and pGFP plasmid. (B) Histograms of cell viability and GFP intensity in RPE-1 hTert cells 48 h after transfection, mock-transfection and with pGFP plasmid.

To assess the knockdown efficiency of various siRNA sequences targeting CAP-H and SMC2, Western blotting was performed following the transfection of these siRNA sequences, along with a negative control siRNA that does not target any known gene sequence in the organism under study. The results indicated that siSMC2-1 and siSMC2-4 exhibited superior knockdown efficiency compared to the other siRNA sequences tested. The protein levels of SMC2 were reduced by approximately 80% following transfection (Figure 17A). Consequently, a combination of siSMC2-1 and siSMC2-4 at equal amounts was selected for subsequent investigations.

Regarding the siCAP-H sequences, a cocktail comprising siCAP-H-1, siCAP-H-2, siCAP-H-3 and siCAP-H-4 demonstrated the most effective knockdown efficiency, resulting in over 80% suppression of CAP-H protein levels (Figure 17B). Therefore, this siCAP-H cocktail was utilized in subsequent studies to achieve efficient knockdown of CAP-H expression.

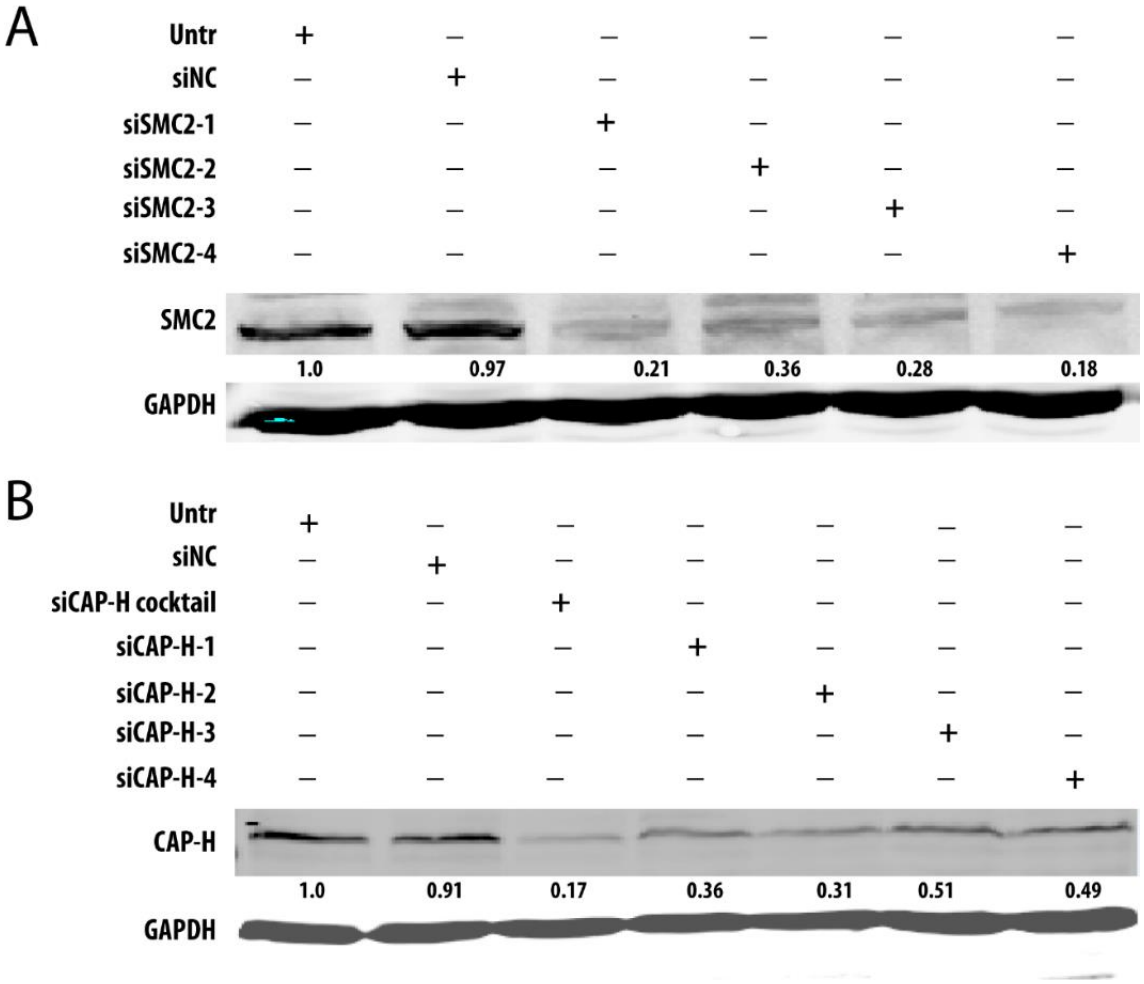

Figure 17: The expression of CAP-H and SMC2 proteins was analyzed post-transfection with different siRNA sequences using western blotting. (A) The expression of SMC2 was analyzed 48 hours after transfection with different siRNA sequences and a control negative siRNA; untreated cells are also shown. (B) the expression of CAP-H was analyzed 48 hours after transfection with different siRNA sequences and a control negative siRNA; untreated cells are also shown.

5.4 Effects of condensin knockdown on RPE-1 hTert cells and A549 cells radiosensitivity

To investigate the functions of condensin in DSB repair, we employed a clonogenic survival assay as discussed above to assess the radiosensitivity of cells following condensin suppression. The results obtained are discussed next.

5.4.1 Effects of condensin I knockdown on RPE-1 hTert cells radiosensitivity

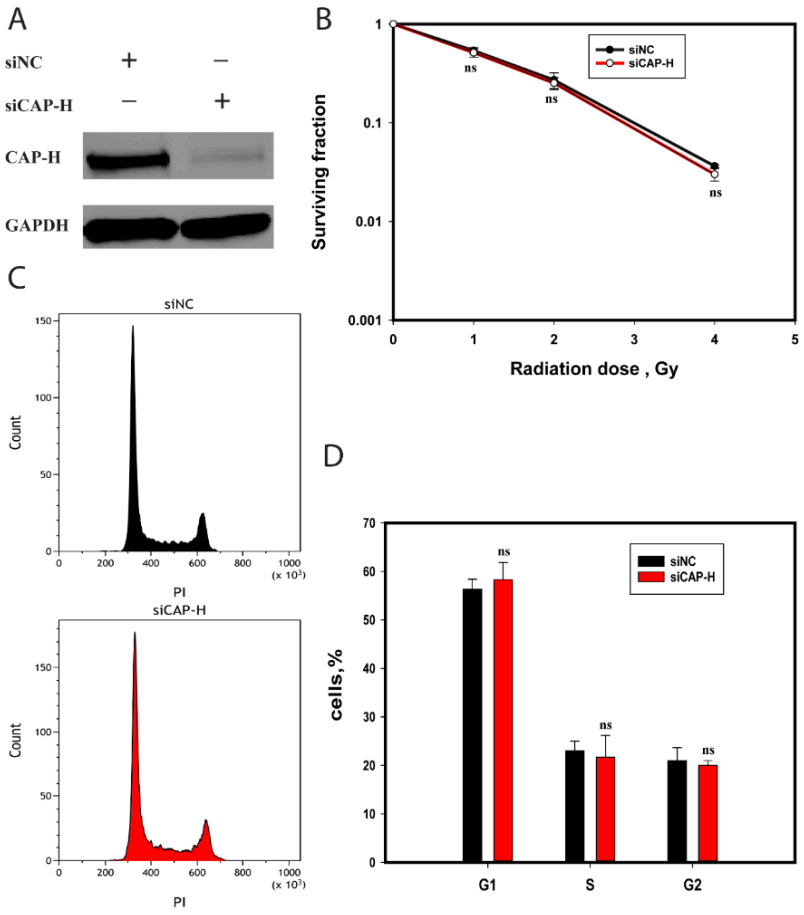

Figure 18: Effect of condensin I knockdown on radiosensitivity of RPE-1 hTert cells (A)Western blot analysis of CAP-H in RPE-1 hTert cells 48 h post transfection with specific siRNA targeting CAP-H protein; GAPDH serves as loading control. (B) Clonogenic survival experiments of RPE-1 hTert cells transfected with siCAP-H and negative control siRNA. (C) Flow cytometry histograms of RPE-1 hTert cells after transfection with siCAP-H and negative control siRNA. (D) Distribution of CAP-H knockdown RPE-1 hTert cells in different cell cycle phases. The analysis shows no significant differences between negative control (siNC) and CAP-H knockdown (siCAP-H) cells. Data represent the mean ± SD from three independent experiments. The significance level, or p-value, is calculated using the two-tailed. Student's t-test: ns (not significant).

In the context of condensin I, CAP-H serves as one of its subunits. By knocking down CAP-H, the functionality of condensin I can be inhibited. Interestingly, in contrast to the

control group, when the expression of condensin I was suppressed, the surviving fraction remained unchanged, and there was no significant alteration observed in the distribution of cells in the cell cycle (Figure 18C, D). Consequently, it can be concluded that the suppression of condensin I did not have any discernible impact on the radiosensitivity of RPE-1 hTert cells (see Figure 18B).

5.4.2 Condensin II surpression has no effect on the radiosensitivity of RPE-1 cells

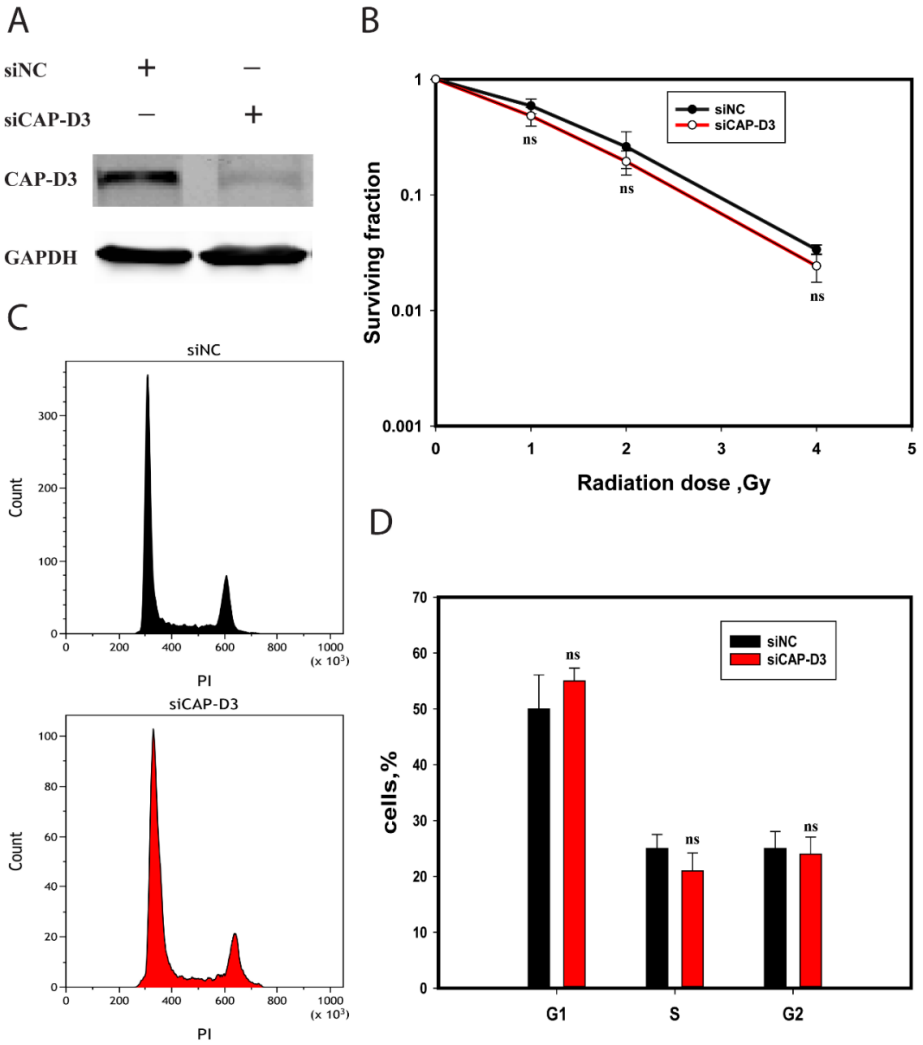

Figure 19: Effect of condensin II knockdown on radiosensitivity of RPE-1 hTert cells. (A) Western blot analysis of CAP-D3 in RPE-1 hTert cells 48 h post transfection with a specific siRNA targeting CAP-D3 protein; GAPDH serves as loading control. (B) Clonogenic survival experiments of RPE-1 hTert cells transfected with siCAP-D3 and negative control siRNA. (C) Flow cytometry histograms of RPE-1 hTert cells after transfection with siCAP-D3 and negative control siRNA. (D) Distribution of CAP-D3 knockdown RPE-1 hTert cells in different cell cycle phases. Data represent the mean ± SD from three independent experiments. The significance level, or p-value, is calculated using the two-tailed Student's t-test: ns (not significant).

In the context of condensin II, CAP-D3 serves as one of its subunits. The knockdown of CAP-D3 can effectively inhibit the function of condensin II. Compared to the control group, suppressing condensin II resulted in a slight rise in the number of cells in the G1.

5.4.3 Combined knockdown of condensin I and condensin II radiosensitizes RPE-1 hTert cells and A549 cells

Following our investigation of the radiosensitivity of RPE-1 hTert cells with individual knockdown of Condensin I and Condensin II, we proceeded to study the impact of double knockdown targeting both Condensin I and Condensin II. At 48 h after transfection, compared to the control group, cells with suppressed Condensin I and Condensin II (referred to as condensins) exhibited a slight, but not significant, increase in the number of cells in the G1 phase. Significantly, the surviving fraction of these cells was lower than that of the control group (Figure 20B). This observation was additionally verified in the A549 tumor cell line (Figure 20F). These findings strongly indicate that the suppression of condensins sensitizes RPE-1 hTert cells and A549 cells to radiation and suggest that these proteins play important functions in their response to IR.

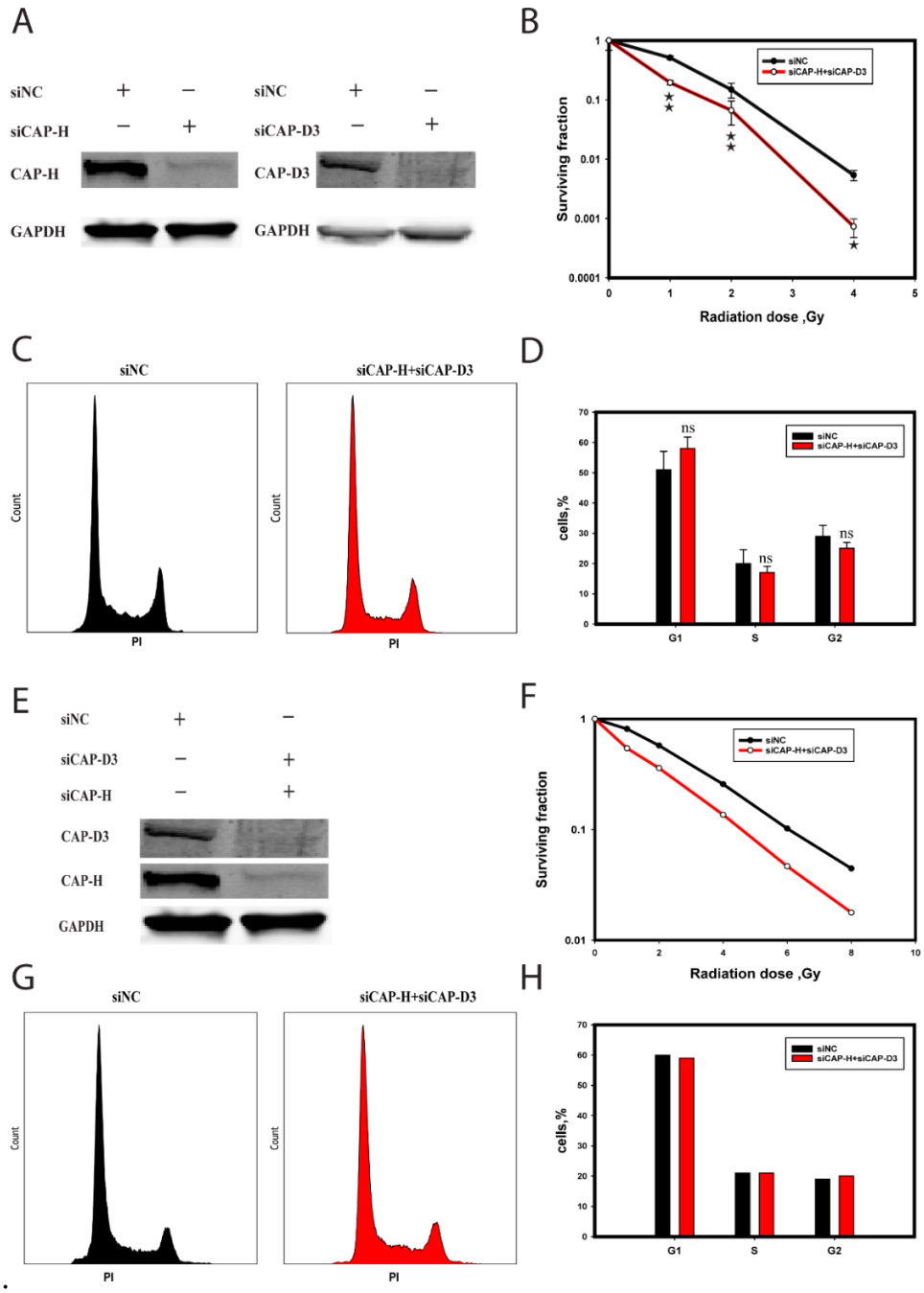

Figure 20: Effect of condensin I and condensin II knockdown on radiosensitivity of RPE-1 hTert cells and A549 cells. (A) Western blot analysis of CAP-H and CAP-D3 protein levels in RPE-1 hTert cells 48 h post transfection with siCAP-H+siCAP-D3, or a negative control siRNA; GAPDH serves as loading control. (B) Clonogenic survival experiments of RPE-1 hTert cells transfected with siCAP-H + siCAP-D3 and negative control siRNA. (C) Flow cytometry histograms of RPE-1 hTert cells after transfection with siCAP-H + siCAP-D3 and negative control siRNA. (D) Distribution of CAP-H + CAP-D3 knockdown RPE-1 hTert cells in different cell cycle phases. (E) Same as panel (A), but for A549 cells. (F) Same as panel (B), but for A549 cells. (G) Same as panel (C), but for A549 cells. (H) Same as panel (D), but for A549 cells. Data for RPE-1 hTert cells represent the mean ± SD from three independent experiments. The significance level, or p-value, is calculated using the two-tailed Student's t-test: ns (not significant), * $p < 0.05$, ** $p < 0.01$.

5.4.4 SMC2 suppression impacts the survival of RPE-1 hTert cells and A549 cells

SMC2 serves as a common subunit for both condensin I and condensin II. Knocking down SMC2 can therefore effectively inhibit the function of both condensin I and condensin II. To investigate using a different approach the combined effects of suppressing both Condensin I and Condensin II on cell cycle distribution and cell survival, experiments were conducted on RPE-1 hTert cells and A549 cells (Figure 21). The results demonstrated that the suppression of Condensins led to a noteworthy increase in the number of cells in the G1 phase and a significant decrease in the number of cells in the S phase compared to the control group. However, no significant difference was observed in the G2 phase fraction (Figure 21C, D, G, H). In addition, the plating efficiency was 61% in RPE-1 hTert cells and 79.5% in A549 cells for the control group, but dropped to just 1.1% and 2.1% in SMC2 knockdown cells, respectively (Figure 21B, F). These findings strongly indicate that combined suppression of both condensins through their SMC2 subunit has such an effect on cell viability that precludes analysis of radiosensitization.

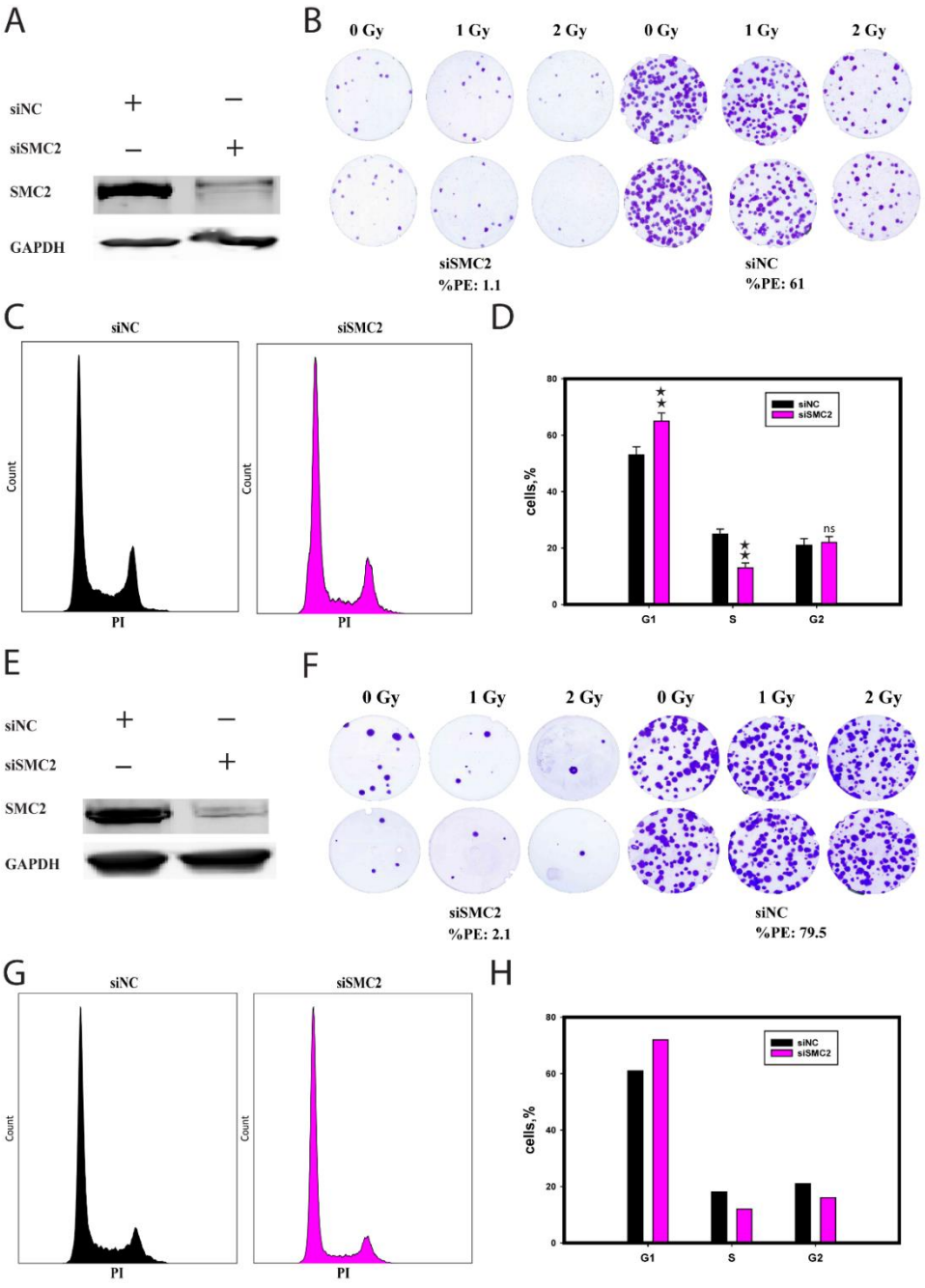

Figure 21: Effect of SMC2 knockdown on radiosensitivity of RPE-1 hTert cells. (A) Western blot analysis of SMC2 protein levels in RPE-1 hTert cells 48 h post transfection with siSMC2 or negative control siRNA; GAPD-H serves as loading control. (B) Representative images clonogenic survival assays of RPE-1 hTert cells after transfection with siSMC2 or negative control siRNA. (C) Flow cytometry histograms of RPE-1 hTert cells after transfection with siSMC2 or negative control siRNA. (D) Distribution of siSMC2 knockdown RPE-1 hTert cells in different cell cycle phase. (E) Same as panel (A), but for A549 cells. (F) Same as panel (B), but for A549 cells. (G) Same as panel (C), but for A549 cells. (H) Same as panel (D), but for A549 cells. Data for RPE-1 hTert cells represent the mean ± SD from three independent experiments. The significance level, or p-value, is calculated using the two-tailed Student's t-test: ns (not significant), ** $p < 0.01$.

5.5 Effects of condensins on DSB signaling

γH2AX is the most widely used markers for DSBs. ATM, the primary kinase responsible for H2AX phosphorylation that generates γH2AX and extends this phosphorylation bidirectionally from the break sites, creating binding sites for signal transducers (more detail in introduction).

53BP1 is a crucial protein in the cellular response to DNA DSBs. Upon occurrence of DSBs, it is rapidly recruited to the break sites, forming distinct nuclear foci. 53BP1 protects DNA ends from excessive resection, thereby favoring NHEJ over HR. While promoting NHEJ, 53BP1 concurrently inhibits HR by preventing extensive DNA end resection, a critical step for HR to proceed (Zimmermann and de Lange 2014).

In this study, we examine the impact of condensins depletion on DDR signaling, as documented by the formation of γH2AX and 53BP1 foci.

Under control conditions, analysis of γH2AX foci in RPE-1 hTert cells reveals a maximum of approximately 36 foci 1 h after 1 Gy of IR exposure. After 6 h, more than 70% of these foci are resolved, indicating ongoing DSB repair. In contrast, cells with condensins knockdown show a slightly higher initial number of foci, with around 40 foci observed 1 h after 1 Gy of IR. Six h post-IR, there is only a 15% reduction in the number of DSBs that develop γH2AX foci (Figure 22B, C). The number of residual γH2AX foci at 6 h is significantly higher than in control cells.

The results obtained in A549 cells were consistent with those observed in RPE-1 hTert cells. Specifically, condensins depletion led to an increase in the formation of γH2AX foci, and significantly compromised their resolution. This indicates that the ability of cells to effectively repair this damage is markedly impaired in the absence of condensins.

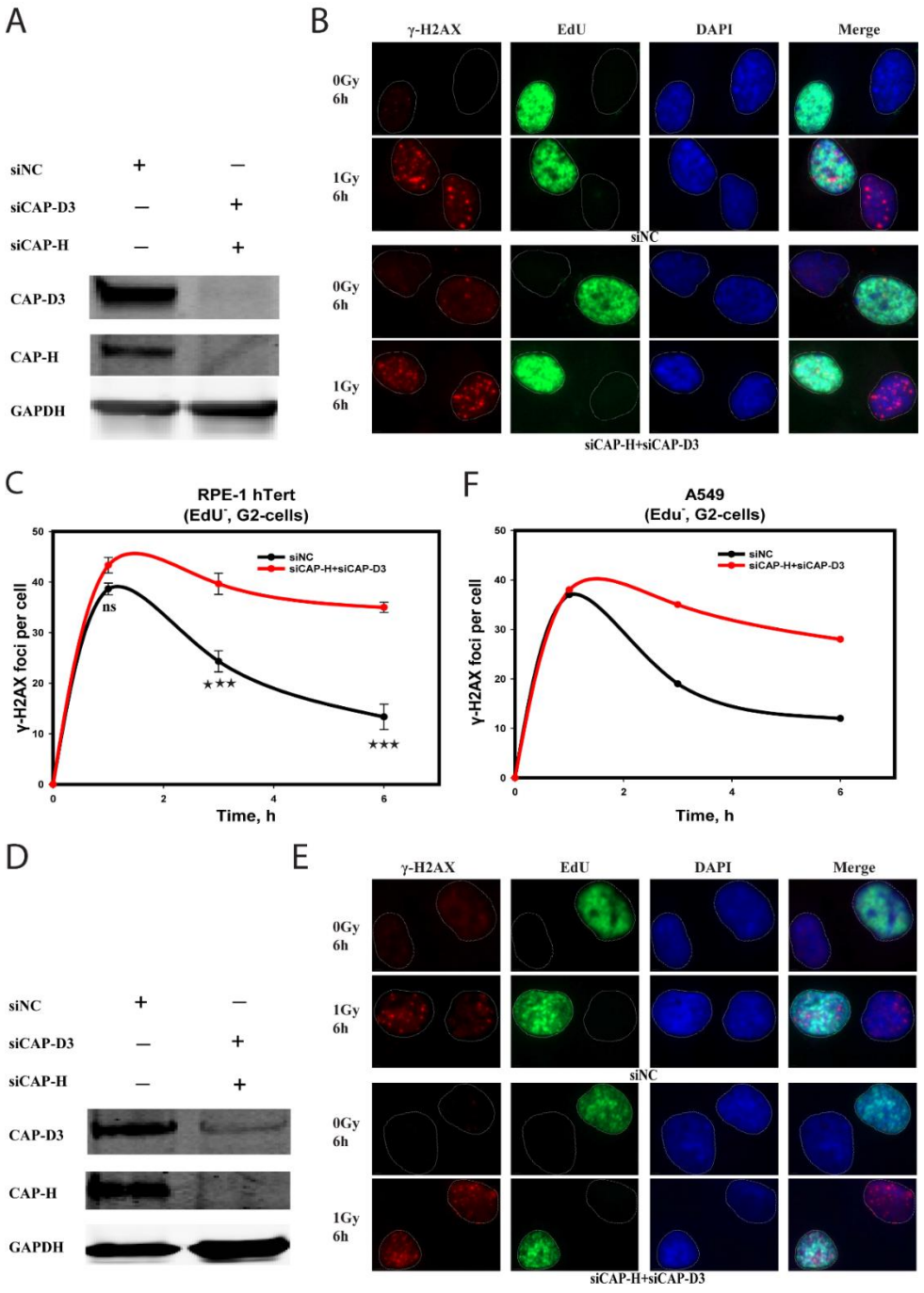

Figure 22: Condensins deficiency increases IR-induced DSBs signaling as γH2AX foci. (A) Western blot analysis of CAP-H and CAP-D3 protein levels in RPE-1 hTert cells 48 h post transfection with siCAP-H + siCAP-D3; GAPDH serves as loading control. (B) Representative images of γH2AX foci in RPE-1 hTert cells, irradiated with 1 Gy of X-rays and collected at the indicated times after irradiation. 48h before irradiation, cells were transfected with siNC or siCAP-H + siCAP-D3. (C) Quantification of γH2AX foci in siNC and siCAP-H + siCAP-D3, RPE-1 hTert, EdU-, G2-cells. (D) Same as panel (A), but for A549 cells. (E) Same as panel (B), but for A549 cells. (F) Same as panel (C), but for A549 cells. Cell cycle-specific γH2AX foci analysis was performed in EdU negative, G2 phase cells (EdU-, G2-cells) as described in Materials and Methods. The scale bar is 30 μm for all images. Data for RPE-1 hTert cells represent the mean ± SD from three independent determinations. The significance level, or p-value, is calculated using the two-tailed Student´s t-test: *** $p < 0.001$.

Following ATM activation, the mediator protein 53BP1 is activated in response to DSBs. This protein, in conjunction with BRCA1, is believed to influence the repair pathway choice by promoting cNHEJ and inhibiting end resection. Consequently, we examine here the formation of 53BP1 foci in cells deficient in condensins after IR exposure.

Under control conditions, analysis of 53BP1 foci in RPE-1 hTert cells shows a maximum of about 46 foci 1 h after 1 Gy of IR. After 6 h, over 75% of these foci are resolved, indicating ongoing DSB repair. In cells with condensin knockdown, there is a slightly higher initial count of about 50 foci 1 h after 1 Gy of IR. 6 h post-IR, only a 25% reduction in DSBs is observed, and the number of residual 53BP1 foci at 6 h is significantly higher than in control cells (Figure 23B, C).

The results from A549 cells aligned with those seen in RPE-1 hTert cells. Specifically, condensins depletion caused a slight increase in 53BP1 foci formation but significantly impaired their resolution (Figure 23E, F).

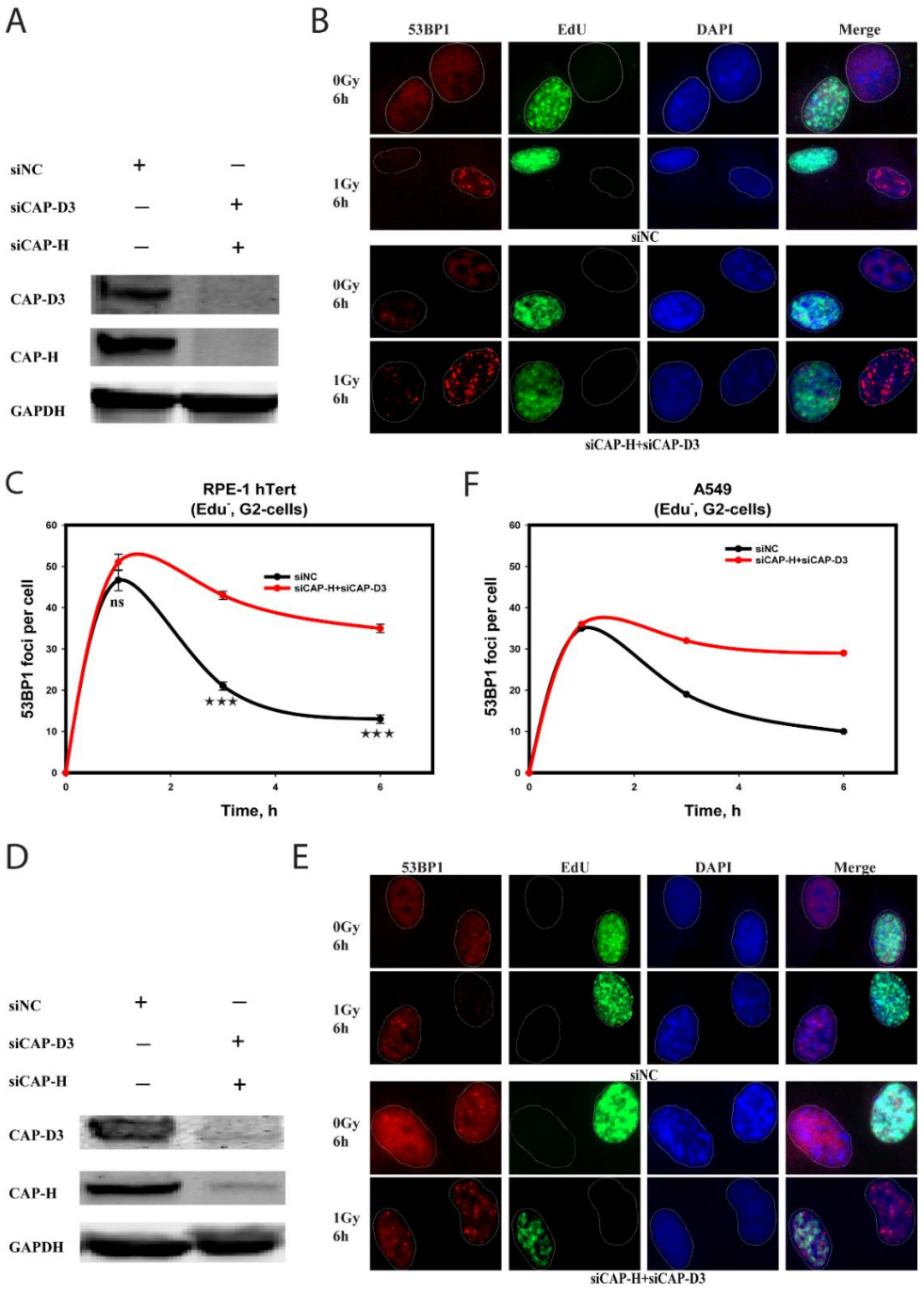

Figure 23: Condensins deficiency increases IR-induced DSBs signaling in the form of 53BP1 foci. (A) Western blot analysis of CAP-H and CAP-D3 protein levels in RPE-1 hTert cells 48 h post transfection with siCAP-H + siCAP-D3; GAPDH serves as loading control. (B) Representative images of 53BP1 foci in RPE-1 hTert cells, irradiated with 1 Gy of X-rays and collected at the indicated times after irradiation. 48 h before irradiation, cells were transfected with siNC or siCAP-H + siCAP-D3. (C) Quantification of 53BP1 foci in siNC and siCAP-H + siCAP-D3, RPE-1 hTert, EdU$^-$, G2-cells. (D) Same as panel (A), but for A549 cells. (E) Same as panel (B), but for A549 cells. (F) Same as panel (C), but for A549 cells. Cell cycle-specific 53BP1 foci analysis was performed in EdU negative, G2 phase cells (EdU$^-$, G2-cells) as described in Materials and Methods. The scale bar is 30 μm for all images. Data for RPE-1 hTert cells represent the mean ± SD from three independent determinations. The significance level, or p-value, is calculated using the two-tailed Student´s t-test: *** $p < 0.001$.

5.6 The role of condensins in DSB repair pathway choice

To explore the impact of condensins knockdown on the four known DSB repair pathways, we utilized a set of U2OS GFP reporter cell lines. These cell lines have been established as a useful tool for investigating DSB repair pathway engagement and inhibition. Each of the four U2OS GFP reporter cell lines carries a stable integration of a specific construct in their genomes, designed to monitor the activity of a distinct DSB repair pathway. The introduction of the I-SceI meganuclease (Figure 24), achieved through transient transfection of the corresponding expression plasmid, induces a DSB in the targeted site.

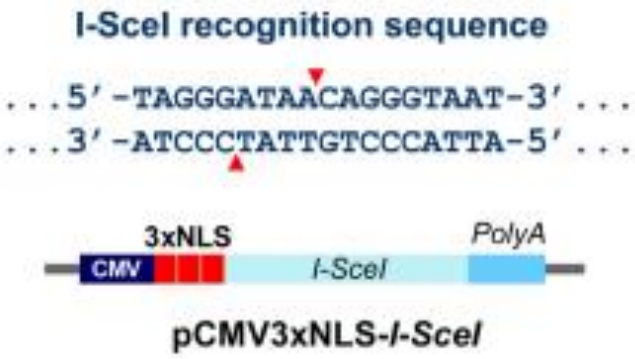

Figure 24: Schematic of the I-SceI RE system. Top: recognition sequence of I-SceI endonuclease. Note the generation of 3′ 4-bp overhangs. Bottom: the relevant domain structure of an expression vector, pCMV3xnls-I-SceI, used frequently in transient transfection experiments to express I-SceI. Note the three NLS sites that ensure the nuclear localization of the expressed enzyme(Mladenova, Mladenov, and Iliakis 2016).

The following specific repair pathway functions are monitored in each cell line (Mladenova, Mladenov, and Iliakis 2016).

1. U2OS DR-GFP cells: These cells specifically monitor homologous recombination (HR) function (Figure 25A).

2. U2OS SA-GFP cells: These cells monitor single-strand annealing (SSA) (Figure 25C).

3. U2OS EJ5-GFP cells: These cells monitor non-homologous end joining (NHEJ) (Figure 25B).

4. U2OS EJ2-GFP cells: These cells monitor alternative end joining (alt-EJ) (Figure 25D).

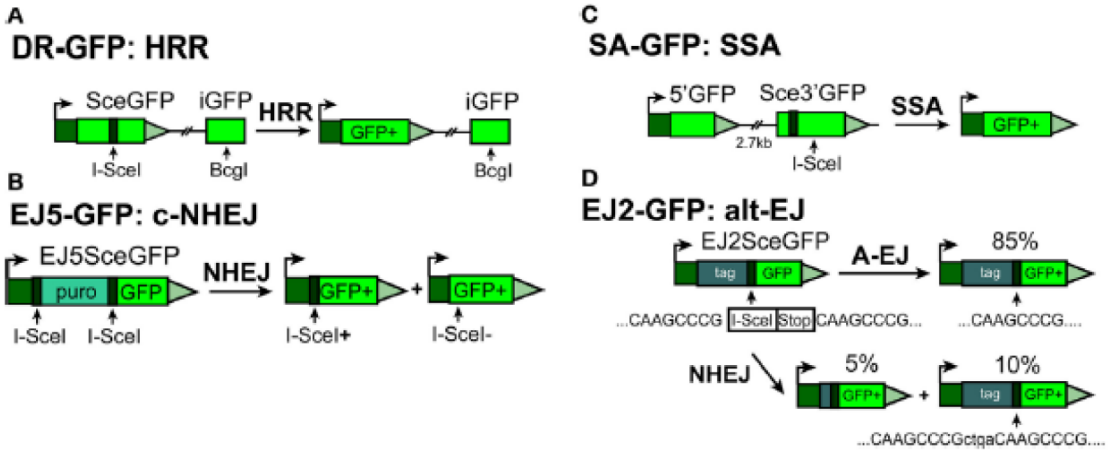

Figure 25: Outline of reporter constructs developed in the laboratory of Dr. J. Stark (Bennardo et al. 2008) **to analyze the efficiency of I-SceI-DSB-processing by different DSB repair pathways in human cells** (Mladenova, Mladenov, and Iliakis 2016)**.**

5.6.1 The role of condensins in NHEJ pathway

The c-NHEJ pathway is a DNA repair mechanism that operates independently of DNA homology and is active throughout the cell cycle. This pathway is widely recognized for its potentially error-prone nature. To investigate the impact of condensins in the NHEJ pathway, we utilized U2OS EJ5-GFP cells, which are specifically designed to monitor the repair of I-SceI-induced DSBs by NHEJ (EJ5-GFP).

To assess the effect of condensins suppression on the c-NHEJ pathway, we compared the GFP expression in U2OS EJ5-GFP cells transfected with negative control siRNA to those in which condensins were suppressed (Figure 26). By analyzing the GFP signal, we can gain insights into the impact of condensins on the efficiency of c-NHEJ-mediated repair of I-SceI-induced DSBs.

In the investigation of the role of condensins in NHEJ pathway, the results showed that the knockdown led to a small albeit significant increase in GFP signal of over 20% compared to cells transfected with a control siRNA. This suggests that condensins may not actively participate in the NHEJ pathway and that their knockdown suppress instead other DSB repair pathways. As a consequence after their inhibition NHEJ unfolds to a greater degree.

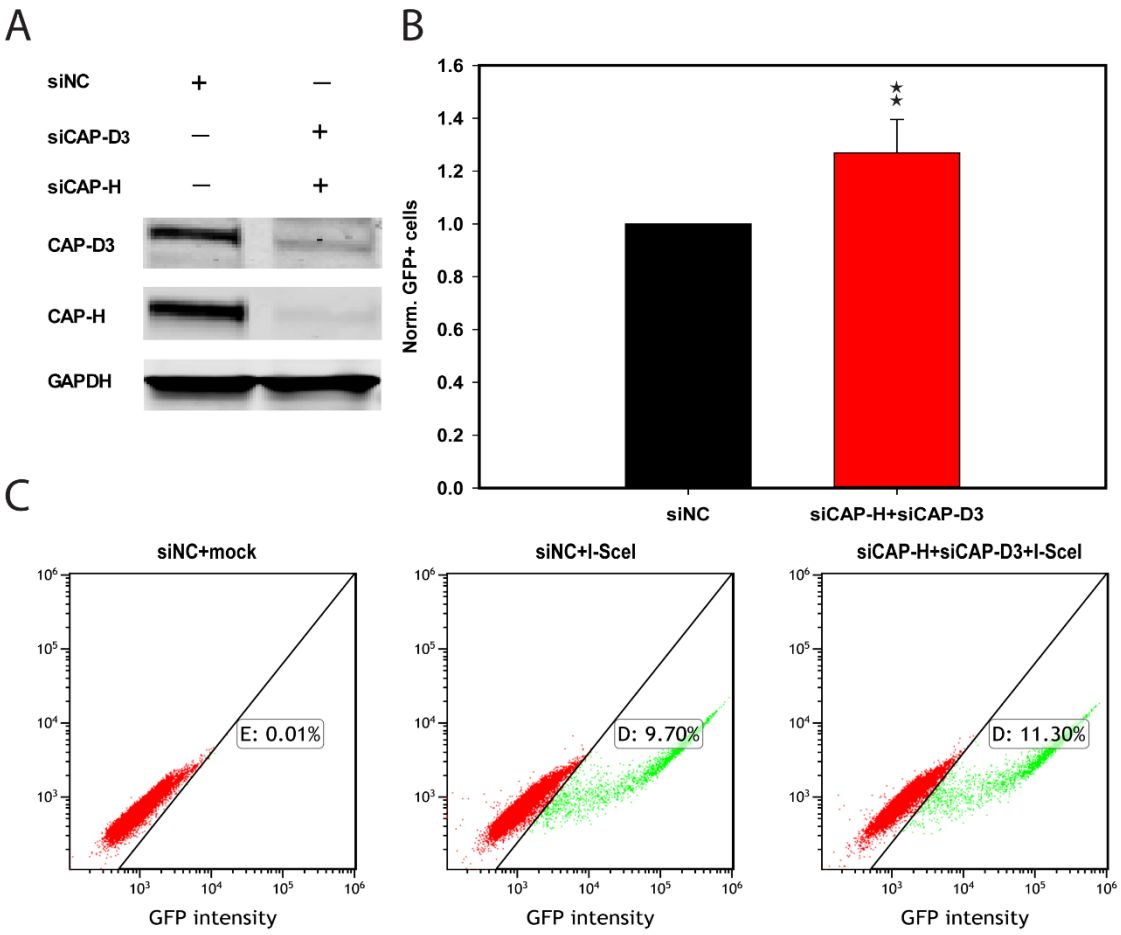

Figure 26: Effect of condensins deficiency on NHEJ pathway. (A) Western blot analysis of CAP-H and CAP-D3 protein level in U2OS EJ5-GFP cells 48 h post transfection with siCAP-H + siCAP-D3; GAPDH serves as loading control. (B) Bar plots reflect the siNC-normalized GFP+ cells. (C) Percentage of GFP positive cells (GFP+), in the negative control (siNC) and CAP-H + CAP-D3 knockdown in EJ5-GFP cells. Data represent the mean ± SD from three independent determinations. The significance level, or p-value, is calculated using the two-tailed Student´s t-test: ** $p < 0.01$.

5.6.2 The role of condensins in HR pathway

Moving on to the role of condensins in HR pathway, which is involved in the precise and error-free repair of DSBs, we focused on the impact of CAP-H and CAP-D3 knockdown on HR using U2OS DR-GFP cells (Figure 27). The findings demonstrated that the suppression of Condensin I and Condensin II resulted in approximately a 50% reduction in HR compared to cells transfected with a control siRNA. These results provide evidence that condensins are indeed involved in the HR pathway, in line with previous reports (Wood et al. 2007; Wood et al. 2008).

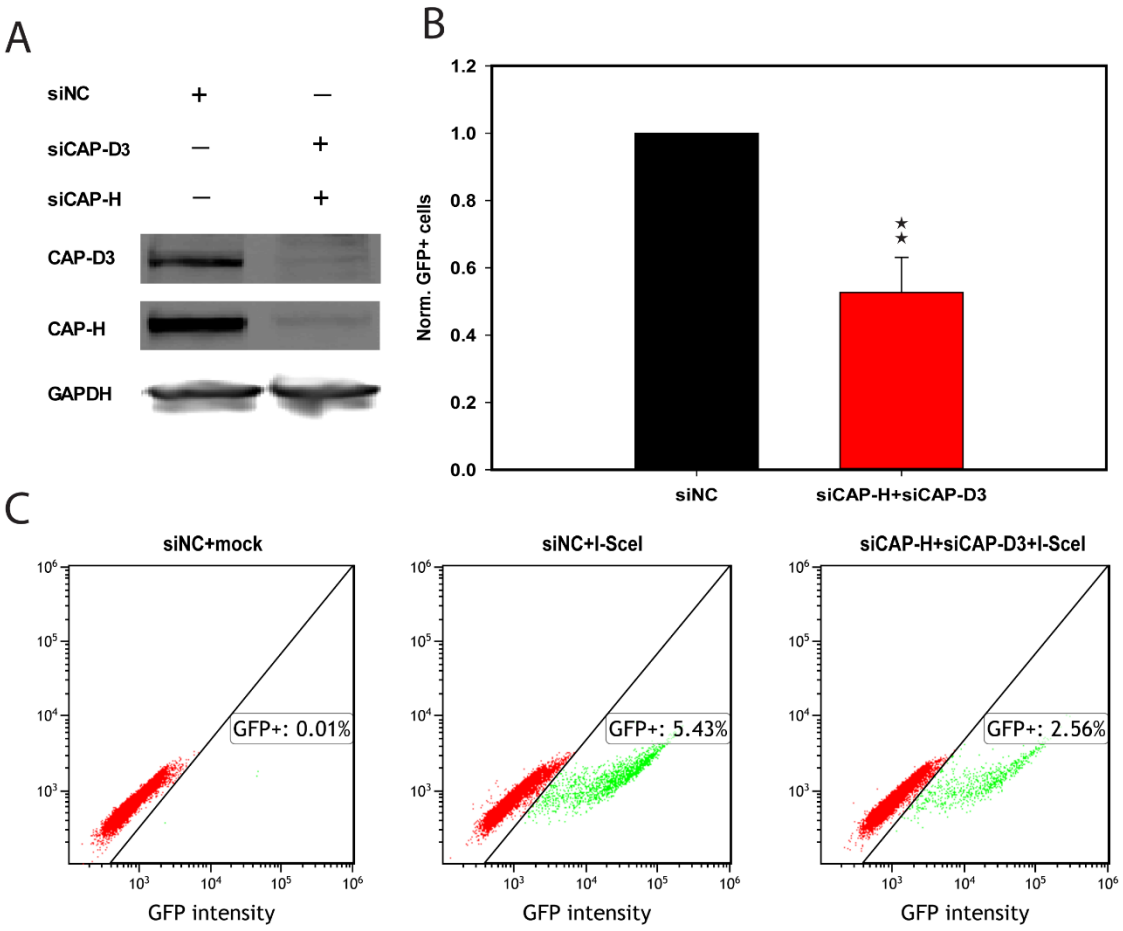

Figure 27: Effect of condensins deficiency on HR pathway. (A) Western blot analysis of CAP-H and CAP-D3 protein levels in U20S DR-GFP cells 48 h post transfection with siCAP-H + siCAP-D3; GAPDH serves as loading control. (B) Bar plots reflect the siNC-normalized GFP+ cells. (C) Percentage of GFP positive cells (GFP+) in the negative control (siNC) and CAP-H + CAP-D3 knock-down of DR-GFP cells. Data represent the mean ± SD from three independent determinations. The significance level, or p-value, is calculated using the two-tailed Student´s t-test: ** $p < 0.01$.

5.6.3 The role of condensins in SSA pathway

In order to investigate the potential involvement of condensins in SSA pathway, an experiment was conducted using U2OS SA-GFP cells. The SSA repair mechanism is known to rely on DNA end resection and is influenced by the cell cycle stage. The objective was to test the impact of condensins on SSA repair.

The results of this experiment revealed that the suppression of condensins resulted in an approximately 40% decrease in SSA in U2OS SA-GFP cells (Figure 28). These findings strongly suggest that condensins plays a role in the SSA pathway. The involvement of condensin in SSA further highlights its significance in various DSB repair pathways,

emphasizing its broader contribution to DNA repair mechanisms. It is somewhat surprising that depletion of condensins suppress both HR and SSA, as often in experiments of this kind, SSA rises when HR is suppressed. Indeed, the common reduction of HR and SSA upon condensin knockdown suggests that these proteins are involved in steps of the repair process that are common to both pathways.

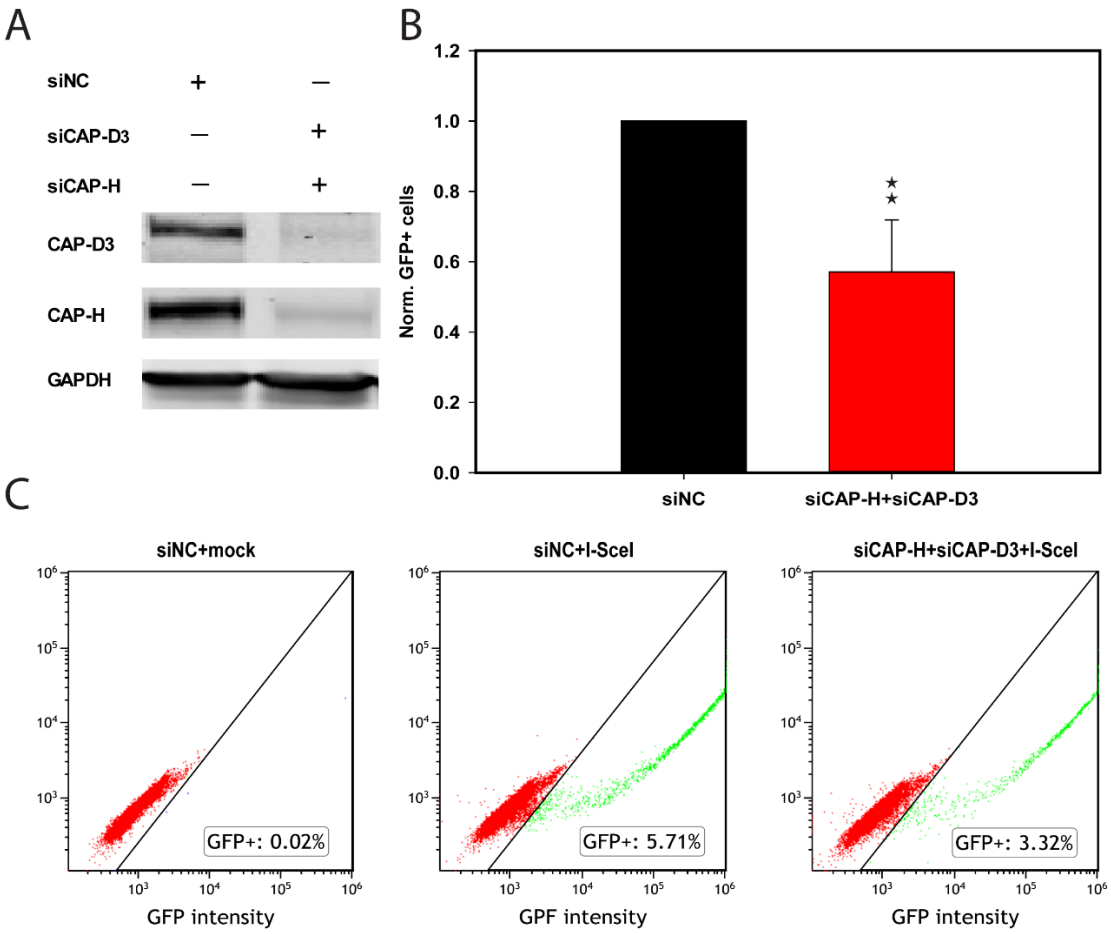

Figure 28: Effect of condensins deficiency on SSA pathway. (A) Western blot analysis of CAP-H and CAP-D3 protein levels in U20S SA-GFP cells 48 h post transfection with siCAP-H + siCAP-D3; GAPDH serves as loading control. (B) Bar plots reflect the siNC-normalized GFP+ cells. (C) Percentage of GFP positive cells (GFP+) in the negative control (siNC) and CAP-H + CAP-D3 knockdown of SA-GFP cells. Data represent the mean ± SD from three independent determinations. The significance level, or p-value, is calculated using the two-tailed Student´s t-test: ** $p < 0.01$.

5.6.4 The role of condensins in alt-EJ pathway

To assess the efficiency of alternative end joining (alt-EJ) under conditions of condensin sknockdown, U2OS EJ2-GFP cells were utilized.

The results demonstrated that the knockdown of CAP-H and CAP-D3 significantly reduced the GFP signal in U2OS EJ2-GFP cells, indicating a decrease in repair via alt-EJ (Figure 29). These findings provide compelling evidence that condensins, represented by CAP-H and CAP-D3, are involved in the alt-EJ pathway.

Based on all aforementioned results collectively, it is evident that inhibition of condensins leads to a decrease in all DNA end resection-dependent pathways. To gain further insights into the effect of condensins on DNA end resection, additional investigations were carried out to directly study the impact of condensins on DNA end resection. Understanding how condensins influence DNA end resection may provide valuable information regarding their role in modulating the balance between different repair pathways and contribute to our overall understanding of DNA repair mechanisms.

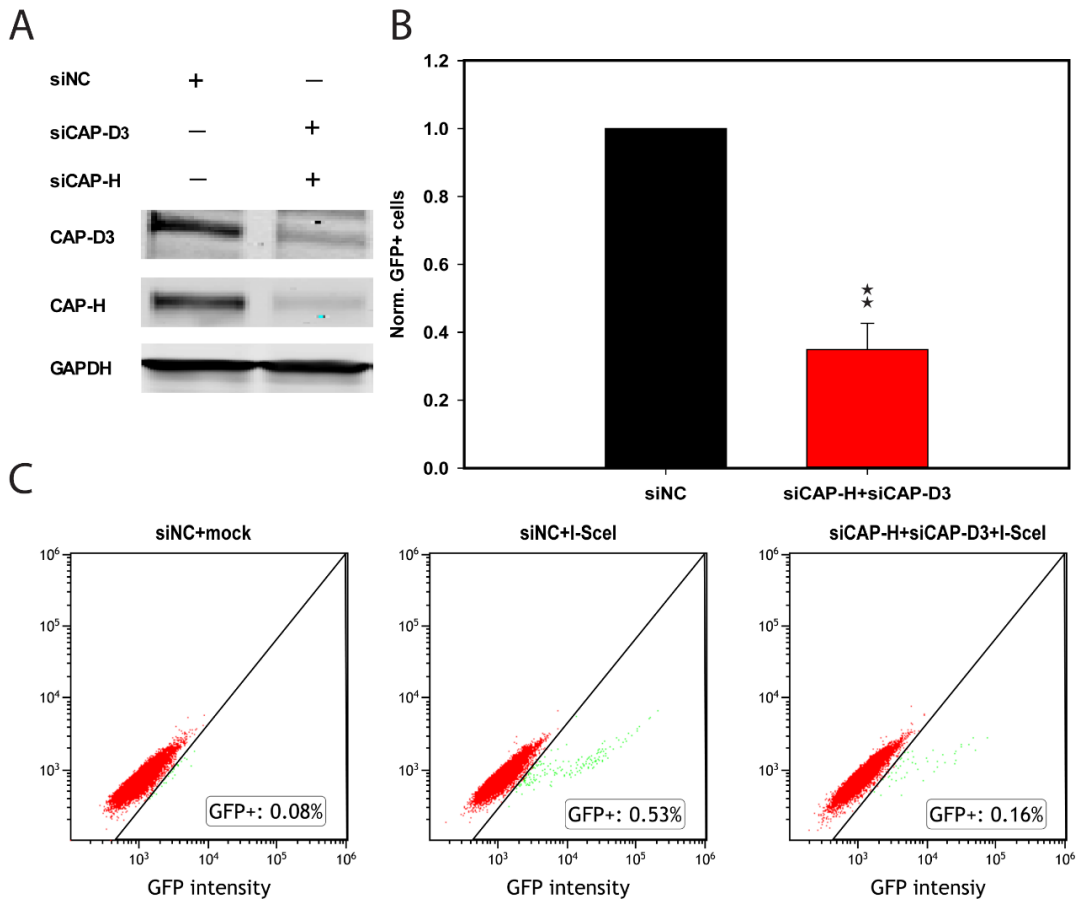

Figure 29: Effect of condensins deficiency on alt-EJ pathway. (A) Western blot analysis of CAP-H and CAP-D3 protein levels in U20S EJ2-GFP cells 48 h post transfection with siCAP-H + siCAP-D3; GAPDH serves as loading control. (B) Bar plots reflect the siNC-normalized GFP+ cells. (C) Percentage of GFP positive cells (GFP+) in the negative control (siNC) and CAP-H + CAP-D3 knockdown of EJ2-GFP cells. Data represent the mean ± SD from three independent determinations. The significance level, or p-value, is calculated using the two-tailed Student´s t-test: ** $p < 0.01$.

5.7 Effect of condensins on resection analysed by quantitating RPA70 foci formation

DNA end resection is a crucial step in several DSB repair pathways, including HR, SSA and alt-EJ. During DNA end resection, a long 3'- ssDNA overhang is generated, which during HR can invades the homologous DNA strand in the sister chromatid, and is also utilized to bring the DNA ends together in SSA and alt-EJ. Multiple proteins participate in this process. At the center is the MRN complex, composed of Rad50, Nbs1, and Mre11, which is responsible for DNA binding and enzymatic functions. CtIP, through its interaction with Nbs1, is crucial for activating the MRN complex and initiating end resection. The extension of the DNA end resection is further supported by Exo1, DNA2, and the helicases WRN and BLM. Following end resection, the RPA protein binds to the generated 3'-ssDNA overhangs to protect them from nuclease degradation and to prevent hairpin formation, which would hinder Rad51 filament assembly (REF). RPA70, in particular, plays a crucial role in stabilizing ssDNA and is necessary for the initiation of DNA end resection in DSB repair.

In the previous experiments investigating the four DSB repair pathways, it was observed that HR, SSA and alt-EJ, which are all DNA end resection-dependent repair pathways, were compromised in condensins deficient RPE-1 hTert cells. However, the specific role of condensins in regulating DNA end resection and whether their effects on DSB repair pathway choice occur upstream or downstream of this step remained unclear. To address this question, we investigated DNA end resection by examining the formation of RPA70 foci following exposure to 2 Gy X-rays (Figure 30). We specifically measured RPA70 foci formation and decay in cells irradiated during the G2 phase of the cell cycle, as these cells are fully proficient for DNA end resection. Exponentially growing cells were pulse-labeled with 10 Mm EdU 30 minutes before exposure to 2 Gy. RPA70 foci were quantified in EdU^--G2 phase cells.

In the negative control cells, RPA70 foci exhibited a rapid increase within the first-hour post-irradiation and remained above 15 foci per cell from 3 to 6 h after irradiation. In contrast, condensins deficient cells showed a similar trend in foci formation but at significantly suppressed levels (Figure 30B, C). Interestingly, this phenomenon is not limited to RPE-1 cells but is also observed in tumor cells such as A549 (Figure 30E, F).

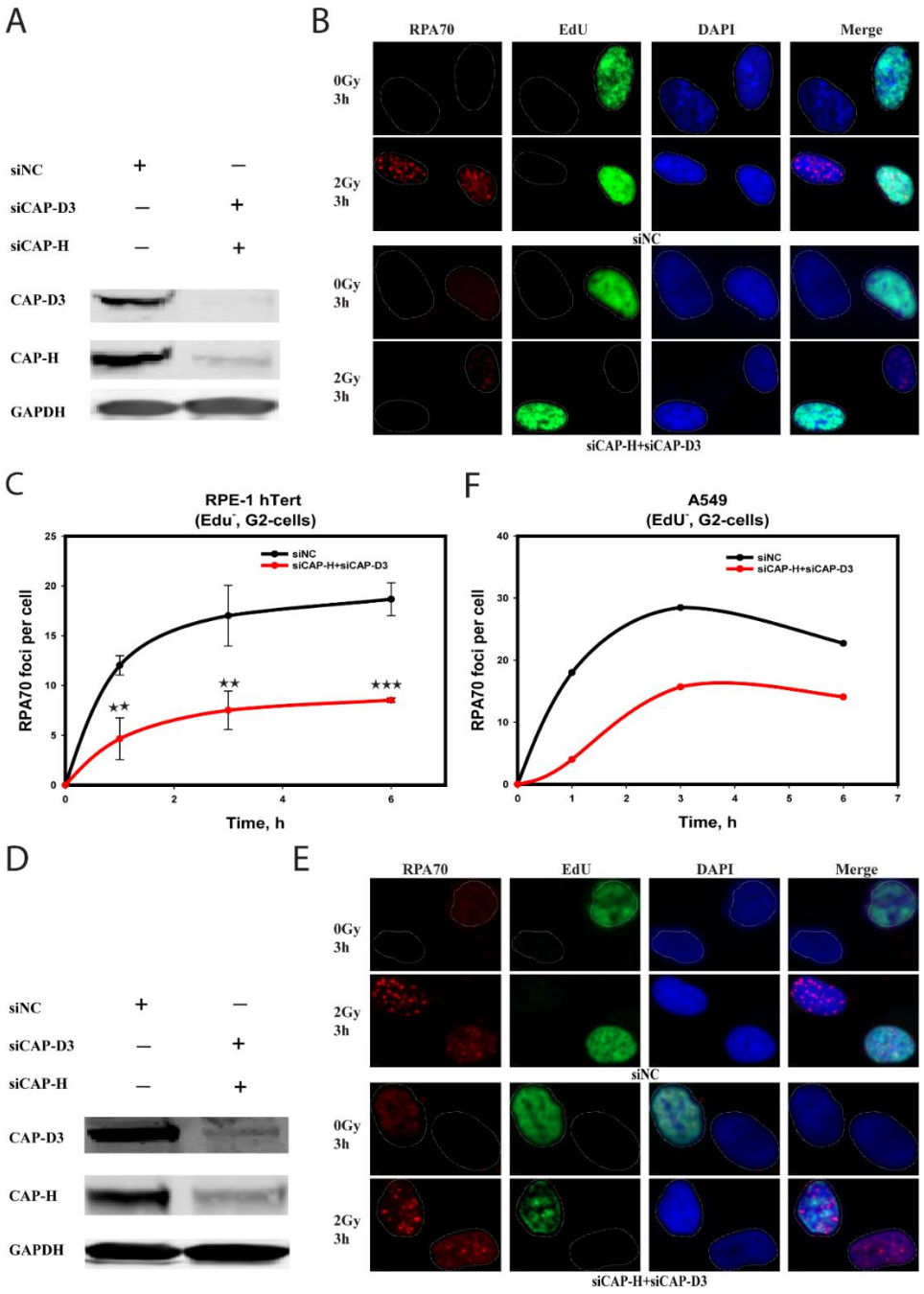

Figure 30: Condensins deficiency decreases IR-induced RPA foci. (A) Western blot analysis of CAP-H and CAP-D3 protein level in RPE-1 hTert cells 48 h post transfection with siCAP-H + siCAP-D3; GAPDH serves as loading control. (B) Representative images of RPA foci in RPE-1 hTert cells, irradiated with 2 Gy of X-rays and collected at the indicated times after irradiation. Forty-eight hours before irradiation, cells were transfected with siNC or siCAP-H + siCAP-D3. (C) Quantification of RPA foci in siNC and siCAP-H + siCAP-D3, RPE-1 hTert, EdU$^-$, G2 cells. (D) Same as panel (A), but for A549 cells. (E) Same as panel (B), but for A549 cells. (F) Same as panel (C), but for A549 cells. Cell cycle-specific RPA foci analysis was performed in EdU negative, G2 phase cells (EdU$^-$, G2 cells) as described in Materials and Methods. The scale bar is 30 µm for all images. Data for RPE-1 hTert cells represent the mean ± SD from three independent determinations. The significance level, or p-value, is calculated using the two-tailed Student´s t-test: ** $p < 0.01$, *** $p < 0.001$.

These results provide direct evidence that DNA end resection is impaired in condensins suppressed cells. These findings align with the previous experiments that demonstrated the inhibition of the three DNA end resection-dependent repair pathways upon condensins suppression.

5.8 Effect of condensins on HR analysed by quantitating Rad51 foci formation

Rad51, playing a crucial role in DSB repair through HR, facilitates the exchange of DNA strands between homologous chromosomes or sister chromatids by catalyzing the search for a homologous DNA sequence. During the repair of DSBs, Rad51 forms a filament on the resected single-stranded DNA (ssDNA) at the break site. This filament then invades the homologous sequence on the sister chromatid or the homologous chromosome, enabling the joint molecule to serve as a template for DNA synthesis and repair of the break. Rad51 is also involved in the repair of DNA damage caused by various sources, including replication fork collapse and interstrand crosslinking, which necessitate homologous recombination repair.

To further elucidate the functionality of DNA end resection and other mechanisms of DSB repair in condensins deficient cells, we measured the formation and decay of IR-induced foci by Rad51 (Figure 31). Specifically, we measured the formation and decay of Rad51 foci in cells irradiated during G2 phase of the cell cycle, as these cells are proficient in HR repair. These methods resemble those used to measure the RPA70 foci formation discussed above.

The results presented in Figure 29 demonstrate that in RPE-1 hTert cells and A549 cells exposed to 2 Gy of IR, Rad51 rapidly accumulates at DSBs (Figure 31B, C, E, F) and forms foci that peak at approximately 11 foci in RPE-1 hTert and 25 foci in A549 per cell after 3 h, followed by decay over time (Figure 31B). The accumulation of Rad51 at DSBs is reduced by approximately 70% in following condensins knockdown. These findings are consistent with our previous observations using reporter cell lines and support the notion that condensins support HR.

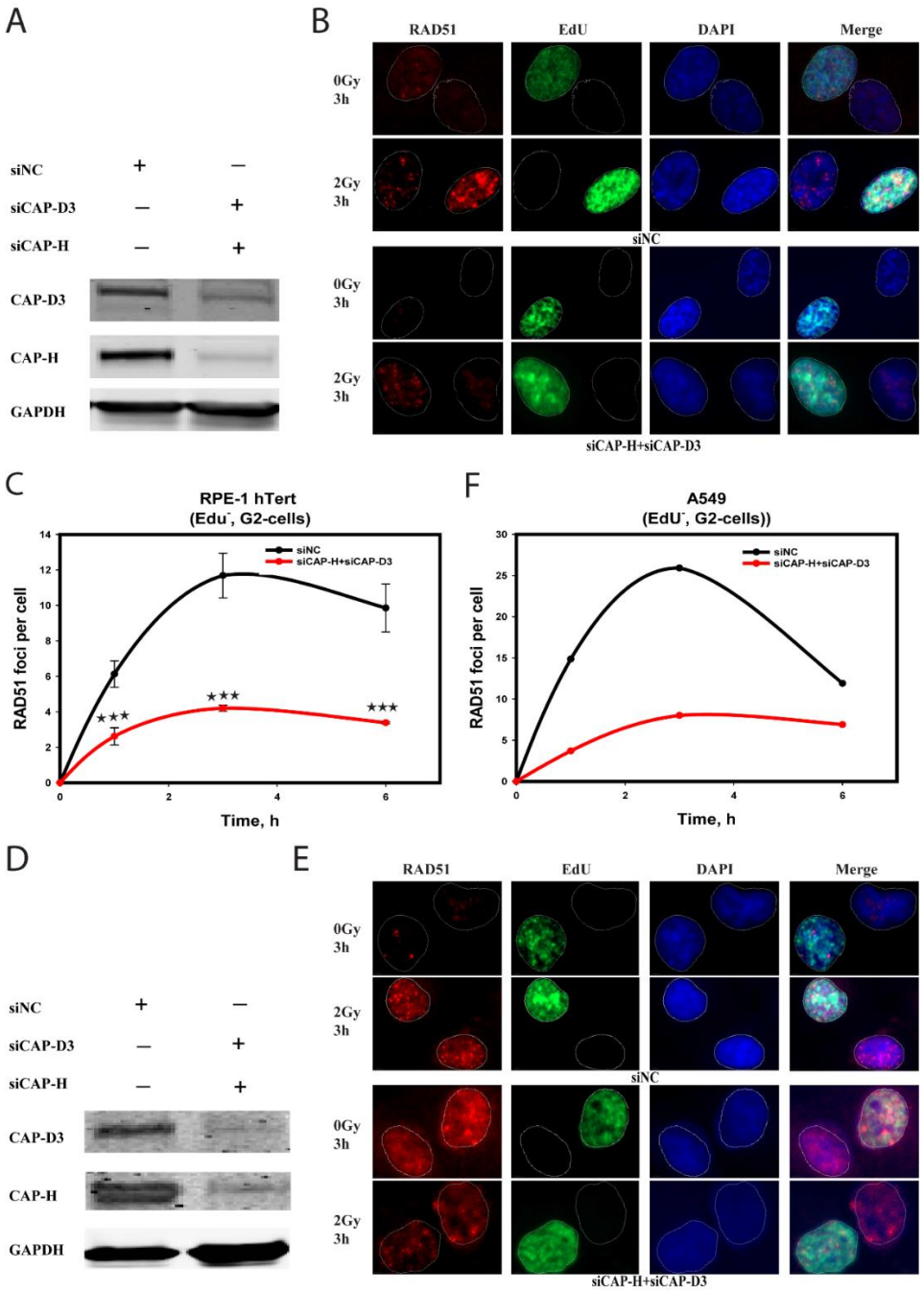

Figure 31: Condensins deficiency decreases number of IR-induced RAD51 repair foci. (A) Western blot analysis of CAP-H and CAP-D3 protein levels in RPE-1 hTert cells 48 h post transfection with siCAP-H + siCAP-D3; GAPDH serves as loading control. (B) Representative images of Rad51 foci in RPE-1 hTert cells, irradiated with 2 Gy of X-rays and collected at the indicated times after irradiation. Forty-eight hours before irradiation, cells were transfected with siNC or siCAP-H + siCAP-D3. (C) Quantification of RAD51 foci in siNC and siCAP-H + siCAP-D3, RPE-1 hTert, EdU-, G2-cells. (D) Same as panel (A), but for A549 cells. (E) Same as panel (B), but for A549 cells. (F) Same as panel (C), but for A549 cells. Cell cycle-specific RAD51 foci analysis was performed in EdU negative, G2 phase cells (EdU$^-$, G2-cells) as described in Materials and Methods. The scale bar is 30 μm for all images. Data for RPE-1 hTert cells represent the mean ± SD from three independent determinations. The significance level, or p-value, is calculated using the two-tailed Student´s t-test: *** $p < 0.001$.

5.9 Effect of condensins on the regulation of G2-Checkpoint

The G2 checkpoint is a crucial cell cycle checkpoint that occurs during the G2 phase, after DNA replication, but before cells enter into mitosis. It ensures that DNA has been properly replicated, checks for unrepaired DNA damage, and verifies the readiness of the cell for division. If there is DNA damage, the checkpoint can delay progression into mitosis, allowing time for repair before cell division takes place. The G2 checkpoint plays a vital role in maintaining genomic stability and preventing the accumulation of mutations that could lead to diseases like cancer.

In our previous report, we established a direct correlation between the activation of the G2 checkpoint and the cell's ability to repair DSBs through HR (Soni, Mladenov, and Iliakis 2021). Given that HR is compromised following the knockdown of condensins, the checkpoint response will likely be affected. This would provide further evidence supporting the suppression of HR after condensins knockdown.

In our present investigation, when RPE-1 hTert cells are irradiated in the G2 phase, they activate a checkpoint that delays their progression into mitosis, resulting in a rapid decrease in the mitotic index (MI) that persists for about 4 hours before recovering at later times. This response indicates the transient activation of the G2 checkpoint, specifically in G2-phase irradiated cells, as only these cells can reach mitosis during the observed time interval (Blackford and Stucki 2020). However, the strong checkpoint response of cells is somewhat compromised at each time point, particularly at 1 and 2 h, when condensins are depleted (Figure 32B, C).

In our investigation using A549 cells, we observed a more significant checkpoint response compared to RPE-1 hTert cells. A549 cells in the G2 phase were irradiated with 2Gy of radiation, leading to a robust suppression of the checkpoint response（Figure 32E, F）.

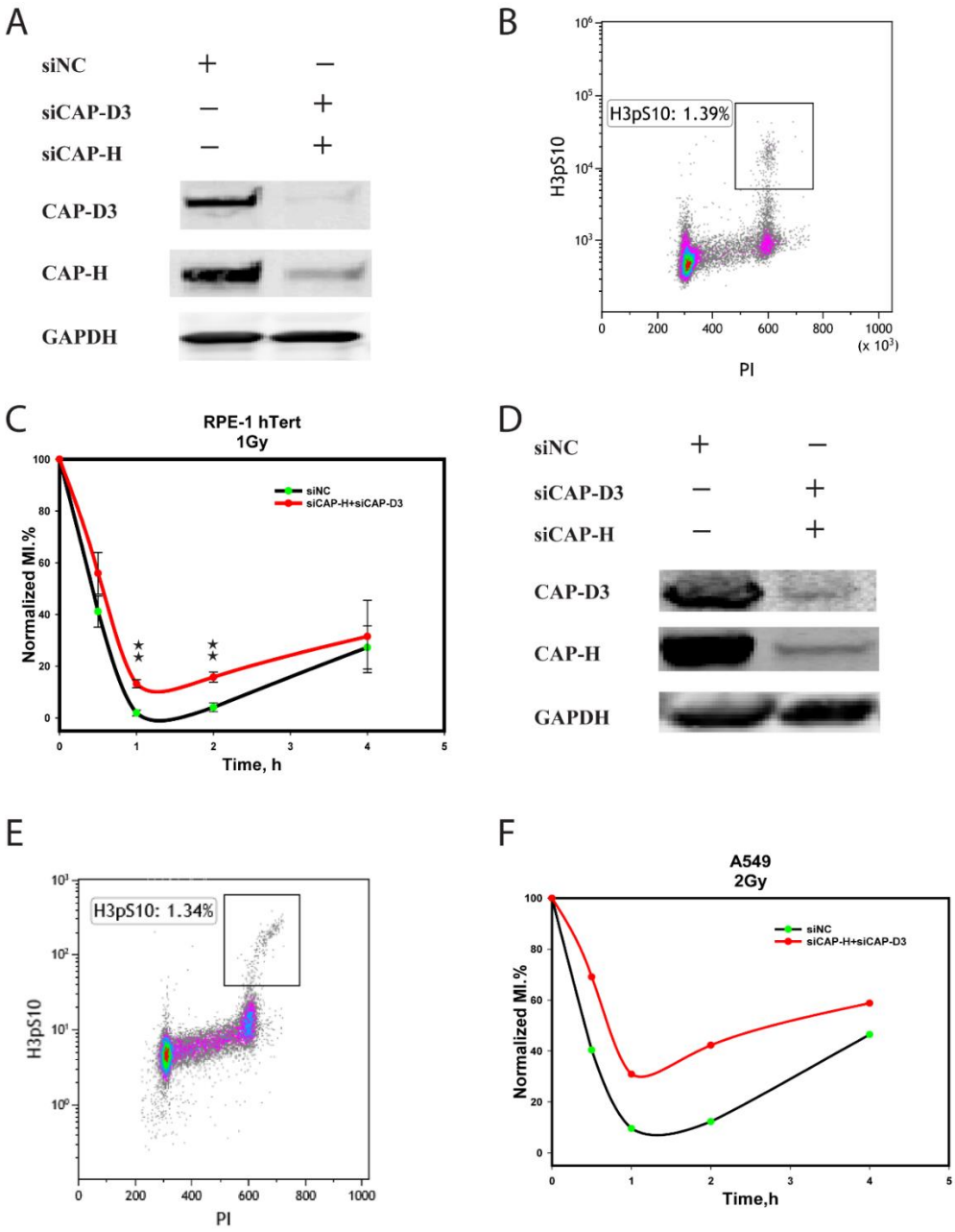

Figure 32: **Condensins knockdown has a small effect on the G2-checkpoint.** The checkpoint activated in cells that are in G2-phase at the time of irradiation is measured by analyzing the mitotic index (MI), using two-parameter flow cytometry detecting DNA through PI staining and phosphorylated H3 at Serine 10 (H3pS10), a specific marker of mitotic cells, by antibody staining. (A) Western blot analysis of CAP-H and CAP-D3 protein level in RPE-1 hTert cells 48 h post transfection with siCAP-H + siCAP-D3; GAPDH serves as loading control. (B) Representative histograms with a rectangle depicting the gating employed to analyze H3pS10 percentage by FACS. (C) Normalized MI in siNC and siCAP-H + siCAP-D3 transfected RPE-1 hTert cells after IR. Normalized MI is calculated by dividing the MI measured in irradiated cells by that of non-irradiated cells. (D) Same as panel (A), but for A549 cells. (E) Same as panel (B), but for A549 cells. (F) Same as panel (C), but for A549 cells. Data for RPE-1 hTert cells represent the mean ± SD from three independent determinations. The significance level, or p-value, is calculated using the two-tailed Student´s t-test: ** $p < 0.01$.

When cells are irradiated with 1 Gy, inhibition of ATM or ATR abolishes the activation of the G2 checkpoint. The same result is observed when cells are transfected with siNC and siCAP-H+siCAP-D3. This indicates that the functions of ATM and ATR in the regulation of the G2 checkpoint remains intact after knockdown of Condensins (Figure 33).

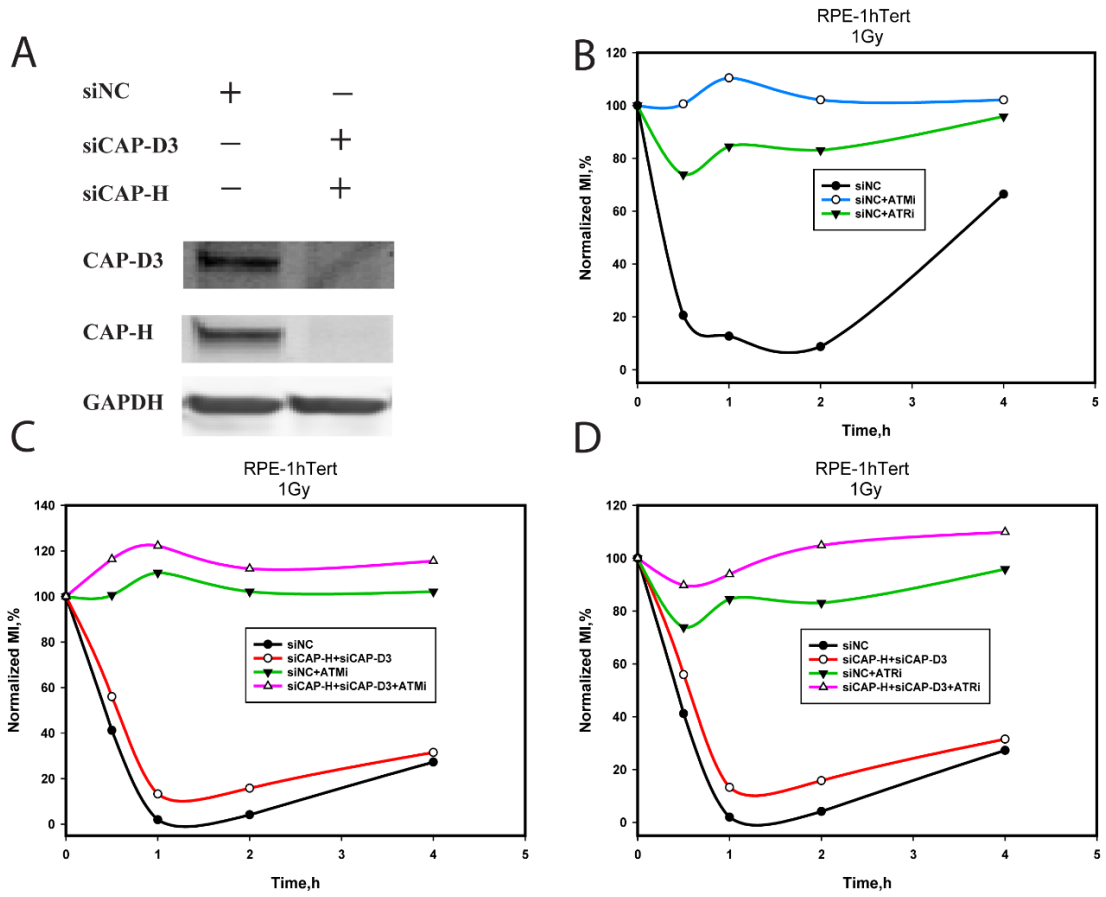

Figure 33: Condensins deficiency leaves intact the functions of ATM and ATR in G2 checkpoint regulation. (A) Western blot analysis of CAP-H and CAP-D3 protein level in RPE-1 hTert cells 48 h post transfection with siCAP-H + siCAP-D3; GAPDH serves as loading control. (**B**) Normalized MI of RPE-1 hTert cells treated with siNC, siNC+10 µM KU55933 (ATMi), or siNC+5 µM VE-821 (ATRi) after 1 Gy of IR. (**C**) Normalized MI of RPE-1 hTert cells treated with siNC, siNC+10 µM KU55933, siCAP-H+siCAP-D3, or siCAP-H+siCAP-D3+10 µM KU55933 after 1 Gy IR. (D) Normalized MI of RPE-1 hTert cells treated with siNC, siNC+5 µM VE-821, siCAP-H+siCAP-D3, or siCAP-H+siCAP-D3+5 µM VE-821 after 1 Gy IR. Normalized MI is calculated by dividing the MI measured in irradiated cells by that of non-irradiated cells.

5.10 Condensins suppression impairs G2 phase chromatid break repair

To investigate the impact of condensins deficiencies on the processing of chromatid breaks, we conducted experiments in G2-phase RPE-1 hTert cells. We utilized Calyculin-

A administration to induce chromatin condensation in interphase cells. This method allows for the direct visualization and assessment of damage in G2 cells, bypassing the influence of the G2 checkpoint on repair processes. G2-phase premature chromosome condensation generated prematurely condensed chromosomes (G2-PCCs) that were easily distinguishable from metaphase chromosomes due to the absence of a centromeric constriction.

In this experimental setup, exponentially growing cells treated with negative control siRNA (siNC) and siRNA targeting both CAP-H and CAP-D3 (siCAP-H+siCAP-D3) were irradiated with 0.5 Gy X-rays. The chromatid breaks in G2-PCCs were quantified at 1 h and 4 h post-irradiation. The results obtained using RPE-1 hTert cells are presented in Figure 34.

Following the suppression of condensins, we observed widespread alterations in chromosome structure, as evidenced by significant decondensation (Figure 34D, F). These findings support the essential role of condensins in chromosome compaction. Interestingly, we observed that the initial level of damage was slightly higher in condensins deficient cells compared to siNC cells. However, while the siNC cells demonstrated normal repair ability, a substantial portion, approximately 80%, of the breaks remained unrepaired in condensins deficient cells (Figure 34B). Even though cells lacking functional condensins exhibited a slightly elevated level of chromosome breaks upon initial induction, the repair process was significantly compromised after condensin knockdown.

These findings from G2-PCC measurements are consistent with previous results, which underscore the essential role of functional condensins in the repair of IR-induced DSBs. For instance, earlier studies demonstrated that the condensin II binding region of MCPH1 is also required for HR function (Wood et al. 2008). Additionally, research has shown that decondensation of chromosome by incubating cells in hypotonic medium delayed their repair as measured by scoring G2-PCC breaks over time and HypoS markedly suppresses HR (Krieger et al. 2021). These results, along with the present PCC data, provide compelling evidence that functional condensins are indispensable for the effective repair of IR-induced DSBs.

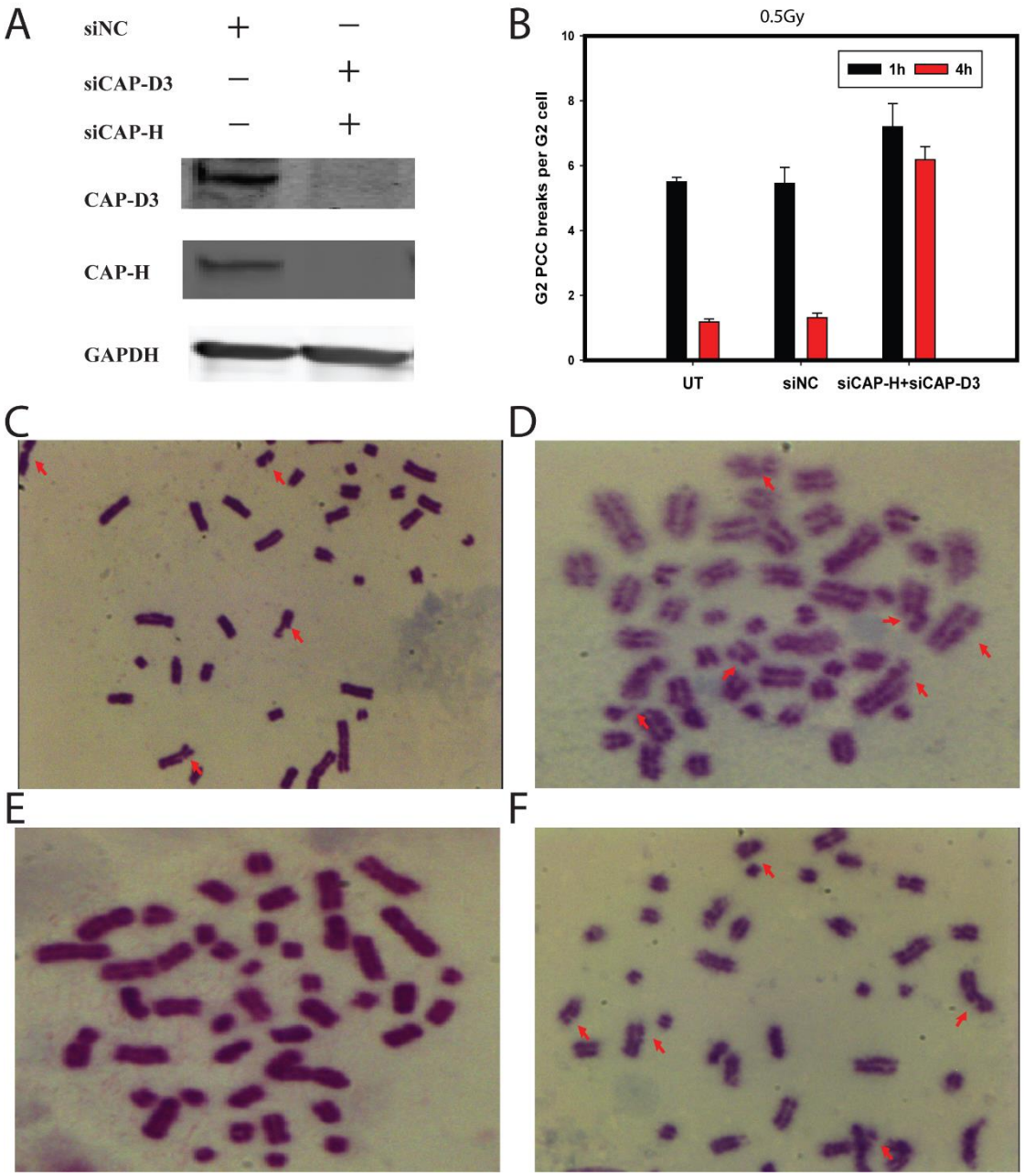

Figure 34: G2-PCC breaks in exponentially growing condensins depleted cells irradiated with 0.5 Gy X-rays. Cells were allowed to repair to up-to 4 h. G2-PCCs were induced by adding 50 nM calyculin A for 45 min and this time is included in the repair time. The number of G2-PCC breaks is plotted against time. Arrows represent PCC-breaks. (A) Western blot analysis of CAP-H and CAP-D3 protein level in RPE-1 hTert cells 48 h post transfection with siCAP-H + siCAP-D3; GAPDH serves as loading control. (B) Bar plots reflect chromatid breaks at different times post irradiation in untreated, siNC, and siCAP-H + siCAP-D3 transfected exponentially growing RPE-1 hTert cells. (C) Representative image at 1 h post IR in siNC transfected cells. (D) Representative image at 1 h post IR in siCAP-H + siCAP-D3 transfected cells. (E) Representative image at 4 h post IR in siNC transfected cells. (F) Representative image at 4 h post IR in siCAP-H + siCAP-D3 transfected cells. Data represent the mean ± SD from three independent determinations.

6. Discussion

Every cell in the human body encounters tens of thousands of DNA damage events daily. These lesions can interfere with genome replication and transcription. Biological systems are in place to detect, signal, and repair DNA damage. Unrepaired or inaccurately repaired lesions can lead to mutations or severe genomic abnormalities, threatening cell viability and overall health.

Cancer often begins with DNA mutations or alterations resulting from unrepaired or inaccurately repaired DNA damage, including DSBs. Research in the field focuses on understanding these processes in order to develop effective prevention and treatment strategies.

In eukaryotes, condensin is a crucial protein complex consisting of two structural maintenance of chromosomes (SMC) subunits and three regulatory non-SMC subunits. Condensin is vital for chromosome dynamics, including mitotic chromosome condensation, segregation, and DNA repair. Repairing DNA damage, especially unresolved DSBs, is essential for cell health; failure to do so can lead to tumorigenesis, senescence, or apoptosis. However, the exact molecular mechanisms by which condensin functions in DNA repair are not well understood.

To explore condensin's role in DNA damage repair, we used RPE-1 hTert, U2OS GFP reporter, and A549 cells to study responses to ionizing radiation (IR) in both condensing depleted and non-depleted cells. By examining these responses, we aimed to clarify condensin's involvement in DNA repair processes and enhance our understanding of its functional repair contributions.

6.1 The role of condensins in radiosensitivity

We used clonogenic survival assays to assess the effects of condensin suppression in RPE-1 hTert and A549 cells. Understanding the involvement of condensins in DNA repair mechanisms has potential implications for improving radiotherapy strategies.

We initially focused on condensin I by knocking down CAP-H, a key subunit. Our results showed that suppressing condensin I did not affect the surviving fraction of RPE-1 hTert cells post-irradiation, as compared to the control group. Additionally, cell cycle analysis revealed no significant changes in cell cycle distribution. This observation suggests that

Condensin I does not have an essential role in the DSB repair process in RPE-1 hTert cells, under the conditions tested (Figure 18).

Next, we examined Condensin II by knocking down CAP-D3. While the suppression of Condensin II resulted in a slightly increased number of cells in the G1 phase and a marginally decreased number in the S phase, there was no significant alteration in the G2 phase. Despite these changes in cell cycle distribution, the surviving fraction post-irradiation remained unchanged. This indicates that similar to Condensin I, Condensin II suppression does not significantly impact the radiosensitivity of RPE-1 hTert cells (Figure 19).

We then explored the combined effects of suppressing both Condensin I and Condensin II. Interestingly, the dual knockdown of these proteins led to a slight, albeit not statistically significant, increase in the number of cells in the G1 phase. More notably, the surviving fraction of these cells was significantly lower than that of the control group (Figure 20). This suggests a that in the absence of condensin I, condensin II can compensate and suppression of both condensins is required to see measurable effects. To further validate our findings, we targeted SMC2, a common subunit for both Condensin I and II. Suppression of SMC2 significantly increased the number of cells in the G1 phase and decreased the number of cells in the S phase, with no significant change in the G2 phase. The plating efficiency of SMC2 knockdown cells was drastically reduced, compared to in the control group, highlighting a severe impact on cell survival. This profound decrease in plating efficiency precludes detailed analysis of radiosensitivity but underscores the critical role of condensins in cell viability (Figure 21).

To generalize our findings, we conducted condensins knockdown on A549 cells. There was a marked increase in radiosensitivity, akin to the effects observed in RPE-1 hTert cells (Figure 20). This consistency across different cell lines suggests that condensins suppression universally enhances radiosensitivity, potentially providing a therapeutic avenue for improving radiotherapy outcomes.

The findings from our study indicate that while individual suppression of Condensin I or II alone may not significantly alter radiosensitivity, their combined suppression, but not through targeting common subunit SMC2, can markedly increase radiosensitivity.

6.2 The role of condensins in DSB signaling

γH2AX is a well-established marker for DSBs, with its phosphorylation by ATM kinase occurs rapidly at the sites of DNA damage. This phosphorylation extends bidirectionally from the break sites, facilitating the recruitment of other DDR proteins.

In our study, control cells showed efficient DNA repair after radiation, while condensins knockdown cells had a slower repair, indicating condensins are crucial for effective DSB repair (Figure 22).

53BP1 is another crucial DDR protein that plays a significant role in determining the pathway choice for DSB repair. By promoting NHEJ and inhibiting HR through the prevention of extensive DNA end resection, 53BP1 ensures the protection of DNA ends. Our analysis showed that in control cells, 53BP1 foci resolved efficiently after radiation, while in condensin-knockdown cells, foci persisted longer, indicating impaired DSB repair and highlighting the importance of condensins in the process (Figure 23).

To validate our findings, we extended our investigation to A549 cells. The results in A549 cells mirrored those observed in RPE-1 hTert cells.

The observed impairment in the resolution of γH2AX and 53BP1 foci upon condensins depletion highlights the critical role of condensins in the efficient repair of DSBs. Despite a slightly heightened initial DNA damage response, the inability to effectively repair the damage in the absence of condensins suggests that these proteins are crucial for maintaining genomic integrity.

Our study underscores the essential role of condensins in the DDR, particularly in the efficient repair of DSBs. The compromised resolution of γH2AX and 53BP1 foci in condensins deficient cells indicates that these proteins are integral to the DSB repair machinery.

6.3 The role of condensins in DSB repair pathway balance

Using U2OS GFP reporter cell lines, we explored the effect of condensins knockdown on c-NHEJ, HR, SSA and alt-EJ. Additionally, we examined the influence of condensins on DNA end resection by assessing the formation of RPA70 foci, a critical step in several DNA repair pathways. We also investigated the formation of RAD51 foci to evaluate the impact of condensins on homologous recombination (HR).

The c-NHEJ pathway repairs double-strand breaks (DSBs) without requiring a homologous template. Our experiments using U2OS EJ5-GFP cells revealed a significant increase in GFP signal following condensins knockdown (Figures 26). This suggests that condensins do not actively participate in the c-NHEJ pathway. Instead, their suppression appears to facilitate the repair of DSBs via c-NHEJ, implying that condensins may be more involved in other DSB repair pathways that rely on DNA end resection.

Homologous recombination (HR) is a high-fidelity repair mechanism that utilizes a homologous sequence as a template. Analysis using U2OS DR-GFP cells showed that condensins knockdown led to approximately a 50% reduction in HR activity (Figures 27). This substantial decrease underscores the critical role of condensins in HR. Similarly, our assessment of the SSA pathway using U2OS SA-GFP cells revealed an approximately 40% decrease in SSA activity following condensins suppression (Figures 28). Alt-EJ, a repair mechanism dependent on microhomology, was examined using U2OS EJ2-GFP cells. Condensins knockdown significantly reduced alt-EJ activity (Figures 29). Interestingly, the concurrent reduction of HR, SSA, and alt-EJ following condensins knockdown suggests that condensins are involved in shared steps of these pathways, potentially in the initial DNA end resection process.

Given the observed impacts on HR, SSA, and alt-EJ, we further investigated the role of condensins in DNA end resection by measuring RPA70 foci formation in irradiated RPE-1 hTert and A549 cells. RPA70 binds to ssDNA generated during end resection, protecting it and facilitating subsequent repair steps. Our results showed a significant reduction in RPA70 foci formation in condensins deficient cells (Figures 30), providing direct evidence that condensins are essential for efficient DNA end resection.

To assess the functionality of DNA end resection and HR repair, we measured RAD51 foci formation. RAD51 is critical for the search and strand invasion steps of HR. Our results demonstrated a significant reduction in RAD51 accumulation at DSBs in condensin-deficient RPE-1 hTert and A549 cells (Figures 31). This reduction was consistent with our observations from the GFP reporter assays, further supporting the role of condensins in facilitating HR.

Our findings indicate that condensins are crucial for maintaining the balance between different DSB repair pathways by promoting DNA end resection. The suppression of

condensins shifts the repair pathway preference from HR, SSA, and alt-EJ towards c-NHEJ. This shift likely occurs due to the impaired ability to process DNA ends, which is essential for HR, SSA, and alt-EJ but not for c-NHEJ. Previous studies, including our own, have demonstrated that chromosomal alterations can influence DNA repair pathways (Krieger et al. 2021). Notably, there are reports that Condensin II may play a role in promoting HR (Wood et al. 2007; Wood et al. 2008), while Condensin I has been shown to cooperate with poly(ADP-ribose) polymerase 1 during interphase to facilitate the repair of single-stranded DNA breaks (Kong et al. 2011; Heale et al. 2006). However, the effects of condensins on other repair pathways have not been extensively studied. Our results, which demonstrate the involvement of condensins in multiple resection-dependent pathways, emphasize their broader significance in the overall DSB repair process. The broad involvement of condensins in multiple resection-dependent pathways highlights their significance in the overall DSB repair process.

6.4 The role of condensins in the G2/M checkpoint

In response to DSBs, cells activate regulatory mechanisms known as checkpoints, which result in a delay in cell cycle progression. This delay provides the cell with additional time to repair DSBs before cell cycle transitions alter the repair pathway landscape or the lesion itself. The G2 phase is particularly critical, as transitioning into the M phase poses a risk to the processing of DSBs (Richardson and Jasin 2000) and increases the likelihood of DSBs transforming into chromosome breaks. Our previous findings (Soni, Mladenov, and Iliakis 2021) have established a direct correlation between the activation of the G2 checkpoint and the cell's ability to process DSBs through homologous recombination (HR). This connection is particularly significant as it underscores the importance of the G2 checkpoint in facilitating DNA repair mechanisms. In our recent report, we discovered that approximately 50% of DNA DSBs repaired during the G2 phase, were repaired through the process of HR at low doses of ionizing radiation (< 1 Gy). However, as the radiation dose increased, the contribution of HR diminished and became undetectable beyond 8 Gy (Mladenov et al. 2020).

In our previous investigation, we have shown that condensins knockdown compromises HR. Given this, we hypothesized that the G2 checkpoint response would also be affected

following condensins depletion. This would provide additional evidence supporting the suppression of HR following condensins knockdown.

To test this hypothesis, In the present study, we investigated the function of condensins in the G2 checkpoint and analyzed their function separately for cells irradiated in the G2 or S phase. We irradiated RPE-1 hTert cells in the G2 phase with 1 Gy and A549 cells in the G2 phase with 2 Gy X-ray. We utilized a two-parameter flow cytometry approach, combining staining techniques for PI and H3pS10.

This treatment activated the G2 checkpoint, resulting in a temporary decrease in the mitotic index (MI) for approximately 4 hours, after which the MI recovered (Figure 32). This response indicates the transient activation of the G2 checkpoint specifically in G2-phase irradiated cells, as only these cells can reach mitosis during the observed time interval (Blackford and Stucki 2020). However, when condensins were depleted, the robust checkpoint response observed at each time point, particularly at 1 and 2 h post-irradiation, was compromised (Figure 32). This finding supports our hypothesis that the suppression of HR following condensins knockdown also affects the G2 checkpoint response, further emphasizing the interdependence of these two processes.

Interestingly, while the knockdown of condensins had a pronounced effect on the G2 checkpoint, it did not directly affect the function of ATM and ATR, the primary kinases involved in the G2 checkpoint (Figure 32). In cells irradiated with 1 Gy, inhibition of ATM or ATR abolished the activation of the G2 checkpoint, similar to the effect seen in cells transfected with siNC and siCAP-H+siCAP-D3 (Figure 33). This indicates that condensins do not directly influence ATM and ATR functions in the G2 checkpoint pathway.

Additionally, we extended our investigation to A549 cells, which were irradiated with 2 Gy of radiation. The results (Figure 32F) showed a more pronounced inactivation of the checkpoint response in these cells compared to RPE-1 hTert cells. This observation suggests that different cell types may exhibit varying sensitivities to radiation-induced DNA damage and checkpoint activation, potentially due to intrinsic differences in their DNA repair capabilities and cell cycle regulation mechanisms.

Our study highlights the crucial role of condensins in maintaining the integrity of the G2 checkpoint and the effectiveness of HR in DNA repair. The compromised checkpoint

response following condensins knockdown underscores the delicate balance required for genomic stability. These findings provide valuable insights into the molecular mechanisms underlying cell cycle regulation and DNA repair, with significant implications for understanding cancer development and potential therapeutic interventions.

6.5 Condensins play an important role in the repair of G2 chromosomal breaks

The above analysis confirms the role of condensins in the HR pathway. In our previous study, we discovered the essential role of HR in processing chromatid breaks at doses within the range of 1 Gy (Soni et al. 2020). To further investigate the impact of condensins defects on the processing of chromatid breaks using G2-PCC analysis, we conducted appropriate experiments.

In our experimental setup, exponentially growing cells treated with negative control siRNA (siNC) and siRNA targeting both CAP-H and CAP-D3 irradiated with 0.5 Gy X-rays. Chromatid breaks in G2-PCCs were quantified at 1 hour and 4 hours post-irradiation. The results, as presented in Figure 34, reveal widespread alterations in chromosome structure following the suppression of condensins. This was evidenced by significant chromosome decondensation (Figure 33D, F), highlighting the essential role of condensins in chromosome compaction.

Interestingly, our observations showed that the initial level of damage was slightly higher in condensins deficient cells compared to siNC cells. Despite this initial difference, the repair capabilities diverged significantly. While siNC cells demonstrated normal repair capability, approximately 80% of the breaks remained unrepaired in condensins deficient cells (Figure 34B). This stark contrast underscores the compromised repair process in the absence of functional condensins.

These findings align with previous studies that emphasize the critical role of functional condensins in the repair of IR-induced DSBs. For example, earlier research demonstrated that the condensin II binding region of MCPH1 is essential for homologous recombination (HR) function, highlighting a novel role of MCPH1 in modulating HR repair through Condensin II to maintain genome integrity (Wood et al. 2008). Furthermore, it has been shown that decondensation of chromosomes by incubating cells

in a hypotonic medium delayed their repair, as measured by scoring G2-PCC breaks over time, with HypoS markedly suppressing HR (Krieger et al. 2021). These results, along with our current PCC data, provide compelling evidence that functional condensins are indispensable for the effective repair of IR-induced DSBs.

Our study reinforces the fundamental role of condensins in chromosome compaction and the efficient repair of chromatid breaks. The compromised repair observed in condensins deficient cells highlights the critical function of condensins in maintaining genomic stability. These findings not only advance our understanding of the molecular mechanisms underlying DNA repair but also have significant implications for therapeutic strategies targeting genome stability in cancer treatment.

7. Summary

The role of the condensin protein complex, crucial for chromosome dynamics and DNA repair, was investigated to understand its function in DNA damage repair. Suppression of condensins in RPE-1 hTert and A549 cells showed increased radiosensitivity, indicating their importance in maintaining cell viability post IR.

Detailed studies revealed that while individual downregulation of condensin I or II expression did not significantly affect radiosensitivity, combined suppression of both condensins did, highlighting a potential therapeutic target for radiotherapy. Further investigation into DNA damage signaling demonstrated that condensins knockdown impaired the resolution of γH2AX and 53BP1 foci, critical markers for DSB repair, underscoring the role of condensins in effective DSB repair.

Condensins knockdown also affected the balance of DSB repair pathways. It reduced activities in HR, SSA, and alt-EJ while promoting c-NHEJ. This was linked to impaired DNA end resection, crucial for HR and SSA, as evidenced by reduced RPA70 and RAD51 foci formation.

Additionally, condensins play a vital role in the progression of the cells through the G2/M phases (checkpoint activation), which is necessary for DNA repair before cell division. Condensins deficient cells showed a compromised checkpoint response, affecting HR-mediated repair. This interdependence of HR and the G2 checkpoint emphasizes the importance of condensins in genomic stability.

Finally, the study confirmed condensins' crucial role in repairing chromatid breaks. Condensins suppression led to significant chromosomal decondensation and impaired DNA repair, supporting their essential function in chromosome compaction and DSB repair. These findings highlight the potential of targeting condensins in cancer therapies to enhance radiotherapy effectiveness and maintain genomic stability. Collectively, these novel findings substantially increase our knowledge in the field.

8. Zusammenfassung

Die Rolle des Condensin-Proteinkomplexes, der für Chromosomendynamik und DNA-Reparatur von entscheidender Bedeutung ist, wurde untersucht, um seine Funktion in der DNA-Schadensreparatur zu verstehen. Die Unterdrückung von Condensinen in RPE-1 hTert- und A549-Zellen zeigte eine erhöhte Strahlenempfindlichkeit, was auf ihre Wichtigkeit für die Aufrechterhaltung der Zellviabilität nach ionisierender Strahlung (IR) hinweist.

Detaillierte Studien ergaben, dass die Herunterregulierung der Expression von Condensin I oder II die Strahlenempfindlichkeit nicht signifikant beeinflusste, während die kombinierte Unterdrückung beider Condensine dies tat, was ein potenzielles therapeutisches Ziel für die Strahlentherapie aufzeigt. Weitere Untersuchungen zur DNA-Schadenssignalübertragung zeigten, dass die Herunterregulation von Condensinen die Auflösung von γH2AX- und 53BP1-Foci, kritischen Markern für den Doppelstrangbruch (DSB)-Reparatur, beeinträchtigte und somit die Rolle der Condensine in der effektiven DSB-Reparatur unterstreicht.

Die Herunterregulation non Condensinen beeinflusste auch das Gleichgewicht der DSB-Reparaturwege. Es reduzierte die Aktivität der homologen Rekombination (HR), Single-single-strand annealing (SSA) und alternativer End-Verknüpfung (alt-EJ), während es das klassische nicht-homologe End-Verknüpfung (c-NHEJ) förderte. Dies wurde mit einer Beeinträchtigung der DNA-Endresektion in Verbindung gebracht, die für HR und SSA entscheidend ist, welches durch eine reduzierte Bildung von RPA70- und RAD51-Foci belegt wurde.

Darüber hinaus spielen Condensine eine wichtige Rolle bei der Progression der Zellen durch die G2/M-Phasen (Checkpoint-Aktivierung), die für die DNA-Reparatur vor der Zellteilung notwendig ist. Condensin-defiziente Zellen zeigten eine beeinträchtigte Kontrollpunkt-Antwort, was die HR-vermittelte Reparatur beeinflusste. Diese wechselseitige Abhängigkeit von HR und dem G2-Kontrollpunkt betont die Bedeutung von Condensinen für die genomische Stabilität.

Schließlich bestätigt die Studie die zentrale Rolle der Condensine bei der Reparatur von Chromatidbrüchen. Die Unterdrückung von Condensinen führte zu einer signifikanten Chromosomendekondensation und beeinträchtigten DANN Reparatur, was ihre

essenzielle Funktion bei der Chromosomenkondensation und der DSB-Reparatur hervorhebt. Diese Ergebnisse unterstreichen das Potenzial des Targetings von Condensinen in der Krebstherapie, um die Wirksamkeit der Strahlentherapie zu verbessern und die genomische Stabilität aufrechtzuerhalten. Zusammenfassend erweitern diese neuen Erkenntnisse erheblich unser Wissen auf diesem Gebiet.

9. References

Abe, S., K. Nagasaka, Y. Hirayama, H. Kozuka-Hata, M. Oyama, Y. Aoyagi, C. Obuse, and T. Hirota. 2011. 'The initial phase of chromosome condensation requires Cdk1-mediated phosphorylation of the CAP-D3 subunit of condensin II', *Genes Dev*, 25: 863-74.

Allen, C., A. K. Ashley, R. Hromas, and J. A. Nickoloff. 2011. 'More forks on the road to replication stress recovery', *J Mol Cell Biol*, 3: 4-12.

Bazett-Jones, D. P., K. Kimura, and T. Hirano. 2002. 'Efficient supercoiling of DNA by a single condensin complex as revealed by electron spectroscopic imaging', *Mol Cell*, 9: 1183-90.

Bennardo, N., A. Cheng, N. Huang, and J. M. Stark. 2008. 'Alternative-NHEJ is a mechanistically distinct pathway of mammalian chromosome break repair', *PLoS Genet*, 4: e1000110.

Bhargava, R., D. O. Onyango, and J. M. Stark. 2016. 'Regulation of Single-Strand Annealing and its Role in Genome Maintenance', *Trends Genet*, 32: 566-75.

Blackford, A. N., and M. Stucki. 2020. 'How Cells Respond to DNA Breaks in Mitosis', *Trends Biochem Sci*, 45: 321-31.

Bodnar, A. G., M. Ouellette, M. Frolkis, S. E. Holt, C. P. Chiu, G. B. Morin, C. B. Harley, J. W. Shay, S. Lichtsteiner, and W. E. Wright. 1998. 'Extension of life-span by introduction of telomerase into normal human cells', *Science*, 279: 349-52.

Boteva, L., R. S. Nozawa, C. Naughton, K. Samejima, W. C. Earnshaw, and N. Gilbert. 2020. 'Common Fragile Sites Are Characterized by Faulty Condensin Loading after Replication Stress', *Cell Rep*, 32: 108177.

Bryant, P. E., and P. J. Johnston. 1993. 'Restriction-endonuclease-induced DNA double-strand breaks and chromosomal aberrations in mammalian cells', *Mutat Res*, 299: 289-96.

Ciccia, A., and S. J. Elledge. 2010. 'The DNA damage response: making it safe to play with knives', *Mol Cell*, 40: 179-204.

Cortez, D., S. Guntuku, J. Qin, and S. J. Elledge. 2001. 'ATR and ATRIP: partners in checkpoint signaling', *Science*, 294: 1713-6.

Covo, S., J. W. Westmoreland, D. A. Gordenin, and M. A. Resnick. 2010. 'Cohesin Is limiting for the suppression of DNA damage-induced recombination between homologous chromosomes', *PLoS Genet*, 6: e1001006.

Dantzer, F., G. de La Rubia, J. Ménissier-De Murcia, Z. Hostomsky, G. de Murcia, and V. Schreiber. 2000. 'Base excision repair is impaired in mammalian cells lacking Poly(ADP-ribose) polymerase-1', *Biochemistry*, 39: 7559-69.

Dueva, Rositsa, and George Iliakis. 2013. 'Alternative pathways of non-homologous end joining (NHEJ) in genomic instability and cancer', *Translational Cancer Research; Vol 2, No 3 (June 19, 2013): Translational Cancer Research (DNA Damage and Repair)*.

Falck, J., J. Coates, and S. P. Jackson. 2005. 'Conserved modes of recruitment of ATM, ATR and DNA-PKcs to sites of DNA damage', *Nature*, 434: 605-11.

Gerlich, D., T. Hirota, B. Koch, J. M. Peters, and J. Ellenberg. 2006. 'Condensin I stabilizes chromosomes mechanically through a dynamic interaction in live cells', *Curr Biol*, 16: 333-44.

Gibcus, J. H., K. Samejima, A. Goloborodko, I. Samejima, N. Naumova, J. Nuebler, M. T. Kanemaki, L. Xie, J. R. Paulson, W. C. Earnshaw, L. A. Mirny, and J. Dekker. 2018. 'A pathway for mitotic chromosome formation', *Science*, 359.

Goloborodko, A., M. V. Imakaev, J. F. Marko, and L. Mirny. 2016. 'Compaction and segregation of sister chromatids via active loop extrusion', *Elife*, 5.

Gunn, A., and J. M. Stark. 2012. 'I-SceI-based assays to examine distinct repair outcomes of mammalian chromosomal double strand breaks', *Methods Mol Biol*, 920: 379-91.

Hall, E.J., and A.J. Giaccia. 2006. *Radiobiology for the Radiologist* (Lippincott Williams & Wilkins).

Harrison, J. C., and J. E. Haber. 2006. 'Surviving the breakup: the DNA damage checkpoint', *Annu Rev Genet*, 40: 209-35.

Heale, J. T., A. R. Ball, Jr., J. A. Schmiesing, J. S. Kim, X. Kong, S. Zhou, D. F. Hudson, W. C. Earnshaw, and K. Yokomori. 2006. 'Condensin I interacts with the PARP-1-XRCC1 complex and functions in DNA single-strand break repair', *Mol Cell*, 21: 837-48.

Hirano, T. 2012. 'Condensins: universal organizers of chromosomes with diverse functions', *Genes Dev*, 26: 1659-78.

Hirota, T., D. Gerlich, B. Koch, J. Ellenberg, and J. M. Peters. 2004. 'Distinct functions of condensin I and II in mitotic chromosome assembly', *J Cell Sci*, 117: 6435-45.

Hoeijmakers, J. H. 2009. 'DNA damage, aging, and cancer', *N Engl J Med*, 361: 1475-85.

Hoencamp, C., O. Dudchenko, A. M. O. Elbatsh, S. Brahmachari, J. A. Raaijmakers, T. van Schaik, Á Sedeño Cacciatore, V. G. Contessoto, Rghp van Heesbeen, B. van den Broek, A. N. Mhaskar, H. Teunissen, B. G. St Hilaire, D. Weisz, A. D. Omer, M. Pham, Z. Colaric, Z. Yang, S. S. P. Rao, N. Mitra, C. Lui, W. Yao, R. Khan, L. L. Moroz, A. Kohn, J. St Leger, A. Mena, K. Holcroft, M. C. Gambetta, F. Lim, E. Farley, N. Stein, A. Haddad, D. Chauss, A. S. Mutlu, M. C. Wang, N. D. Young, E. Hildebrandt, H. H. Cheng, C. J. Knight, T. L. U. Burnham, K. A. Hovel, A. J. Beel, P. J. Mattei, R. D. Kornberg, W. C. Warren, G. Cary, J. L. Gómez-Skarmeta, V. Hinman, K. Lindblad-Toh, F. Di Palma, K. Maeshima, A. S. Multani, S. Pathak, L. Nel-Themaat, R. R. Behringer, P. Kaur, R. H. Medema, B. van Steensel, E. de Wit, J. N. Onuchic, M. Di Pierro, E. Lieberman Aiden, and B. D. Rowland. 2021. '3D genomics across the tree of life reveals condensin II as a determinant of architecture type', *Science*, 372: 984-89.

Hoencamp, C., and B. D. Rowland. 2023. 'Genome control by SMC complexes', *Nat Rev Mol Cell Biol*, 24: 633-50.

Iliakis, G., E. Mladenov, and V. Mladenova. 2019. 'Necessities in the Processing of DNA Double Strand Breaks and Their Effects on Genomic Instability and Cancer', *Cancers (Basel)*, 11.

Ivanov, E. L., N. Sugawara, J. Fishman-Lobell, and J. E. Haber. 1996. 'Genetic requirements for the single-strand annealing pathway of double-strand break repair in Saccharomyces cerevisiae', *Genetics*, 142: 693-704.

Jackson, S. P., and J. Bartek. 2009. 'The DNA-damage response in human biology and disease', *Nature*, 461: 1071-8.

Jasin, M. 1996. 'Genetic manipulation of genomes with rare-cutting endonucleases', *Trends Genet*, 12: 224-8.

Jiang, X. R., G. Jimenez, E. Chang, M. Frolkis, B. Kusler, M. Sage, M. Beeche, A. G. Bodnar, G. M. Wahl, T. D. Tlsty, and C. P. Chiu. 1999. 'Telomerase expression in human somatic cells does not induce changes associated with a transformed phenotype', *Nat Genet*, 21: 111-4.

Kedar, P. S., D. F. Stefanick, J. K. Horton, and S. H. Wilson. 2012. 'Increased PARP-1 association with DNA in alkylation damaged, PARP-inhibited mouse fibroblasts', *Mol Cancer Res*, 10: 360-8.

Kim, J. S., T. B. Krasieva, V. LaMorte, A. M. Taylor, and K. Yokomori. 2002. 'Specific recruitment of human cohesin to laser-induced DNA damage', *J Biol Chem*, 277: 45149-53.

Kong, M., E. E. Cutts, D. Pan, F. Beuron, T. Kaliyappan, C. Xue, E. P. Morris, A. Musacchio, A. Vannini, and E. C. Greene. 2020. 'Human Condensin I and II Drive Extensive ATP-Dependent Compaction of Nucleosome-Bound DNA', *Mol Cell*, 79: 99-114.e9.

Kong, X., J. Stephens, A. R. Ball, Jr., J. T. Heale, D. A. Newkirk, M. W. Berns, and K. Yokomori. 2011. 'Condensin I recruitment to base damage-enriched DNA lesions is modulated by PARP1', *PLoS One*, 6: e23548.

Krieger, L. M., E. Mladenov, A. Soni, M. Demond, M. Stuschke, and G. Iliakis. 2021. 'Disruption of Chromatin Dynamics by Hypotonic Stress Suppresses HR and Shifts DSB Processing to Error-Prone SSA', *Int J Mol Sci*, 22.

Lancaster, L., H. Patel, G. Kelly, and F. Uhlmann. 2021. 'A role for condensin in mediating transcriptional adaptation to environmental stimuli', *Life Sci Alliance*, 4.

Löbrich, M., and P. Jeggo. 2017. 'A Process of Resection-Dependent Nonhomologous End Joining Involving the Goddess Artemis', *Trends Biochem Sci*, 42: 690-701.

Luo, D., E. Mladenov, A. Soni, M. Stuschke, and G. Iliakis. 2023. 'The p38/MK2 Pathway Functions as Chk1-Backup Downstream of ATM/ATR in G(2)-Checkpoint Activation in Cells Exposed to Ionizing Radiation', *Cells*, 12.

Maeshima, K., and U. K. Laemmli. 2003. 'A two-step scaffolding model for mitotic chromosome assembly', *Dev Cell*, 4: 467-80.

Massagué, J. 2004. 'G1 cell-cycle control and cancer', *Nature*, 432: 298-306.

Matsunaga, H., J. T. Handa, A. Aotaki-Keen, S. W. Sherwood, M. D. West, and L. M. Hjelmeland. 1999. 'Beta-galactosidase histochemistry and telomere loss in senescent retinal pigment epithelial cells', *Invest Ophthalmol Vis Sci*, 40: 197-202.

Mladenov, E., S. Magin, A. Soni, and G. Iliakis. 2016. 'DNA double-strand-break repair in higher eukaryotes and its role in genomic instability and cancer: Cell cycle and proliferation-dependent regulation', *Semin Cancer Biol*, 37-38: 51-64.

Mladenov, E., C. Staudt, A. Soni, T. Murmann-Konda, M. Siemann-Loekes, and G. Iliakis. 2020. 'Strong suppression of gene conversion with increasing DNA double-strand break load delimited by 53BP1 and RAD52', *Nucleic Acids Res*, 48: 1905-24.

Mladenova, V., E. Mladenov, and G. Iliakis. 2016. 'Novel Biological Approaches for Testing the Contributions of Single DSBs and DSB Clusters to the Biological Effects of High LET Radiation', *Front Oncol*, 6: 163.

Nasmyth, K. 2001. 'Disseminating the genome: joining, resolving, and separating sister chromatids during mitosis and meiosis', *Annu Rev Genet*, 35: 673-745.

Nastasi, C., L. Mannarino, and M. D'Incalci. 2020. 'DNA Damage Response and Immune Defense', *Int J Mol Sci*, 21.

Ochs, F., K. Somyajit, M. Altmeyer, M. B. Rask, J. Lukas, and C. Lukas. 2016. '53BP1 fosters fidelity of homology-directed DNA repair', *Nat Struct Mol Biol*, 23: 714-21.

Patel, J., B. A. Baptiste, E. Kim, M. Hussain, D. L. Croteau, and V. A. Bohr. 2020. 'DNA damage and mitochondria in cancer and aging', *Carcinogenesis*, 41: 1625-34.

Pei, X., E. Mladenov, A. Soni, F. Li, M. Stuschke, and G. Iliakis. 2022. 'PTEN Loss Enhances Error-Prone DSB Processing and Tumor Cell Radiosensitivity by Suppressing RAD51 Expression and Homologous Recombination', *Int J Mol Sci*, 23.

Piazza, A., H. Bordelet, A. Dumont, A. Thierry, J. Savocco, F. Girard, and R. Koszul. 2021. 'Cohesin regulates homology search during recombinational DNA repair', *Nat Cell Biol*, 23: 1176-86.

Piazza, I., A. Rutkowska, A. Ori, M. Walczak, J. Metz, V. Pelechano, M. Beck, and C. H. Haering. 2014. 'Association of condensin with chromosomes depends on DNA binding by its HEAT-repeat subunits', *Nat Struct Mol Biol*, 21: 560-8.

Polo, S. E., and S. P. Jackson. 2011. 'Dynamics of DNA damage response proteins at DNA breaks: a focus on protein modifications', *Genes Dev*, 25: 409-33.

Ribezzo, F., Y. Shiloh, and B. Schumacher. 2016. 'Systemic DNA damage responses in aging and diseases', *Semin Cancer Biol*, 37-38: 26-35.

Richardson, C., and M. Jasin. 2000. 'Frequent chromosomal translocations induced by DNA double-strand breaks', *Nature*, 405: 697-700.

Riggs, A. D. 1990. 'DNA methylation and late replication probably aid cell memory, and type I DNA reeling could aid chromosome folding and enhancer function', *Philos Trans R Soc Lond B Biol Sci*, 326: 285-97.

Rothenberg, E., J. M. Grimme, M. Spies, and T. Ha. 2008. 'Human Rad52-mediated homology search and annealing occurs by continuous interactions between overlapping nucleoprotein complexes', *Proc Natl Acad Sci U S A*, 105: 20274-9.

Rouet, P., F. Smih, and M. Jasin. 1994. 'Expression of a site-specific endonuclease stimulates homologous recombination in mammalian cells', *Proc Natl Acad Sci U S A*, 91: 6064-8.

Ryu, J. K., S. H. Rah, R. Janissen, J. W. J. Kerssemakers, A. Bonato, D. Michieletto, and C. Dekker. 2022. 'Condensin extrudes DNA loops in steps up to hundreds of base pairs that are generated by ATP binding events', *Nucleic Acids Res*, 50: 820-32.

Schipler, A., and G. Iliakis. 2013. 'DNA double-strand-break complexity levels and their possible contributions to the probability for error-prone processing and repair pathway choice', *Nucleic Acids Res*, 41: 7589-605.

Soni, A., E. Mladenov, and G. Iliakis. 2021. 'Proficiency in homologous recombination repair is prerequisite for activation of G(2)-checkpoint at low radiation doses', *DNA Repair (Amst)*, 101: 103076.

Soni, A., T. Murmann-Konda, M. Siemann-Loekes, G. E. Pantelias, and G. Iliakis. 2020. 'Chromosome breaks generated by low doses of ionizing radiation in G(2)-phase are processed exclusively by gene conversion', *DNA Repair (Amst)*, 89: 102828.

Ström, L., C. Karlsson, H. B. Lindroos, S. Wedahl, Y. Katou, K. Shirahige, and C. Sjögren. 2007. 'Postreplicative formation of cohesion is required for repair and induced by a single DNA break', *Science*, 317: 242-5.

Ström, L., H. B. Lindroos, K. Shirahige, and C. Sjögren. 2004. 'Postreplicative recruitment of cohesin to double-strand breaks is required for DNA repair', *Mol Cell*, 16: 1003-15.

Sulli, G., R. Di Micco, and F. d'Adda di Fagagna. 2012. 'Crosstalk between chromatin state and DNA damage response in cellular senescence and cancer', *Nat Rev Cancer*, 12: 709-20.

Terakawa, T., S. Bisht, J. M. Eeftens, C. Dekker, C. H. Haering, and E. C. Greene. 2017. 'The condensin complex is a mechanochemical motor that translocates along DNA', *Science*, 358: 672-76.

Tiwari, V., and D. M. Wilson, 3rd. 2019. 'DNA Damage and Associated DNA Repair Defects in Disease and Premature Aging', *Am J Hum Genet*, 105: 237-57.

Unal, E., A. Arbel-Eden, U. Sattler, R. Shroff, M. Lichten, J. E. Haber, and D. Koshland. 2004. 'DNA damage response pathway uses histone modification to assemble a double-strand break-specific cohesin domain', *Mol Cell*, 16: 991-1002.

Unal, E., J. M. Heidinger-Pauli, and D. Koshland. 2007. 'DNA double-strand breaks trigger genome-wide sister-chromatid cohesion through Eco1 (Ctf7)', *Science*, 317: 245-8.

Wang, M., W. Wu, W. Wu, B. Rosidi, L. Zhang, H. Wang, and G. Iliakis. 2006. 'PARP-1 and Ku compete for repair of DNA double strand breaks by distinct NHEJ pathways', *Nucleic Acids Res*, 34: 6170-82.

Wang, Z., Y. Gong, B. Peng, R. Shi, D. Fan, H. Zhao, M. Zhu, H. Zhang, Z. Lou, J. Zhou, W. G. Zhu, Y. S. Cong, and X. Xu. 2019. 'MRE11 UFMylation promotes ATM activation', *Nucleic Acids Res*, 47: 4124-35.

Williams, R. S., G. Moncalian, J. S. Williams, Y. Yamada, O. Limbo, D. S. Shin, L. M. Groocock, D. Cahill, C. Hitomi, G. Guenther, D. Moiani, J. P. Carney, P. Russell, and J. A. Tainer. 2008. 'Mre11 dimers coordinate DNA end bridging and nuclease processing in double-strand-break repair', *Cell*, 135: 97-109.

Wood, J. L., Y. Liang, K. Li, and J. Chen. 2008. 'Microcephalin/MCPH1 associates with the Condensin II complex to function in homologous recombination repair', *J Biol Chem*, 283: 29586-92.

Wood, J. L., N. Singh, G. Mer, and J. Chen. 2007. 'MCPH1 functions in an H2AX-dependent but MDC1-independent pathway in response to DNA damage', *J Biol Chem*, 282: 35416-23.

Wu, S., N. Fatkhutdinov, L. Rosin, J. M. Luppino, O. Iwasaki, H. Tanizawa, H. Y. Tang, A. V. Kossenkov, A. Gardini, K. I. Noma, D. W. Speicher, E. F. Joyce, and R. Zhang. 2019. 'ARID1A spatially partitions interphase chromosomes', *Sci Adv*, 5: eaaw5294.

Xiao, H., F. Li, E. Mladenov, A. Soni, V. Mladenova, B. Pan, R. Dueva, M. Stuschke, B. Timmermann, and G. Iliakis. 2022. 'Increased Resection at DSBs in G(2)-Phase Is a Unique Phenotype Associated with DNA-PKcs Defects That Is Not Shared by Other Factors of c-NHEJ', *Cells*, 11.

Yu, Z., G. Vogel, Y. Coulombe, D. Dubeau, E. Spehalski, J. Hébert, D. O. Ferguson, J. Y. Masson, and S. Richard. 2012. 'The MRE11 GAR motif regulates DNA double-strand break processing and ATR activation', *Cell Res*, 22: 305-20.

Zetterberg, A., and O. Larsson. 1985. 'Kinetic analysis of regulatory events in G1 leading to proliferation or quiescence of Swiss 3T3 cells', *Proc Natl Acad Sci U S A*, 82: 5365-9.

Zhang, T., J. R. Paulson, M. Bakhrebah, J. H. Kim, C. Nowell, P. Kalitsis, and D. F. Hudson. 2016. 'Condensin I and II behaviour in interphase nuclei and cells undergoing premature chromosome condensation', *Chromosome Res*, 24: 243-69.

Zimmermann, M., and T. de Lange. 2014. '53BP1: pro choice in DNA repair', *Trends Cell Biol*, 24: 108-17.

List of abbreviations

53BP1	p53 binding protein
Ab	antibody
AP	apurinic/apyrimidinic
APS	ammonium persulfate
ATM	ataxia telangiectasia mutated kinase
ATR	ATM and Rad3 related kinase
bp	base pair
BRCA1/2	breast cancer susceptibility protein 1/2
BrPBlue	bromophenol blue
BSA	bovine serum albumin
cm	centimeter
cm^2	square centimeter
CtIP	CtBP interacting protein
d	day
DAPI	4’,6-diamidino-2-phenylindole
D-loop	displacement loop
DMEM	dulbecco’s modified eagle’s medium
DMSO	dimethyl sulfoxide
dsDNA	double-stranded DNA
EDTA	ethylenediaminetetraacetic acid
EdU	5-Ethynyl-2’-deoxyuridine
e.g.	exempli gratia
EGFP	enhanced GFP
et al.	et alii
EtBr	ethidium bromide
etc.	et cetera
eV	electronvolt

FBS	fetal bovine serum
FC	flow cytometry
GFP	green fluorescent protein
Gy	Gray
h	hour
H3pS10	phosphorylated serine10 of histone H3
hTert	human telomerase catalytic subunit component
i	inhibitor
i.e.	id est
IF	immunofluorescence
kb	kilobases
KCl	potassium chloride
kg	kilogram
kV	kilovolt
LET	linear energy transfer
LIF	leica image format
Lig1/3/4	ligase 1/3/4
m	meter
mA	milliampere
µg	microgram
MI	mitotic index
min	minute/s
mM	millimolar
µm	micrometer
µM	micromolar
Mre11	meiotic recombination 11
MRN complex	Mre11/Rad50/Nbs1 complex
NaCl	sodium chloride
NASA	National Aeronautics and Space Administration

NLS	N-Lauroylsarcosine
nm	nanometer
nM	nanomolar
PAXX	paralog of XRCC4 and XLF
PBS	phosphate buffered saline
PI	propidium iodide
RIF1	RAP1-interacting factor 1
RPA	replication protein A
RPE-1	retinal pigment epithelial cell line 1
rpm	revolutions per minute
RT	room temperature
SD	standard deviation
TBS	tris buffered saline
TBS-T	tris buffered saline and Tween 20
U2OS	human bone osteosarcoma epithelial cell line
UK	Universitätsklinikum
UV	ultra violet
XLF	XRCC4-like factor
XRCC1/2/3/4	X-ray cross-complementing protein 1/2/3/4
γH2AX	phosphorylated H2AX at serine139

List of Figures

Acknowledgments

I would like to begin by expressing my deepest gratitude to my supervisor, Prof. Dr. George Iliakis, for granting me the opportunity to pursue my Ph.D. at the Institute of Medical Radiation Biology. His unwavering support, both professionally and personally, has been a constant source of guidance. I am especially grateful for the trust he placed in me by assigning me important responsibilities, and for his patience and reassurance during challenging times.

My research was generously funded by the Bundesministerium für Bildung und Forschung (BMBF) under grant number 02NUK054B for the project "VERCHROMT: Detection, Processing, and Biological Consequences of Chromatin Damage after Particle Irradiation."

I would also like to extend my sincere thanks to Dr. Lisa Marie Krieger for her invaluable training at the outset of my research, as well as her continuous support in resolving technical and experimental challenges.

A heartfelt acknowledgment goes to Dr. Aashish Soni, Dr. Emil Mladenova, Dr. Veronika Mladenova, and Dr. Fanghua Li for their exceptional assistance and encouragement over the past three years. Their expertise and kindness were pivotal to my progress.

I am equally grateful to my colleagues, especially Ye Qiu, Xixi Lin, Xile Pei, Huaping Xiao, and Bing Pan, whose help and camaraderie have provided both motivation and friendship throughout my studies. I also want to thank Christian Möllers and Al-Dulaimi Nada Faisal Rashid for their instrumental support in ensuring the smooth execution of my experiments.

Finally, I extend my heartfelt appreciation to my friends and family, with special thanks to my husband for his unwavering support and encouragement, and to my two daughters for enduring the stressful moments alongside me.

To all who have contributed to my academic and personal journey, thank you for your invaluable support. Your contributions have enabled me to persevere and successfully complete my studies.

CURRICULUM VITAE

This section has been removed for data protection reasons.